รายงานวิจัยฉบับสมบูรณ์

โครงการการศึกษาบทบาทของโปรตีนกลุ่มแชเปอโรนินภายใต้สภาวะความเครียดแสงของพืช

Investigating the roles of molecular chaperones in irradiance-stress responses of plants

โดย

ผศ. ดร. กิตติศักดิ์ หยกทองวัฒนา **หัวหน้าโครงการวิจัย**

ภาควิชาชีวเคมีและหน่วยวิจัยโครงสร้างและการทำงานของโปรตีน

คณะวิทยาศาสตร์ มหาวิทยาลัยมหิดล 272 ถนนพระรามที่ 6

แขวงทุ่งพญาไท เขตราชเทวี กรุงเทพมหานคร 10400

เดือน ปี ที่สำเร็จโครงการ มิถุนายน พ.ศ. 2556

สัญญาเลขที่ RMU5380037

รายงานวิจัยฉบับสมบูรณ์

โครงการการศึกษาบทบาทของโปรตีนกลุ่มแชเปอโรนินภายใต้สภาวะความเครียดแสงของพืช

Investigating the roles of molecular chaperones in irradiance-stress responses of plants

โดย

ผศ. ดร. กิตติศักดิ์ หยกทองวัฒนา **หัวหน้าโครงการวิจัย**

ภาควิชาชีวเคมีและหน่วยวิจัยโครงสร้างและการทำงานของโปรตีน

คณะวิทยาศาสตร์ มหาวิทยาลัยมหิดล 272 ถนนพระรามที่ 6

แขวงทุ่งพญาไท เขตราชเทวี กรุงเทพมหานคร 10400

สนันสนุนโดยสำนักงานคณะกรรมการการอุดมศึกษา
และสำนักงานกองทุนสนับสนุนการวิจัย

กิตติกรรมประกาศ

I would like to thank the granting agencies that jointly support this research: Thailand Research Fund, the Office of the Higher Education Commissions, and Mahidol University. Acknowledgements must also go to all the students and colleagues that participated more or less in this research.

บทคัดย่อ

รหัสโครงการ : RMU5380037

ชื่อโครงการ : การศึกษาบทบาทของโปรตีนกลุ่มแชเปอโรนินภายใต้สภาวะความเครียดแสงของพืช

ชื่อนักวิจัย : ผศ. ดร. กิตติศักดิ์ หยกทองวัฒนา

E-mail Address : kittisak.yok@mahidol.ac.th

ระยะเวลาโครงการ : 3 ปี

ในงานวิจัยนี้ ผลการทดลองที่เกิดจากการศึกษาด้วยวิธีโปรตีโอมิกส์ของสาหร่ายเซลล์เดียว *Chlamydomonas reinhardtii* ระหว่างการตอบสนองต่อสภาพวะแสงสูงได้บ่งบอกถึงความเป็นไปได้ที่โปรตีน CPN60 อาจจะมีบทบาทการทำงานที่สำคัญในการปกป้องเซลล์และโปรตีนจากการถูกทำลายด้วยแสงที่มากเกินไป เราได้พบว่าสาหร่ายชนิดนี้ซึ่งเป็นสาหร่ายที่ไม่ชอบแสงสูง ไม่สามารถรักษาระดับของโปรตีน CPN60 ไว้ได้เมื่อได้รับแสงสูงเป็นเวลานาน คาดว่าเพราะเหตุนี้จึงเป็นเหตุให้สาหร่ายชนิดนี้ไม่ทนแสง เพื่อยืนยันสมมติฐานนี้ เราได้ทำการ knock down การแสดงออกของยีน *cpn60B1* และ *cpn60B2* ซึ่งแปลรหัสได้เป็นโปรตีนหน่วยย่อยของ CPN60 และได้ทำการศึกษาผลของการยับยั้งนี้ต่อประสิทธิภาพการสังเคราะห์ด้วยแสง พบว่าในสาหร่ายพันธุ์กลายที่มีการแสดงออกของยีน *cpn60B1* และ *cpn60B2* ลดลงนั้น ระบบแสงที่สอง (PSII) จะถูกทำลายได้เร็วกว่าสาหร่ายพันธุ์ wild type ในชั่วโมงแรก ๆ เมื่อได้รับแสงสูง

คำหลัก : *Chlamydomonas reinhardtii*, heat-shock protein, irradiance stress, molecular chaperones, photoinhibition

Abstract

Project Code : RMU5380037

Project Title : Investigating the roles of molecular chaperones in irradiance-stress responses of plants

Investigator : Dr. Kittisak Yokthongwattana, Assistant Professor

E-mail Address : kittisak.yok@mahidol.ac.th

Project Period : 3 ปี

Through proteomic screenings and reverse genetic approaches, we have found a clue for possible active role of a chloroplast-localized chaperonin protein (CPN60) in protecting plants from irradiance stress. A light-sensitive unicellular green alga, *Chlamydomonas reinhardtii*, was used as a model organism. When subjected to excessive light, the alga was unable to maintain the level of the CPN60 chaperone. Such failure to keep the chaperonin level under irradiance stress may explain the light-sensitive nature of this alga. Reverse genetic approach of knocking down the *cpn60B1* and *cpn60B2* genes encoding for beta 1 and beta 2 subunit of the chaperonin was performed. Results showed that the transformants with knocked down phenotype of *cpn60B1* or *cpn60B2* exhibit faster rate of PSII photodamge, especially in the initial period of irradiance stress.

Keywords : *Chlamydomonas reinhardtii*, heat-shock protein, irradiance stress, molecular chaperones, photoinhibition

เนื้อหางานวิจัย

Introduction and Literature Reviews

Rationale of the project

Although light is essential for photosynthesis, a process that governs plant productivity, too much light rather causes inhibitory effects. Absorption of excessive irradiance often leads to photo-oxidative damage to photosynthetic apparatus as well as to chloroplast membrane lipids (Niyogi 1999). Without remediation, photosynthetic reactions are arrested, leading to declines in crop productivity. This phenomenon is commonly known as irradiance stress or photoinhitition, and if prolonged, may eventually lead to plant death (Melis 1999). For survival, photosynthetic organisms have evolved protective and repair mechanisms (of photosystem II) to rectify themselves from such adverse effect (Niyogi 1999; Yokthongwattana and Melis 2006; Yokthongwattana et al. 2009). These two research areas have been subjects of interest from scientists around the world. However, to date such protective and repair mechanisms are still not fully understood. Various factors contributing to photoprotection and repair have been reported in the literature each year.

As Thailand is a country located very close to the equator, the region where a lot of sunlight reaches the earth surface more than other parts of the world, important agricultural crops often face with photoinhibitory conditions. Understanding at the molecular level how plants can successfully cope with irradiance stress may allow scientist to help boost productivity of agricultural crops, which is important for the country's economy. Molecular chaperones have been suggested to play important role in successful plant adaptation to suboptimal growth conditions. In this research proposal, therefore, the roles of molecular chaperones in plant response to irradiance-stress conditions were investigated using a unicellular green alga, *Chlamydomonas reinhardtii*, as a model organism.

Irradiance stress and photoinhibition

In oxygenic photosynthetic organisms, light absorption, rate of electron transport and carbon metabolism are synchronized to maximize photosynthesis yield. Under limiting irradiance, light energy is captured and utilized with high efficiency by employing a large chlorophyll (Chl) antenna. Increasing light intensities will result in more photon absorptions and enhanced rates of CO_2 assimilation. However, at the light intensity where the rate of CO_2 fixation becomes a limiting factor, photosynthesis is saturated (Stitt 1986). Absorption of excitation energy in excess of that required for the saturation of photosynthesis can bring about

photo-oxidative damage to chloroplast membranes and proteins. Under irradiance stress, the chloroplast is saturated with ensuing flux of excitation energy, reduced form of redox mediators and molecular oxygen. This condition favors the generation of reactive oxygen species (ROS). Over-reduction of the plastoquinone (PQ) pool under excess irradiance results in the Q_B binding site of the PSII being devoid of oxidized PQ, resulting in a longer lifetime of reduced primary quinone acceptor (Q_A^-). The long-lived Q_A^-, in turn, blocks electron transfer from the subsequent charge separation between the reaction center chlorophyll (P680) and pheophytin (Pheo). The increasing lifetime of the $P680^+/Pheo^-$ is not stable and has a tendency to recombine and produce a long-lasting triplet excited state of the P680 ($^3P680^*$) (Vass et al. 1992). Under oxygenic photosynthesis conditions, this $^3P680^*$ can be quenched efficiently by ground-state triplet oxygen ($^3O_2$), resulting in the formation of singlet oxygen ($^1O_2$). $^1O_2$ is a highly reactive oxygen species capable of causing adverse effects to the P680 itself and/or to other PSII components in the nearby vicinity, rendering the PSII inactive. Light-induced irreversible inactivation of the PSII is a well-known phenomenon that entails a permanent damage to the D1 reaction center protein (Aro et al. 1993; Melis 1999; Yokthongwattana and Melis 2006). In the vicinity of photosystem I (PSI), superoxide anion (O_2^-) can be generated by molecular oxygen intercepting electron from reduced ferredoxin. O_2^- can further be metabolized to hydrogen peroxide (H_2O_2) and/or hydroxyl radical (OH•) (Niyogi 1999). These latter ROS species generated at the acceptor side of the PSI can cause damage to key enzymes of the CO_2 assimilation pathway and to chloroplast membrane lipids.

Throughout evolution, oxygenic photosynthetic organisms have not been able to prevent these photo-oxidative damages from occurring. Nevertheless, to alleviate the adverse effect of the excessive irradiance, photosynthetic organisms have evolved photoprotective mechanisms, which range from molecular to the whole plant level (Niyogi 1999). Additionally, plants have also evolved a repair mechanism by which they rectify the apparently unavoidable PSII photodamage. There is interplay between the processes of photoprotection, photodamage and repair. Whenever the rates of photo-oxidative damage exceed the capacity of photoprotection and of the repair mechanism, then the damaged PSII reaction centers accumulate in the thylakoid membrane. This condition is known as ‘photoinhibition’ of photosynthesis, which is manifested as an overall decline in the rate of photosynthesis (Kok 1956; Powles 1984; Long et al. 1994). In addition to light, other environmental stress factors that lead to an imbalance in the photosynthetic reactions can also elicit photoinhibition, even under moderate light intensities. Such conditions include drought, chilling or freezing temperature and heat stress (Powles 1984; Havaux 1992; Król et al. 1997).

Photoprotection and photosystem II repair process

Photoprotection is the term defined for the plant's overall preventive mechanism against the harmful effect of high light. At the molecular level, photoprotection includes synthesis of antioxidant molecules and enzymes, nonphotochemical quenching (NPQ) of excessive excitation energy and modification of photosynthetic machineries to optimize photon absorption and utilization (Niyogi, 1999). Synthesis of antioxidant enzymes, such as superoxide dismutase (SOD), ascorbate peroxidase (APX) and 2-Cys peroxiredoxin (2-CP), is enhanced under irradiance stress. In addition to these antioxidant enzymes, plants also accumulate several antioxidant molecules, including hydrophobic molecules like carotenoids and tocopherals, and water-soluble compounds such as ascorbate, glutathione, etc. NPQ is a mechanism that quenches the excitation from singlet-excited chlorophyll and safely dissipates at heat before the energy is transferred to O_2 (Niyogi, 1999; 2000; Horton and Ruban 2005).

Although the plants employ protective mechanisms to prevent the drastic consequence from irradiance stress, photo-oxidative damage, particularly to the PSII, can still take place. The PSII photodamage is an inevitable process that can occur at any light intensity but is accelerated under excessive irradiance. One of the intriguing facts regarding the nature of PSII photoinactivation by excessive light is that only the D1 reaction center protein undergoes photodamage while the remaining subunits are unaffected (Aro et al. 1993; Melis 1999). For survival, plants have evolved the PSII repair mechanism to regenerate active complexes from the ones that are damaged. The PSII repair process, of which the damaged D1 protein is selectively degraded and replaced with the de novo synthesized copy, therefore, is an essential biochemical process in plant for maintaining photosynthetic activity. The repair process is in continuous operation under normal and adverse photosynthesis conditions and affords chloroplast recovery from photodamage. The term 'photosystem II damage and repair cycle' has been established for this naturally occurring phenomenon in all oxygenic-evolving organisms (Aro et al. 1993; Melis 1999; Yokthongwattana and Melis 2006). A temporal and spatial sequence of events in the PSII repair process includes: i) protection and stabilization of the inactive PSII, ii) partial disassembly of the damaged PSII holocomplex, iii) biodegradation of inactive D1 protein by specific proteases, iv) biosynthesis, reinsertion of the newly active D1 into the PSII core complex, v) reassembly of fully active PSII and its incorporation in the grana partition. These molecular events are the broad phenomenon accepted by scientists in the field. However, detail mechanisms in each step of the repair process have not been fully

elucidated (for in-depth reviews regarding the PSII damage and repair cycle, please see Yokthongwattana and Melis 2006; Yokthongwattana et al. 2009).

Roles of molecular chaperones in irradiance stress response

The presented literature review so far only summarizes the currently known processes of plant responses toward high-light stress. Although most of the responses described above seem to be conserved among different photosynthetic organisms, yet, many plant species exhibit different level of tolerance toward irradiance stress. Some plants can sustain extreme irradiance very well while others are shade-obligated. Obviously, a lot of missing information is still waiting to be uncovered. A group of proteins called heat shock protein is commonly known for their involvement in stress responses, includeing irradiance stress. The first evidence supporting the active role of molecular chaperones during plant adaption to irradiance stress came from the work from Michael Schroda and his colleagues in Germany. Using *C. reinhardtii* as a model, this group of scientists discovered that down-regulation of a chloroplast-localized heat-shock protein 70 (HSP70B) by antisense technique makes the transformants more susceptible to photo-oxidative damage than wild type (Schroda et al. 1999). On the contrary, the transformants overexpressing such protein are more resistant to high light compared to the wild type counterpart (Schroda et al. 1999). Yokthongwattana et al. (2001) further demonstrated that HSP70B could be part of the PSII repair intermediate complex.

HSP70 is a large protein family found in all living organisms. Although HSP70 chaperones have been reported to carry out a wide range of specialized cellular functions, including the PSII repair process, their predominant role is thought to be for helping renature the unfolded or misfolded proteins during stresses. HSP70A is a well-known cytosolic protein (Müller et al. 1992) believed to function as a typical chaperonin. HSP70E, on the other hand, was identified during the *C. reinhardtii* genome sequencing (Merchant et al. 2007) as an ORF that shares some degree of homology to the HSP70 and HSP110 protein family (Schroda 2004). It is predicted to encode for a cytosolic protein of about 87 kDa, the function of which has not been characterized.

HSP100 or Clp is also a large protein family found in both prokaryotes and eukaryotic organisms (Schirmer et al. 1996). The renowned function of Clp chaperones, especially ClpB, is their ability to dissociate protein aggregates and help them refold (Goloubinoff et al. 1999). In the chloroplast stroma of plants and green algae, ClpC and ClpD are the two homologues of the HSP100 protein family (Zheng et al. 2002). So far, the only reported function of ClpC is believed to facilitate protein import into the chloroplast (Nielsen et al. 1997).

CPN60 or HSP60 is a plastid homologue of bacterial GroEL (Viitanen et al. 1995). It is assumed that CPN60 functions to help refold the denatured proteins, by the same mechanism as that of the famous bacterial GroES/GroEL system (Schroda 2004), of which the primary target could be RubisCO large subunit.

In the literature, the main functions of molecular chaperones are thought to be for assisting protein folding/refolding. However, as molecular chaperones are the housekeeping proteins, they could have many other specialized functions, including translation, protein trafficking, proteolytic cleavage, stabilization of the PSII repair intermediate, etc. To date, direct roles of the molecular chaperones in the acclimation response of plants to irradiance stress have not been reported. This research, therefore, aimed to study the roles of these proteins in plants during the transition from LL⟶HL using *C. reinhardtii* as a model organism.

Experimental Plans and Results

1. Comparative proteomic analysis of *C. reinhardtii* subjected to irradiance stress

As molecular chaperones are important housekeeping proteins usually present in high abundance, changes in their expression pattern are usually found to correlate with stress treatment. We pursue a proteomic analysis of total proteins from *C. reinhardtii* cells grown under optimal condition vs. the one subjected to high-light stress for up to 6 h hoping to see changes (increase) in protein level of certain molecular chaperones.

1.1 Irradiance stress in *C. reinhardtii*

Irradiance stress was imposed on the cells of *C. reinhardtii* by shifting the cultures from LL growth intensity to HL. Under this experimental condition, photo–oxidative damage was manifested as the lowering of the PSII photochemical efficiency (F_v/F_m). The F_v/F_m ratio declined from ~0.85 to a value of ~0.50 within 2 h and was retained at this number during the subsequent 2 to 6 h of HL exposure (Fig. 1). This result affirmed that our HL condition was sufficient to elicit irradiance–stress responses for the subsequent proteomic analysis.

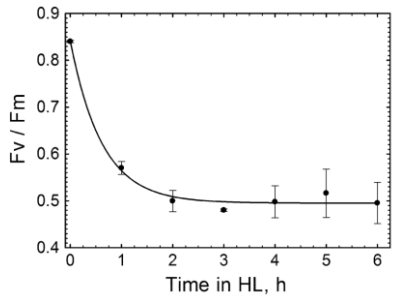

Figure 1. PSII quantum efficiency as determined by the F_v/F_m ratio. *Chlamydomonas* cultures were grown under LL at time 0 and then shifted to HL for 6 h. Cell aliquots were taken at every h and subjected to analysis using PAM fluorometer. Error bars represent SD.

1.2 Proteomic analysis

Total proteins extracted from cell aliquots of *C. reinhardtii*, which include both soluble and membrane polypeptides, were resolved on 2–DE and stained with colloidal Commassie Brilliant Blue G. We opted for the use of colloidal Coomassie as the intensity of the protein spots stained by this type of dye is more consistent and is quantifiable. Although many of the low–abundant proteins might be undetectable by the Coomassie staining, we could already discern a large number of polypeptide spots in this study. Fig. 2 shows representatives of the 2–DE–resolved gels of the samples collected at time 0 (LL), 1.5, 3 and 6 h after HL exposure. Initially a broader range of pH gradient (pH 3–10) was employed for the 1st dimension. However, as most of the proteins scattered between pH 4–7, we therefore used the latter narrow pH range for better resolution. In the 4–7 pH range, we could detect approximately 514 protein spots 'consistently' present in all 3 independent biological replicates of the LL samples (Fig. 2a). Using the same comparative criteria, proteome of *C. reinhardtii* cultures exposed to photoinhibitory condition for 1.5 h contained ~526 protein spots (Fig. 2b). At 3 h after the transition to HL, ~530 proteins could be detected in our study (Fig. 2c). After *C. reinhardtii* was exposed to irradiance stress for 6 h, about 527 total protein spots were consistently observed (Fig. 2d).

Stringent cross comparison of the proteome profiles between that of the LL–grown alga and of the cells harvested at time 1.5, 3, and 6 h after the LL⟶HL shift revealed that totally 99 proteins, at any point in time, showed statistically–significant up– or down–regulation pattern. Those proteins (numbered in Fig. 2) were subjected identification by LC-MS/MS. After mass spectrometry and database search, their identities are presented in Table 1 with the relative spot intensities at different time intervals listed in Table 2 and 3. Table 2 shows the averaged spot densities of proteins that were down–regulated whilst Table 3 presents those that were up–regulated during the 6 h exposure of *C. reinhardtii* to irradiance stress. The italic numbers in Table 2 and in Table 3 signify the time point where the averaged spot intensity of the corresponding proteins became 'statistically significant' different from that of the control LL values.

At 1.5 h after transition from LL to HL, we observed significant down–regulation pattern of 19 proteins (Table 2) while the intensities of 18 spots were enhanced (Table 3). Among the proteins that their expression deviates from the pattern under LL at this time point, we could detect up– and down–regulation of LHC–II proteins, several of which were identified as the same proteins with different p*I* values. It is interesting to note the increasing LHC–II tended to have lower p*I* values than those underexpressed, suggesting that the proteins could undergo

posttranslational modification that results in lowering of the p*I*. Protein phosphorylation is one of such modifications. However, as our data could not provide proof on such modification, we refrain from claiming that phosphorylation is the cause of such lower p*I* values. Besides the light-harvesting proteins, expression of several other proteins involved in metabolic pathways as well as proteins involved in translation and degradation also changed (Table 2 and 3). Of particular remark, we observed enhanced expression of the oxygen evolution enhancer (OEE) proteins. However, as the corresponding spot of this protein had much lower observed M_r than the calculated values, it is most likely that they are degradation fragments of the OEE polypeptides. Several amino acid biosynthesis enzymes were found to be down–regulated in response to HL whereas expressions of proteins involved in carbohydrate metabolism were enhanced. Abundance of two spots corresponding to triose phosphate isomerase and a spot each of phytoene desaturase and ChlI subunit of Mg–chelatase were also found to be elevated at this period.

When the alga was exposed to HL for 3 h, the expressions of 27 proteins were decreased when compared to the LL profile (Table 2), several of which were already found to be down–regulated at time 1.5 h. On the other hand, 30 protein spots showed significant increase in spot densities from the control values, 12 of which were non-redundant with those observed at the time 1.5 h in HL. At this time point, we could still observe up– and down–regulation of the Chl antenna proteins, particularly the minor LHC, as well as the increase in the abundance of the OEE fragments. Proteins involved in cytoskeleton, flagella structure and general cellular metabolism were also down-regulated. A notable up–regulated protein observed after 3 h of HL exposure is the chloroplast–localized heat–shock protein 70 (HSP70B). Expression of HSP70B, at both transcript and protein levels, has been reported to be enhanced under HL (Drzymalla et al. 1996; Schroda et al. 1999; Yokthongwattana et al. 2001). Therefore, the finding that protein level of HSP70B was enhanced after exposure of *C. reinhardtii* to irradiance stress for 3 h can, as well, serve as an internal validation of our experiment. To our surprise was the observation that level of the chaperonin 60 B1 subunit (CPN60) was decreased after 3 h of the LL⟶HL shift. As CPN60 is one of the molecular chaperones that help the denatured proteins to regain their proper conformation during stresses (Schroda 2004), its expression was rather expected to be the opposite.

After prolonged exposure of *C. reinhardtii* cultures to irradiance stress for 6 h, 67 proteins were underexpressed while the level of 29 proteins were elevated (Table 2 and 3). Within the set of down–regulated proteins at this period, 32 spots were not redundant with those found at time 1.5 and 3 h of HL exposure. In contrast, spot# 7530 (phosphoglycerate

kinase) was the only unique protein up–regulated at 6 h of irradiance stress response in *C. reinhardtii*. Of those down-regulated, most are proteins involved in wide range of general cellular processes, such as amino acid and carbohydrate metabolisms, cytoskeleton and cell movement, etc. We also noticed the decline in the amount of the antenna proteins without concomitant increase of other isoforms. This observation suggested that at 6 h of HL exposure, the Chl antenna size may start to be truncated in response to the excessive irradiance. Furthermore, our proteomic analysis (see Table 2) also revealed a remarkable down regulation of several other molecular chaperones beside the CPN60. Such chaperones include HSP70A, HSP70E, and ClpC (HSP100 family).

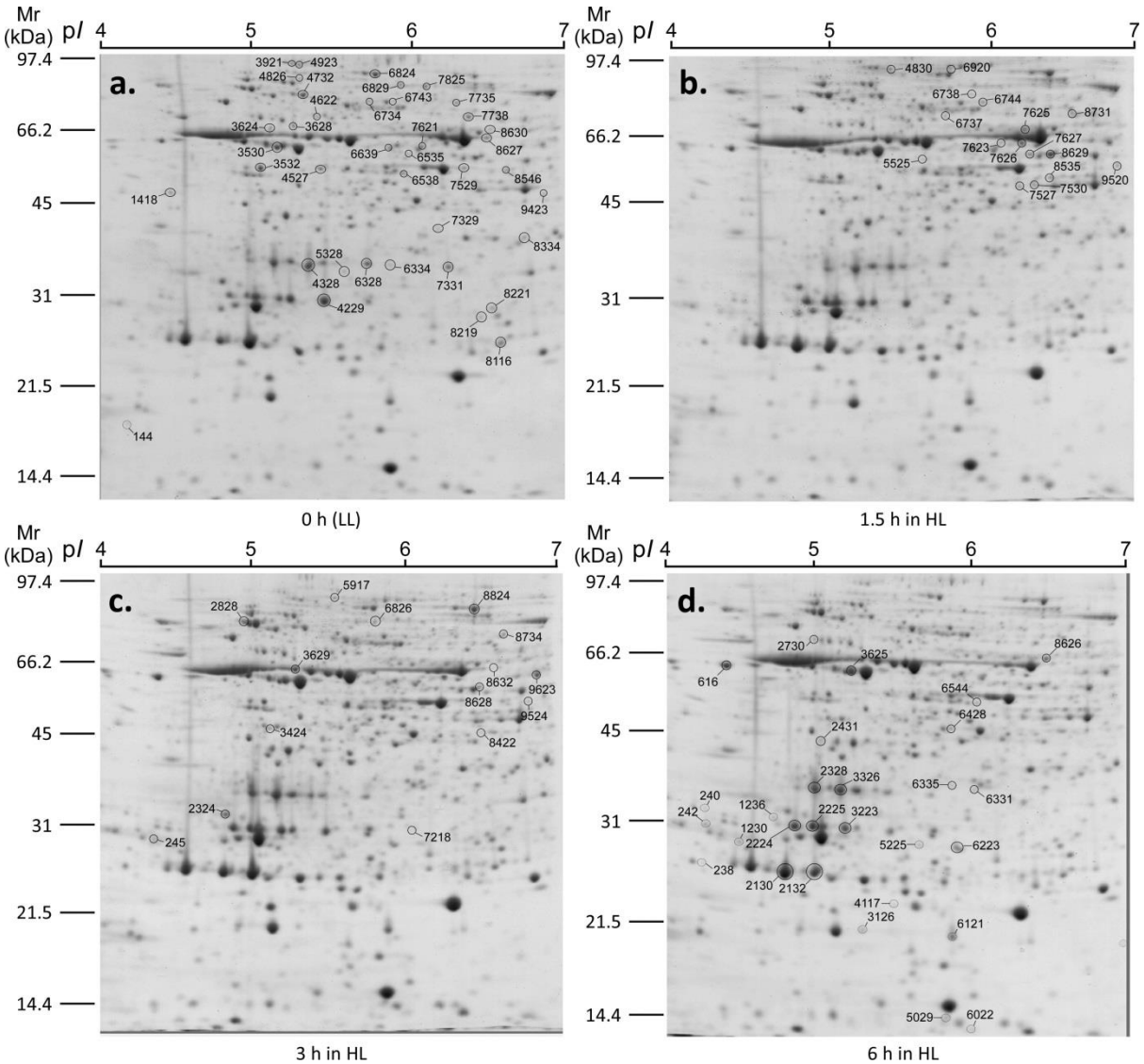

Figure 2. Gel images showing total proteins of *C. reinhardtii* resolved by 2-dimensional gel electrophoresis. Immobilized strips with pH gradient of 4-7 were used for the 1st dimension. The 2nd dimension separation was performed using 12.5% acrylamide gels. Protein spots were visualized by staining with colloidal Coomassie Blue G. Proteomes of LL-grown cells (a), and cells after shifted from LL⟶HL for 1.5 h (b), 3 h (c) and 6 h (d) are presented.

Table 1 List of identified protein spots that the expression level showed significant deviation during the 6 h transition from LL → HL

Spot #	Matched protein	Organism	NCBI Accession #	Observed MW/p*I*	Theoretical MW/p*I*	MOWSE score	# Of matched peptide	% Sequence coverage
Photosynthetic proteins								
240	LI818r-1	*C. reinhardtii*	gil1865771	33.2/4.3	21.7/4.53	58	1	7
242	Stress-related chlorophyll *a*/*b* binding protein 2	*C. reinhardtii*	gil159475924	31.0/4.4	28.2/4.88	227	4	24
1230	Stress-related chlorophyll *a*/*b* binding protein 1	*C. reinhardtii*	gil159476046	28.9/4.6	27.5/4.94	108	2	12
1236	Major light-harvesting complex II protein m3	*C. reinhardtii*	gil159491492	31.9/4.8	27.4/5.68	152	1	6
2130	Major light-harvesting complex II protein m1	*C. reinhardtii*	gil20269804	25.8/4.8	27.6/5.96	271	9	17
2132	Major light-harvesting complex II protein m1	*C. reinhardtii*	gil20269804	25.4/5.1	27.6/5.96	252	8	17
2224	Major light-harvesting complex II protein m3	*C. reinhardtii*	gil159491492	30.9/4.9	27.4/5.68	103	1	6
2228	Chlorophyll *a*-*b* binding protein of LHCII type I	*C. reinhardtii*	gil115827	31.1/5.0	27.0/5.96	73	1	5
2328	Minor chlorophyll *a*-*b* binding protein of PSII	*C. reinhardtii*	gil159475641	35.9/5.1	30.7/5.38	245	3	12
2730	RuBisCO large subunit-binding protein subunit alpha	*C. reinhardtii*	gil2493647	71.6/5.0	62.0/5.57	760	12	23
3126	Oxygen-evolving enhancer protein 2	*C. reinhardtii*	gil131389	19.6/5.3	25.9/9.14	361	8	30
3223	Chlorophyll *a*-*b* binding protein of LHCII type I	*C. reinhardtii*	gil115827	30.5/5.3	27.0/5.96	301	1	4
3326	Minor chlorophyll *a*-*b* binding protein of PSII	*C. reinhardtii*	gil159475641	35.2/5.2	30.7/5.38	182	2	8
4117	Oxygen-evolving enhancer protein 2	*C. reinhardtii*	gil131389	21.7/5.5	25.9/9.14	437	8	35
4328	Chlorophyll *a*/*b* binding protein Lhcb5	*C. incerta*	gil87313239	35.2/5.4	27.6/4.66	54	1	3
5029	Oxygen evolving enhancer protein 3	*C. reinhardtii*	gil159486609	13.5/5.9	21.8/9.58	312	7	25
6022	Photosystem I reaction center subunit XI	*C. reinhardtii*	gil159465747	13.0/6.0	20.4/9.37	53	1	4
6121	Chlorophyll *a*/*b*-binding protein	*C. reinhardtii*	gil19421770	19.1/5.9	23.9/9.41	249	7	35
6328	Chlorophyll *a*-*b* binding protein of PSII	*C. reinhardtii*	gil159478202	35.0/5.8	30.1/6.22	294	7	20
6334	Chlorophyll *a*-*b* binding protein of PSII	*C. reinhardtii*	gil159478202	34.5/5.9	30.1/6.22	93	2	6
7331	Chlorophyll *a*-*b* binding protein of PSII	*C. reinhardtii*	gil159478202	35.5/6.3	30.1/6.22	219	7	25
7529	RuBisCO large subunit	*C. reinhardtii*	gil41179049	55.7/6.4	53.2/6.14	420	10	21
8116	Chlorophyll *a*/*b* binding protein Lhca3	*C. reinhardtii*	gil87313217	26.0/6.6	27.1/8.14	117	2	10
8219	Chlorophyll *a*-*b* binding protein of LHCII	*C. reinhardtii*	gil159478875	29.0/6.5	28.7/7.79	69	2	7
8627	RuBisCO large subunit	*C. reinhardtii*	gil41179049	65.9/6.5	53.2/6.14	471	2	18
Stress proteins								
2828	Heat shock protein 70B	*C. reinhardtii*	gil159476666	83.2/5.0	72.1/5.31	99	2	2
3624	T-complex protein, theta subunit	*C. reinhardtii*	gil159490756	66.4/5.2	58.0/5.16	265	4	8
3921	Heat shock protein 70E	*C. reinhardtii*	gil159475503	93.3/5.3	88.1/5.22	1133	26	28
4622	Chaperonin 60B1	*C. reinhardtii*	gil159486163	70.7/5.5	62.3/6.38	583	6	19
4732	Heat shock protein 70A	*C. reinhardtii*	gil159486599	80.1/5.4	71.5/5.25	1466	30	40
4923	Heat shock protein 70E	*C. reinhardtii*	gil159475503	93.5/5.4	88.1/5.22	663	13	17
6824	Chaperone, Hsp100 family, ClpC-type	*O. lucimarinus*	gil145356586	89.1/5.8	92.7/5.27	517	9	11
8630	Ascorbate peroxidase	*C. reinhardtii*	gil159487873	68.6/6.5	36.0/8.67	174	2	8
Pigment biosynthesis								
3424	Magnesium chelatase subunit chlI	*C. reinhardtii*	gil20137882	47.6/5.2	45.5/6.22	411	9	21

Table 1 continued

Spot #	Matched protein	Organism	NCBI Accession #	Observed MW/p*I*	Theoretical MW/p*I*	MOWSE score	# Of matched peptide	% Sequence coverage
6535	4-Hydroxy-3-methylbut-2-enyl diphosphate reductase	*C. reinhardtii*	gil159486551	58.1/6.0	51.9/6.19	392	7	16
8535	Delta-aminolevulinic acid dehydratase	*C. reinhardtii*	gil159487537	52.3/6.4	43.1/7.72	340	6	20
8632	Phytoene desaturase	*C. reinhardtii*	gil159465297	66.1/6.6	63.0/7.68	106	1	2
Carbohydrate metabolism								
2431	Sedoheptulose-1,7-bisphosphatase	*C. reinhardtii*	gil159467635	43.8/5.1	42.4/8.59	607	15	36
3532	Fructose-1,6-bisphosphatase	*C. reinhardtii*	gil159465323	53.9/5.1	44.9/5.61	86	2	5
3628	Galactose kinase	*C. reinhardtii*	gil159487006	67.7/5.3	55.9/6.17	141	3	5
4229	Ribose-5-phosphate isomerase	*C. reinhardtii*	gil159467673	30.0/5.5	29.0/7.63	95	3	14
5225	Triose phosphate isomerase	*C. reinhardtii*	gil159463610	28.5/5.7	30.4/7.56	272	4	18
6223	Triose phosphate isomerase	*C. reinhardtii*	gil159463610	28.5/6.0	30.4/7.56	540	8	32
6538	Sugar nucleotide epimerase	*C. reinhardtii*	gil159462534	52.4/6.0	43.8/5.78	186	2	6
6428	Phosphoribulokinase	*C. reinhardtii*	gil159471788	46.4/5.9	42.1/8.11	310	6	17
6639	ADP-glucose pyrophosphorylase small subunit	*C. reinhardtii*	gil159467349	59.9/5.9	55.9/8.38	736	12	31
6743	Phosphoglucomutase	*C. reinhardtii*	gil159479834	76.9/6.0	64.8/7.12	238	3	6
7527	Phosphoglycerate kinase	*C. reinhardtii*	gil159482940	49.8/6.2	49.2/8.92	304	6	15
7530	Phosphoglycerate kinase	*C. reinhardtii*	gil1172455	49.8/6.3	49.3/8.84	250	4	11
8731	6-Phosphogluconate dehydrogenase	*C. reinhardtii*	gil159477567	73.1/6.6	61.3/8.35	516	9	20
Amino acid metabolism								
5328	Diaminopimelate epimerase	*C. reinhardtii*	gil159479426	33.8/5.6	34.8/6.95	366	6	21
7738	Acetohydroxyacid dehydratase	*C. reinhardtii*	gil159470063	72.9/6.4	64.8/7.51	335	7	11
8546	LL-Diaminopimelate aminotransferase	*C. reinhardtii*	gil159469820	55.4/6.6	48.3/8.29	763	13	38
8626	Acetohydroxy acid isomeroreductase	*C. reinhardtii*	gil159489328	67.6/6.5	60.6/8.29	75	2	2
8824	Cobalamin-independent methionine synthase	*C. reinhardtii*	gil159489910	89.6/6.5	87.3/5.94	1265	24	29
9520	LL-Diaminopimelate aminotransferase	*C. reinhardtii*	gil159469820	56.2/6.8	48.3/8.29	943	18	36
9623	Serine hydroxymethyltransferase 2	*C. reinhardtii*	gil159487140	63.0/6.7	52.2/6.25	1095	21	44
9524	Agmatine iminohydrolase	*C. reinhardtii*	gil159484436	57.3/6.7	46.1/6.50	173	4	9
Energy metabolism								
3625	ATP synthase CF1 beta subunit	*C. reinhardtii*	gil41179057	60.3/5.3	53.2/5.21	298	5	14
6734	Vacuolar ATP synthase, subunit A	*C. reinhardtii*	gil159480680	76.4/5.8	68.9/5.68	636	13	25
6744	Vacuolar ATP synthase, subunit A	*C. reinhardtii*	gil159480680	76.9/6.0	68.9/5.68	198	4	6
7735	Succinate dehydrogenase subunit A	*C. reinhardtii*	gil159463224	77.8/6.3	69.5/6.25	160	2	5
Signal transduction								
616	Calreticulin 2, calcium-binding protein	*C. reinhardtii*	gil159462862	63.6/4.5	47.4/4.54	384	9	21
1418	Protein phosphatase 2C	*C. reinhardtii*	gil159477373	49.0/4.6	39.1/4.67	201	4	10
8221	4 Ran-like small GTPase	*C. reinhardtii*	gil159467397	30.2/6.5	25.7/6.25	184	4	15
Cytoskeleton/trafficking/cell movement								
3530	Alpha tubulin 1	*C. reinhardtii*	gil159467393	59.9/5.3	50.2/5.01	687	16	34
4830	Flagellar associated protein	*C. reinhardtii*	gil159476808	92.2/5.4	90.9/5.29	61	1	1
6738	*N*-ethylmaleimide sensitive fusion protein	*C. reinhardtii*	gil159480686	79.9/5.9	78.7/5.68	54	1	1
8734	Dynamin-related GTPase	*C. reinhardtii*	gil159485798	78.5/6.6	67.8/6.50	73	1	1
9423	Flagellar associated protein	*C. reinhardtii*	gil159475749	49.2/6.7	41.4/6.34	549	9	28
Transcription/translation								
4527	Eukaryotic initiation factor 4A-like protein	*C. reinhardtii*	gil159466510	53.4/5.5	47.3/5.50	703	14	30

Table 1 continued

Spot #	Matched protein	Organism	NCBI Accession #	Observed MW/p*I*	Theoretical MW/p*I*	MOWSE score	# Of matched peptide	% Sequence coverage
6737	Aspartyl-tRNA synthetase	*C. reinhardtii*	gil159474374	70.2/5.8	60.7/5.61	385	6	11
6920	Elongation factor 2	*C. reinhardtii*	gil159490505	91.9/5.8	95.0/5.63	139	4	4
7621	Subunit of exon junction complex	*C. reinhardtii*	gil159491657	61.0/6.1	49.4/5.77	205	4	8
7625	Chloroplast polyprotein of elongation factor Ts precursor	*C. reinhardtii*	gil53794015	67.2/6.3	109.2/4.53	329	5	5
8334	Acidic ribosomal protein P0	*C. reinhardtii*	gil159477927	34.7/6.1	34.7/6.07	64	1	3
8422	Plastid-specific ribosomal protein 1	*C. reinhardtii*	gil159479306	47.4/6.5	31.9/9.18	412	11	29
Proteins of miscellaneous functions								
2324	14-3-3-Like protein-related protein	*C. reinhardtii*	gil74272601	32.9/4.9	29.7/4.90	114	2	9
3629	Selenium binding protein	*C. reinhardtii*	gil159490794	64.1/5.3	52.5/5.18	504	13	24
6335	Phosphoglycolate phosphatase	*C. reinhardtii*	gil159464681	36.4/5.9	33.5/5.42	48	1	3
6826	Arsenite translocating ATPase-like protein	*C. reinhardtii*	gil159488560	83.1/5.8	54.4/8.68	333	5	11
7329	26S Proteasome regulatory subunit	*C. reinhardtii*	gil159479806	41.5/6.2	37.1/5.75	143	3	12
7623	*S*-Adenosylmethionine synthetase	*C. reinhardtii*	gil159477124	62.4/6.1	43.1/6.03	271	5	15
7626	*S*-Adenosylmethionine synthetase	*C. reinhardtii*	gil159477124	62.7/6.3	43.1/6.03	412	8	17
7627	*S*-Adenosylmethionine synthetase	*C. reinhardtii*	gil159477124	59.3/6.3	43.1/6.03	416	5	11
7825	Putative chloroplast 1-hydroxy-2-methyl-2-(E)-butenyl-4-diphosphate synthase precursor	*C. reinhardtii*	gil61742128	83.8/6.1	75.2/5.76	239	5	6
8628	Isopropylmalate dehydratase, large subunit	*C. reinhardtii*	gil159488260	60.0/6.5	53.6/7.04	385	7	17
8629	*S*-Adenosylmethionine synthetase	*C. reinhardtii*	gil159477124	59.3/6.5	43.1/6.03	1039	23	47
Unknown proteins								
144	Hypothetical protein	*C. reinhardtii*	gil159465102	17.9/4.2	14.2/8.66	61	1	13
238	Putative membrane protein	*C. reinhardtii*	gil159488214	26.6/4.3	30.0/5.02	288	5	20
245	Hypothetical protein	*C. reinhardtii*	gil159475228	29.6/4.5	27.9/4.94	356	5	25
4826	Hypothetical protein CHLREDRAFT_192147	*C. reinhardtii*	gil159477457	88.1/5.4	73.7/5.29	67	1	1
5525	Predicted protein	*C. reinhardtii*	gil159487851	56.7/5.7	53.9/6.36	232	4	8
5917	Hypothetical protein CHLREDRAFT_120875	*C. reinhardtii*	gil159481287	93.8/5.6	12.3/9.17	80	1	9
6331	Predicted protein	*C. reinhardtii*	gil159463656	36.1/6.0	40.1/9.31	201	4	11
6544	Hypothetical protein CHLREDRAFT_132041	*C. reinhardtii*	gil159482705	52.5/6.0	47.0/6.42	144	4	11
6829	Hypothetical protein CHLREDRAFT_82920	*C. reinhardtii*	gil159488381	84.0/6.0	77.2/5.73	188	3	4
7218	Predicted protein	*C. reinhardtii*	gil159470065	30.6/6.1	31.3/8.18	177	4	14

Proteins were tryptic digested and identified by LC-MS/MS as described in the Materials and Methods section. Spot numbers were assigned arbitrarily by the analysis software. MOWSE search scores of 47 or more are considered as significant match

Table 2 Relative spot intensities of *Chlamydomonas reinhardtii* proteins of which the expression levels were down-regulated during the 6 h HL exposure period

Spot #	Protein	Averaged spot density at time following LL → HL shift			
		Control (LL)	1.5 h	3 h	6 h
2132	Major light-harvesting complex II protein m1	15071 ± 3995	*11437 ± 3031*	*11057 ± 3270*	*7105 ± 949*
4527	Eukaryotic initiation factor 4A-like protein	1209 ± 180	*618 ± 87*	*705 ± 133*	*781 ± 125*
5328	Diaminopimelate epimerase	903 ± 113	*742 ± 82*	*662 ± 57*	*542 ± 102*
6334	Chlorophyll *a-b* binding protein of PSII	452 ± 192	*214 ± 85*	*165 ± 119*	*149 ± 38*
6538	Sugar nucleotide epimerase	891 ± 58	*753 ± 30*	*720 ± 59*	*540 ± 80*
7329	26S Proteasome regulatory subunit	1310 ± 206	*872 ± 192*	*814 ± 22*	*793 ± 124*
7331	Chlorophyll *a-b* binding protein of PSII	1856 ± 230	*1127 ± 218*	*804 ± 159*	*594 ± 240*
7623	S-Adenosylmethionine synthetase	916 ± 16	*663 ± 157*	*561 ± 76*	*465 ± 138*
7625	Chloroplast polyprotein of elongation factor Ts precursor	1382 ± 265	*1032 ± 252*	*963 ± 74*	*807 ± 164*
7738	Acetohydroxyacid dehydratase	1632 ± 121	*1242 ± 109*	*1119 ± 136*	*722 ± 142*
8628	Isopropylmalate dehydratase, large subunit	1192 ± 139	*743 ± 58*	*693 ± 25*	*547 ± 58*
8630	Ascorbate peroxidase	648 ± 39	*401 ± 53*	*414 ± 19*	*326 ± 48*
8731	6-Phosphogluconate dehydrogenase	631 ± 108	*516 ± 101*	*451 ± 103*	*325 ± 55*
9524	Agmatine iminohydrolase	718 ± 29	*570 ± 90*	*622 ± 31*	*459 ± 65*
5917	Hypothetical protein CHLREDRAFT_120875	748 ± 49	*653 ± 26*	632 ± 192	*442 ± 34*
6639	ADP-glucose pyrophosphorylase small subunit	1149 ± 217	*906 ± 216*	936 ± 57	*701 ± 86*
6744	Vacuolar ATP synthase, subunit A	771 ± 106	*552 ± 69*	617 ± 57	*389 ± 136*
7627	*S*-Adenosylmethionine synthetase	1159 ± 192	*880 ± 176*	852 ± 230	*663 ± 58*
7735	Succinate dehydrogenase subunit A	917 ± 95	*760 ± 112*	707 ± 105	*554 ± 72*
2324	14-3-3-Like protein-related protein	2742 ± 452	2388 ± 105	*2228 ± 403*	*1759 ± 192*
3530	Alpha tubulin 1	1715 ± 288	1478 ± 279	*1283 ± 272*	*1027 ± 158*
4328	Chlorophyll *a/b* binding protein Lhcb5	3591 ± 671	2334 ± 645	*1874 ± 191*	*1016 ± 299*
4622	Chaperonin 60B1	548 ± 22	514 ± 207	*367 ± 56*	*427 ± 67*
4826	Hypothetical protein CHLREDRAFT_192147	662 ± 41	599 ± 114	*473 ± 42*	*418 ± 34*
6121	Chlorophyll *a/b*-binding protein	3631 ± 647	3313 ± 421	*2908 ± 269*	*1868 ± 305*
6328	Chlorophyll *a-b* binding protein of PSII	2374 ± 774	1856 ± 426	*1407 ± 196*	*834 ± 56*
6826	Arsenite translocating ATPase-like protein	864 ± 24	703 ± 186	*616 ± 60*	*527 ± 89*
6920	Elongation factor 2	457 ± 39	528 ± 131	*343 ± 58*	*332 ± 58*
7626	*S*-Adenosylmethionine synthetase	2112 ± 585	1332 ± 536	*1202 ± 283*	*846 ± 213*
7825	Putative chloroplast 1-hydroxy-2-methyl-2-(E)-butenyl-4-diphosphate synthase	1016 ± 146	689 ± 330	*467 ± 306*	*55 ± 10*
8116	Chlorophyll *a/b* binding protein Lhca3	1919 ± 376	1676 ± 155	*1378 ± 141*	*1200 ± 175*
9423	Flagellar associated protein	839 ± 155	710 ± 59	*517 ± 41*	513 ± 145
144	Hypothetical protein	1344 ± 821	1264 ± 25	1024 ± 245	*612 ± 58*
1418	Protein phosphatase 2C	1310 ± 186	1031 ± 225	827 ± 160	*765 ± 141*
3532	Fructose-1,6-bisphosphatase	2562 ± 540	2068 ± 154	1985 ± 52	*1587 ± 176*
3624	T-complex protein, theta subunit	908 ± 94	739 ± 134	691 ± 103	*607 ± 61*
3628	Galactose kinase	774 ± 151	749 ± 90	742 ± 93	*471 ± 50*
3629	Selenium binding protein	1930 ± 279	1392 ± 320	1601 ± 32	*1039 ± 296*
3921	Heat shock protein 70E	949 ± 40	933 ± 261	798 ± 250	*603 ± 80*
4732	Heat shock protein 70A	2370 ± 133	2627 ± 386	2837 ± 603	*1719 ± 155*
4830	Flagellar associated protein	872 ± 63	734 ± 301	703 ± 175	*284 ± 22*
4923	Heat shock protein 70E	1264 ± 206	1129 ± 204	1213 ± 306	*641 ± 148*
5525	Predicted protein	410 ± 140	343 ± 37	320 ± 6	*188 ± 113*
6022	Photosystem I reaction center subunit XI	1652 ± 298	1487 ± 187	1194 ± 130	*1062 ± 207*
6535	4-Hydroxy-3-methylbut-2-enyl diphosphate reductase	501 ± 81	385 ± 85	338 ± 59	*315 ± 3*

Table 2 continued

Spot #	Protein	Averaged spot density at time following LL → HL shift			
		Control (LL)	1.5 h	3 h	6 h
6734	Vacuolar ATP synthase, subunit A	614 ± 118	571 ± 153	511 ± 25	*370 ± 35*
6737	Aspartyl-tRNA synthetase	469 ± 115	353 ± 78	318 ± 14	*239 ± 29*
6738	*N*-ethylmaleimide sensitive fusion protein	425 ± 55	375 ± 93	351 ± 55	*235 ± 39*
6743	Phosphoglucomutase	442 ± 89	377 ± 112	343 ± 17	*185 ± 62*
6824	Chaperone, Hsp100 family, ClpC-type	2941 ± 135	2344 ± 595	2639 ± 547	*1773 ± 143*
6829	Hypothetical protein CHLREDRAFT_82920	772 ± 53	598 ± 193	676 ± 136	*474 ± 62*
7218	Predicted protein	796 ± 77	589 ± 155	610 ± 111	*528 ± 58*
7527	Phosphoglycerate kinase	971 ± 144	780 ± 129	668 ± 119	*630 ± 46*
7529	RuBisCO large subunit	1116 ± 192	856 ± 103	937 ± 205	*699 ± 80*
7621	Subunit of exon junction complex	866 ± 112	721 ± 230	702 ± 172	*330 ± 70*
8219	Chlorophyll *a*-*b* binding protein of LHCII	1044 ± 128	1163 ± 301	968 ± 233	*639 ± 21*
8221	4 Ran-like small GTPase	1415 ± 234	1249 ± 209	1131 ± 222	*715 ± 197*
8334	Acidic ribosomal protein P0	816 ± 355	424 ± 185	859 ± 372	*337 ± 126*
8535	Delta-aminolevulinic acid dehydratase	950 ± 203	774 ± 96	692 ± 179	*575 ± 21*
8546	LL-Diaminopimelate aminotransferase	980 ± 217	835 ± 167	665 ± 159	*587 ± 108*
8626	Acetohydroxy acid isomeroreductase	1942 ± 83	1612 ± 264	1714 ± 145	*1155 ± 131*
8627	RuBisCO large subunit	1631 ± 210	996 ± 371	1084 ± 443	*567 ± 103*
8629	*S*-Adenosylmethionine synthetase	1764 ± 323	1683 ± 630	1984 ± 202	*837 ± 121*
8734	Dynamin-related GTPase	960 ± 8	861 ± 147	881 ± 131	*516 ± 69*

Averaged spot densities of proteins (3 biological replicates each ± SD) at time 1.5, 3 and 6 h after the transition from LL → HL were subjected to pair-wise *t* test statistical analysis against the respective values of the LL control. The *italicised* values indicates the time points where the expression level of that particular protein was significantly different from the control level. *P* values of all samples were less than 0.05

Table 3 Averaged spot densities of proteins that were up-regulated during transition of *C. reinhardtii* from LL to HL

Spot #	Matched protein	Averaged spot density at time following LL → HL shift			
		Control (LL)	1.5 h	3 h	6 h
238	Putative membrane protein	n/d	*883 ± 281*	*624 ± 78*	*677 ± 197*
242	Stress-related chlorophyll *a*/*b* binding protein 2	n/d	*795 ± 306*	*861 ± 264*	*920 ± 118*
1230	Stress-related chlorophyll *a*/*b* binding protein 1	n/d	*1030 ± 253*	*899 ± 101*	*829 ± 139*
1236	Major light-harvesting complex II protein m3	79 ± 5	*1099 ± 239*	*1002 ± 86*	*953 ± 64*
2130	Major light-harvesting complex II protein m1	5510 ± 1424	*14242 ± 596*	*10195 ± 2322*	*12561 ± 2012*
2224	Major light-harvesting complex II protein m3	2441 ± 695	*4029 ± 97*	*4131 ± 213*	*4316 ± 1081*
2431	Sedoheptulose-1,7-bisphosphatase	n/d	*1108 ± 162*	*1092 ± 202*	*1148 ± 198*
2730	RbcL-binding protein subunit alpha	n/d	*688 ± 145*	*675 ± 111*	*886 ± 187*
3126	Oxygen-evolving enhancer protein 2	693 ± 77	*1400 ± 188*	*1379 ± 53*	*1454 ± 442*
3223	Chlorophyll *a*-*b* binding protein of LHCII type I	2254 ± 439	*4081 ± 509*	*3814 ± 642*	*3499 ± 304*
3424	Magnesium chelatase subunit chlI	n/d	*392 ± 63*	*422 ± 50*	*452 ± 58*
5225	Triose phosphate isomerase	n/d	*751 ± 193*	*728 ± 98*	*871 ± 196*
6223	Triose phosphate isomerase	1441 ± 97	*2455 ± 483*	*2033 ± 251*	*2127 ± 264*
6428	Phosphoribulokinase	n/d	*605 ± 68*	*620 ± 37*	*690 ± 92*
6544	Hypothetical protein CHLREDRAFT_132041	n/d	*688 ± 204*	*689 ± 69*	*449 ± 56*
8422	Plastid-specific ribosomal protein 1	n/d	*431 ± 68*	*477 ± 135*	*437 ± 80*
8632	Phytoene desaturase	n/d	*345 ± 106*	*274 ± 66*	*291 ± 47*
2228	Chlorophyll *a*-*b* binding protein of LHCII type I	2620 ± 453	*4737 ± 611*	3954 ± 508	*5216 ± 633*
9623	Serine hydroxymethyltransferase 2	1325 ± 156	*1645 ± 110*	*1710 ± 178*	1162 ± 306
240	LI818r-1	n/d	n/d	*746 ± 134*	*854 ± 206*
245	Hypothetical protein	n/d	n/d	*968 ± 147*	*949 ± 82*
616	Calreticulin 2, calcium-binding protein	1777 ± 165	2260 ± 248	*2722 ± 367*	*2780 ± 128*
2328	Minor chlorophyll *a*-*b* binding protein of PSII	1920 ± 112	3274 ± 1076	*4790 ± 1157*	*5496 ± 570*
2828	Heat shock protein 70B	731 ± 117	1114 ± 308	*1289 ± 143*	*1515 ± 299*
3625	ATP synthase CF1 beta subunit	2298 ± 554	2568 ± 231	*3110 ± 299*	*3780 ± 385*
4117	Oxygen-evolving enhancer protein 2	n/d	n/d	*946 ± 181*	*956 ± 79*
5029	Oxygen evolving enhancer protein 3	n/d	n/d	*1821 ± 341*	*2506 ± 278*
6331	Predicted protein	n/d	n/d	*630 ± 56*	*721 ± 128*
6335	Phosphoglycolate phosphatase	182 ± 16	212 ± 22	*290 ± 36*	*272 ± 19*
3326	Minor chlorophyll *a*-*b* binding protein of PSII	4576 ± 227	5060 ± 366	*5895 ± 147*	4934 ± 868
8824	Cobalamin-independent methionine synthase	1929 ± 549	2778 ± 1110	*3322 ± 814*	2088 ± 436
7530	Phosphoglycerate kinase	662 ± 70	780 ± 147	1104 ± 334	*1281 ± 80*

Averaged spot densities of proteins (3 biological replicates each ± SD) at time 1.5, 3 and 6 h after the transition from LL → HL were subjected to pair-wise *t* test statistical analysis against the respective values of the LL control. The *italicised* values indicates the time points where the expression level of that particular protein was significantly different from the control level

n/d the protein could not be detected at that time point

P values of all samples were less than 0.05

2. Comparative proteomic analysis between *C. reinhardtii* cells grown under normal condition vs. cells subjected to short-term salinity stress

It has been shown often times in the literature that other types of abiotic stress also exacerbate irradiance stress in plants by causing photoinhtibitory damage at lower threshold. In this part of the work, we collaborate with Dr. Chotika Yokthongwattana at the Department of Biochemistry, Faculty of Science, Kasetsart University to conduct another proteomic study on the effect of salinity stress on *C. reinhardtii* proteins. We expected to see changes in the expression profile of molecular chaperones under NaCl-shock condition.

At first, total proteins of control *C. reinhardtii* culture grown under normal TAP medium and the salt-shocked cells were subjected to 2-DE separation using strips of pH 3–10. However, as more than 80% of the proteins scattered in the middle of the gel, strips with narrower pH gradient range of 4–7 were used for better visibility and resolution. Representative of the 2-DE-based proteome profiles of the control cells is presented in Fig. 3a while that of the salt-shocked samples is illustrated in Fig. 3b. Cross comparison of the proteome profiles between the two sets of samples revealed a large number of differentially-expressed protein spots. As there have already been a lot of proteomic studies reporting on plant proteins that are partially up- or down-regulated under salt stress, we opted for a more stringent criterion of analysis. In this study, the protein spots that their expressions exclusively appeared in one group of samples (either in the control or salt-shocked cells) but not in another group were picked for subsequent identification by tandem mass spectrometry. Even with this strict criterion, we could distinguish more than 100 proteins matched with our screening. Of these, we could elucidate the identities of only 18 spots from the population of proteins that exclusively appeared in *C. reinhardtii* cells grown under normal TAP medium and 99 proteins that are solely discernible in the salt-shocked cells.

Table 4 lists all the 18 proteins that uniquely appeared in the control *Chlamydomonas* cells. Most of the polypeptides in this group are enzymes involved in general metabolic pathways. We found 4 proteins in the group of TCA cycle and energy metabolism including ATP synthase beta (spot #2613) and gamma (#416) subunits and its associated protein (# 9214) as well as isocitrate lyase (#5311). Two spots each of proteins involved in carbohydrate metabolisms (#9209 and 9612) and photosynthesis (#1615 and 2131) were not observed in the salt-shocked cells. There was only one spot each of enzyme in the amino acid and fatty acid metabolism (spot #1022 and 9614, respectively), protein folding (#141), and protein translation (#140). The notable proteins in this group are the telomere-binding proteins (spot #8226, 9207, 9213 in Fig. 3a). The absence of these telomere-binding proteins in the salt-shocked cells may

suggest possible alteration in the chromatin structure under salinity stress condition. Functions of the remaining 3 spots could not be postulated as they were identified as unknown proteins (spot #139, 3915 and 9417).

Of particular remark was the identification of the 99 protein spots that were found only in the salt-shocked but not in the control cells of *C. reinhardtii*. Table 5 shows identities of those proteins as determined by LC–MS/MS, which can be classified into 11 groups based on their cellular functions. Fig. 4 illustrates the proportions of proteins in each group, which include: carbohydrate (11%) and amino acid (12%) metabolisms, metabolism of vitamin and cofactors (4%), metabolism of terpenoids and polyketides (1%), TCA cycle and energy metabolism (10%), photosynthesis (8%), stress-related proteins (~15%), protein translation (13%), protein folding/sorting/degradation (9%), protein of miscellaneous functions (7%) and unknown proteins (10%). Among the 99 proteins, 11 of which are enzymes involved in carbohydrate metabolism. We found 3 spots (#8714, 9709, 9710) matched with splice variant of PEP carboxykinase enzymes, 2 each of phosphoribulokinase (#6218, 7522) and glyceraldehyde-3-phosphate dehydrogenase (#3424, 4426) and 1 spot each of pyruvate dehydrogenase E1 beta subunit (#3425), pyruvate dehydrogenase (#7520), phosphoglycerate kinase (#8518) and succinate-CoA ligase beta chain (#9518).

Twelve proteins that showed exclusive expression in the salt-shocked samples belong to the group of amino acid metabolism. Pyruvate-formate lyase (#8826, 8827, 8829, 8830) and cobalamin-independent methionine synthase (#8822, 8823, 8824) occupy the majority of the protein spots found in this group. Ten polypeptides fall into the group of TCA cycle and energy metabolism, most of which (8 spots) were identified as subunits of ATP synthase enzyme both mitochondrial and chloroplast version (#1417, 1710, 2416, 2729, 3624, 5613, 6619) and its associated protein (#7323). For photosynthetic proteins that appeared only under salinity stress, 6 out of 8 spots were identified as chain A subunit of the Rubisco enzyme (#3621, 3622, 3623, 7620, 7621, 8619) whilst 2 others are LHC-II and a subunit of cytochrome b6f complex (#2221 and 5015, respectively). We also found specific appearance of membrane AAA-metalloprotease (#3825, 3827), chloroplast membrane translocon 7 (#3816, 3817), cyclophilin-type peptidyl-prolyl cis-trans isomerase (#2415, 5424), and one spot each of protein disulfide isomerase (#1621), translocon component Tic40-related protein (#2611) and ubiquitin conjugating enzyme E2 (#2017) in the salt-shocked cells of *C. reinhardtii*.

The two largest groups of proteins that their corresponding spots could only be discerned in the short-term exposure of *Chlamydomonas* to 300 mM NaCl are protein translation and stress-related proteins (Table 5). Protein spots distinguished as translation machineries

including ribosomal proteins (#2217, 7421, 8220, 9416), initiation (#2126, 2519, 8419) and elongation (#4822, 4823, 4824, 7626) factors occupy the majority population in the former group. To our surprise was the finding that in the group of stress proteins, 11 out of 14 spots could be identified as **heat-shock proteins** or **molecular chaperones**. We detected three spots corresponding to HSP90A (#3813, 3814, 3815), four spots to HSP90C (#3818, 3819, 3820, 4825), two spots matched with chaperonin 60C (#5720, 5721), one spot each of chaperonin 60A and HSP70A (#3715 and 4819, respectively). Three other protein spots in the group of stress-related proteins are antioxidant enzyme ascorbate peroxidase (#5321, 6329) and NADPH dependent thioredoxin reductase (#4429). The remaining 22 protein spots exclusively expressed in the salt-shocked were classified as enzymes involved in metabolism of vitamin, cofactors, terpenoids and polyketides as well as proteins of miscellaneous function and unknown proteins

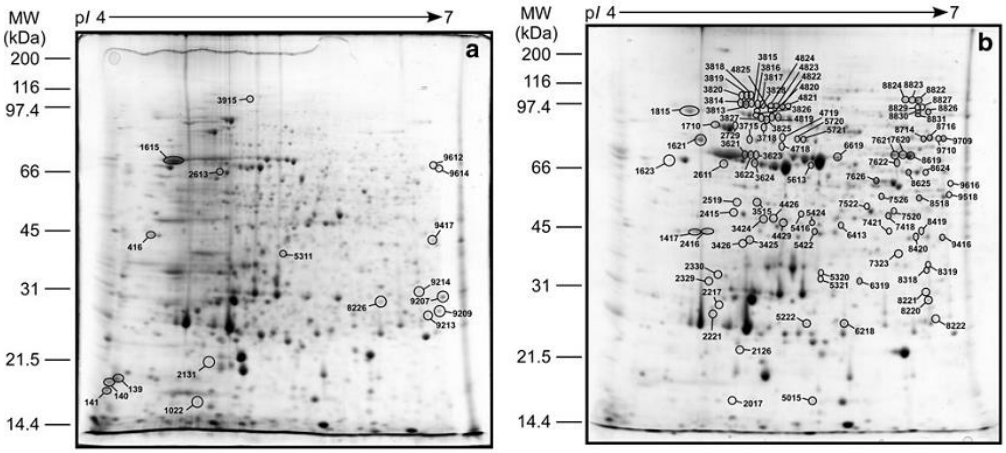

Figure 3. Representative images of 2-DE-resolved protein spot profiles of control *C. reinhardtii* cells grown under normal TAP medium (a) and 2 h salt-shocked cultures (b). Proteins were separated according to their p*I* in the first dimension using 13 cm strip with pH gradient range of 4–7. Separations in the 2nd dimension were carried out using standard SDS-PAGE with 12.5% acrylamide gels. Protein spots were visualized by staining with colloidal Coomassie blue G. Numbered spots correspond to the identified spot # in Table 1 and 2.

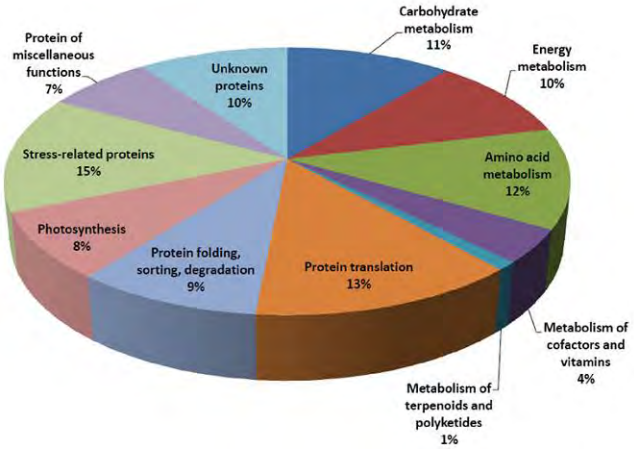

Figure 4. A pie chart showing relative proportions of individual functional groups of the salt-specific proteins from Table 5. The percentage values were rounded to the nearest integer by the computer software.

Table 4. List of identified protein spots that are solely detectable in the cells of *C. reinhardtii* grown in TAP medium but not present in the proteome of the salt-shock cultures.

Spot #	Identified as	NCBI accession #	Organism	Observed MW (kDa)/p*I*	Theoretical MW (kDa)/p*I*	Search score	% Sequence coverage
Carbohydrate metabolism							
9209	Phosphoenolpyruvate carboxykinase	gil74272695	*C. incerta*	27.1/7.0	24.5/8.65	70	4
9612	Dihydrolipoamide dehydrogenase	gil159463380	*C. reinhardtii*	68.4/7.0	60.1/8.73	103	4
Amino acid metabolism							
1022	Homocysteine methyltransferase	gil3334258	*C. reinhardtii*	18.0/4.9	87.2/6.02	80	1
Fatty acid metabolism							
9614	Biotin carboxylase, acetyl-CoA carboxylase component	gil159488652	*C. reinhardtii*	67.7/7.0	52.3/8.96	222	9
TCA cycle and energy metabolism							
416	ATP synthase, gamma subunit	gil228698	*C. reinhardtii*	44.1/4.6	39.1/9.08	150	6
2613	Mitochondrial ATP synthase beta subunit	gil159466892	*C. reinhardtii*	65.8/5.1	62.0/5.00	241	8
5311	Isocitrate lyase	gil619932	*C. reinhardtii*	39.5/5.7	45.8/5.78	73	2
9214	Mitochondrial ATP synthase-associated 31.2-kDa protein	gil159470863	*C. reinhardtii*	30.7/6.9	34.1/6.86	77	3
Photosynthesis							
1615	Rubisco, chain A	gil16975080	*C. reinhardtii*	70.7/4.8	53.1/6.04	174	10
2131	Light-harvesting complex protein I-20	gil18125	*C. reinhardtii*	21.3/5.0	23.5/7.98	63	4
Protein folding, sorting, degradation							
141	Peptidyl-prolyl cis–trans isomerase, cyclophilin-type	gil159484660	*C. reinhardtii*	19.1/4.0	18.6/7.66	48	6
Chromatin structure							
8226	G strand-binding protein 1/telomere-binding protein	gil74272657	*C. incerta*	29.6/6.5	24.5/6.78	132	7
9207	G strand-binding protein 1/telomere-binding protein	gil74272657	*C. incerta*	29.6/7.0	24.5/6.78	393	20
9213	G strand-binding protein 1/telomere-binding protein	gil74272657	*C. incerta*	26.6/6.9	24.5/6.78	212	9
Protein translation							
140	Ribosomal protein L12	gil159477751	*C. reinhardtii*	19.7/4.0	17.8/9.19	222	25
Unknown proteins							
139	Predicted protein	gil159463270	*C. reinhardtii*	20.2/4.0	20.7/5.10	129	13
3915	Predicted protein	gil159471910	*C. reinhardtii*	103.7/5.6	67.6/6.41	156	4
9417	Predicted protein	gil159487124	*C. reinhardtii*	43.7/7.0	31.0/8.50	65	3

Spots were resolved by 2-DE and identified by LC–MS/MS. Observed M_r and p*I* were calculated while the spot numbers were arbitrarily assigned by the PDQuest™ software. Mascot search score beyond 46 is considered as significant match. The identified proteins are listed according to their functional relevance

Table 5. List of proteins exclusively present in the 2 h salt-shocked cells but not in the control cultures of *C. reinhardtii*

Spot #	Protein	NCBI accession #	Organism	Observed M_r (kDa)/p*I*	Theoretical MW (kDa)/p*I*	Search score	% Sequence coverage
Carbohydrate metabolism							
3424	Glyceraldehyde-3-phosphate dehydrogenase	gil159463282	*C. reinhardtii*	48.3/5.3	40.5/9.17	290	17
3425	Pyruvate dehydrogenase E1 beta subunit	gil159482300	*C. reinhardtii*	41.9/5.2	38.5/5.53	500	23
4426	Chloroplast glyceraldehyde-3-phosphate dehydrogenase	gil74272659	*C. incerta*	48.0/5.4	40.0/9.08	207	10
6218	Phosphoribulokinase	gil159471788	*C. reinhardtii*	25.3/5.9	42.1/8.11	108	3
7520	Pyruvate dehydrogenase	gil15223294	*A. thaliana*	50.5/6.3	47.6/7.16	67	2
7522	Phosphoribulokinase	gil159471788	*C. reinhardtii*	51.5/6.1	42.1/8.11	316	17
8518	Phosphoglycerate kinase	gil1172455	*C. reinhardtii*	55.0/6.5	49.3/8.84	358	15
8714	Phosphoenolpyruvate carboxykinase, splice variant	gil159473683	*C. reinhardtii*	78.8/6.6	62.4/6.23	471	17
9518	Succinate-CoA ligase beta chain	gil159466790	*C. reinhardtii*	54.9/6.9	44.7/8.10	313	14
9709	Phosphoenolpyruvate carboxykinase, splice variant	gil159473683	*C. reinhardtii*	77.9/6.9	62.4/6.23	506	23
9710	Phosphoenolpyruvate carboxykinase, splice variant	gil159473683	*C. reinhardtii*	78.0/6.8	62.4/6.23	493	19
Amino acid metabolism							
7418	Glutamine synthetase	gil159469782	*C. reinhardtii*	48.7/6.3	41.7/7.14	368	22
7622	Acetolactate synthase, small subunit	gil159484278	*C. reinhardtii*	68.0/6.3	52.8/8.90	105	6
8625	Argininosuccinate synthase	gil159477301	*C. reinhardtii*	62.9/6.4	49.2/8.41	382	17
8716	Acetohydroxyacid dehydratase	gil159470063	*C. reinhardtii*	79.6/6.7	64.7/7.51	228	9
8822	Cobalamin-independent methionine synthase	gil159489910	*C. reinhardtii*	100.2/6.7	87.3/5.94	689	16
8823	Cobalamin-independent methionine synthase	gil159489910	*C. reinhardtii*	100.4/6.5	87.3/5.94	540	11
8824	Cobalamin-independent methionine synthase	gil159489910	*C. reinhardtii*	100.7/6.4	87.3/5.94	628	16
8826	Pyruvate–formate lyase	gil92084842	*C. reinhardtii*	93.3/6.7	93.7/6.40	512	12
8827	Pyruvate–formate lyase	gil159462978	*C. reinhardtii*	95.8/6.6	91.4/6.49	306	7
8829	Pyruvate–formate lyase	gil159462978	*C. reinhardtii*	96.1/6.6	91.4/6.49	278	7
8830	Pyruvate–formate lyase	gil159462978	*C. reinhardtii*	93.7/6.6	91.4/6.49	434	11
9616	Cystathionine gamma synthase	gil159475262	*C. reinhardtii*	59.3/6.9	51.1/7.28	90	2
Metabolism of vitamins and cofactors							
3426	Gamma glutamyl hydrolase	gil159476168	*C. reinhardtii*	41.1/5.2	41.4/5.34	210	10
3515	Magnesium chelatase subunit chlI	gil20137882	*C. reinhardtii*	53.0/5.3	45.5/6.22	463	22
5422	Thiazole biosynthetic enzyme	gil159481205	*C. reinhardtii*	44.8/5.7	37.0/6.72	112	7
6413	3,8-Divinyl protochlorophyllide *a* 8-vinyl reductase	gil159463876	*C. reinhardtii*	46.1/5.9	44.8/9.01	627	26
Metabolism of terpenoids and polyketides							
8831	1-Deoxy-D-xylulose-5-phosphate synthase	gil4185881	*C. reinhardtii*	91.4/6.5	79.3/7.07	375	9
TCA cycle and energy metabolism							
1417	Chloroplast ATP synthase, gamma chain	gil159476472	*C. reinhardtii*	44.0/4.9	39.1/9.08	336	18
1710	Mitochondrial ATP synthase, beta subunit	gil159466892	*C. reinhardtii*	84.2/5.0	62.0/4.99	783	28
2416	Chloroplast ATP synthase, gamma chain	gil159476472	*C. reinhardtii*	44.1/5.0	39.1/9.08	551	30
2729	Mitochondrial ATP synthase, beta subunit	gil159466892	*C. reinhardtii*	84.6/5.1	62.0/4.99	205	6
3624	ATP synthase CF1, beta subunit	gil41179057	*C. reinhardtii*	67.4/5.3	53.2/5.21	516	19
5222	Soluble inorganic pyrophosphatase	gil159473581	*C. reinhardtii*	25.1/5.6	22.4/5.49	108	13
5613	ATP synthase CF1, beta subunit	gil41179057	*C. reinhardtii*	66.8/5.7	53.2/5.21	390	16
6619	ATP synthase CF1, alpha subunit	gil41179050	*C. reinhardtii*	70.5/5.9	54.8/5.44	531	21

Table 5. continued

Spot #	Protein	NCBI accession #	Organism	Observed M_r (kDa)/p*I*	Theoretical MW (kDa)/p*I*	Search score	% Sequence coverage
7323	Mitochondrial ATP synthase-associated 31.2-kDa protein	gil159470863	*C. reinhardtii*	38.2/6.4	34.1/6.86	369	23
7526	NADP-malate dehydrogenase	gil159477375	*C. reinhardtii*	54.7/6.2	45.3/8.04	458	19
Photosynthesis							
2221	Major light-harvesting complex II protein m1	gil20269804	*C. reinhardtii*	26.9/4.9	27.6/5.96	69	4
3621	Rubisco, chain A	gil16975080	*C. reinhardtii*	70.4/5.2	53.0/6.04	473	17
3622	Rubisco, chain A	gil16975080	*C. reinhardtii*	70.6/5.2	53.0/6.04	450	14
3623	Rubisco, chain A	gil16975080	*C. reinhardtii*	70.9/5.3	53.0/6.04	531	18
5015	Cytochrome b_6f chain C	gil40889430	*C. reinhardtii*	18.6/5.6	13.9/5.74	97	12
7620	Rubisco, chain A	gil16975080	*C. reinhardtii*	71.1/6.4	53.1/6.04	441	16
7621	Rubisco, chain A	gil16975080	*C. reinhardtii*	70.9/6.3	53.1/6.04	508	17
8619	Rubisco, chain A	gil16975080	*C. reinhardtii*	70.9/6.5	53.1/6.04	494	17
Protein folding, sorting, degradation							
1621	Protein disulfide isomerase 1	gil159487489	*C. reinhardtii*	76.5/4.8	58.4/4.80	1,130	36
2017	Ubiquitin conjugating enzyme E2	gil121077798	*V. carteri*	18.5/5.1	17.0/5.04	67	10
2415	Peptidyl-prolyl cis–trans isomerase, cyclophilin-type	gil159467709	*C. reinhardtii*	49.9/5.1	44.8/5.37	283	15
2611	Translocon component Tic40-related protein	gil159465627	*C. reinhardtii*	66.9/5.0	50.0/5.61	434	20
3816	Chloroplast membrane translocon 7	gil159490640	*C. reinhardtii*	97.9/5.3	87.7/5.55	290	7
3817	Chloroplast membrane translocon 7	gil159490640	*C. reinhardtii*	97.7/5.3	87.7/5.55	256	8
3825	Membrane AAA-metalloprotease	gil159465357	*C. reinhardtii*	88.8/5.3	77.7/5.70	429	12
3827	Membrane AAA-metalloprotease	gil159465357	*C. reinhardtii*	89.3/5.3	77.7/5.70	722	20
5424	Peptidyl-prolyl cis–trans isomerase, cyclophilin-type	gil159466422	*C. reinhardtii*	47.0/5.7	42.3/5.69	346	15
Protein translation							
2126	Eukaryotic initiation factor	gil159483583	*C. reinhardtii*	22.4/5.2	18.2/4.97	130	19
2217	Plastid ribosomal protein L3	gil159485314	*C. reinhardtii*	28.6/5.0	27.9/10.26	136	10
2519	Eukaryotic initiation factor	gil159482426	*C. reinhardtii*	53.0/5.1	37.7/4.96	212	12
4822	Chloroplast elongation factor G	gil159487669	*C. reinhardtii*	97.0/5.4	79.9/5.23	767	19
4823	Chloroplast elongation factor G	gil159487669	*C. reinhardtii*	97.8/5.4	79.9/5.23	480	13
4824	Chloroplast elongation factor G	gil159487669	*C. reinhardtii*	97.8/5.4	79.9/5.23	255	8
5320	Heterogeneous nuclear ribonucleoprotein	gil159486121	*C. reinhardtii*	34.2/5.7	31.3/5.79	165	10
7421	Acidic ribosomal protein P0	gil159477927	*C. reinhardtii*	44.0/6.3	34.6/6.07	260	15
7626	Elongation factor Tu	gil226818	*C. reinhardtii*	60.0/6.2	45.7/5.84	242	9
8220	Plastid-specific ribosomal protein 1	gil159479306	*C. reinhardtii*	29.5/6.6	31.9/9.18	501	29
8221	Ran-like small GTPase	gil159467397	*C. reinhardtii*	30.1/6.6	25.7/6.24	252	21
8419	Eukaryotic initiation factor	gil159470237	*C. reinhardtii*	44.0/6.6	36.8/6.01	73	4
9416	Acidic ribosomal protein P0	gil159477927	*C. reinhardtii*	42.8/6.8	34.6/6.07	466	28
Stress-related proteins							
3715	Chaperonin 60A	gil159491478	*C. reinhardtii*	78.0/5.2	61.9/5.49	944	31
3813	Heat-shock protein 90A	gil159474294	*C. reinhardtii*	97.9/5.2	81.0/4.99	643	17
3814	Heat-shock protein 90A	gil159474294	*C. reinhardtii*	97.7/5.2	81.0/4.99	643	14
3815	Heat-shock protein 90A	gil159474294	*C. reinhardtii*	98.2/5.2	81.0/4.99	281	7
3818	Heat-shock protein 90C	gil159490014	*C. reinhardtii*	102.6/5.2	89.5/5.24	574	12
3819	Heat-shock protein 90C	gil159490014	*C. reinhardtii*	103.0/5.2	89.5/5.24	743	15
3820	Heat-shock protein 90C	gil159490014	*C. reinhardtii*	102.7/5.2	89.5/5.24	765	17

Table 5. continued

Spot #	Protein	NCBI accession #	Organism	Observed M_r (kDa)/p*I*	Theoretical MW (kDa)/p*I*	Search score	% Sequence coverage
4429	NADPH-dependent thioredoxin reductase	gil159488145	*C. reinhardtii*	46.9/5.5	37.0/5.26	241	14
4819	Heat-shock protein 70A	gil159486599	*C. reinhardtii*	90.9/5.4	71.5/5.25	980	30
4825	Heat-shock protein 90C	gil159490014	*C. reinhardtii*	95.2/5.4	89.5/5.24	134	3
5321	L-Ascorbate peroxidase	gil159488379	*C. reinhardtii*	32.8/5.7	36.5/9.23	149	7
5720	Chaperonin 60C	gil159466312	*C. reinhardtii*	79.4/5.6	57.2/5.40	482	18
5721	Chaperonin 60C	gil159466312	*C. reinhardtii*	79.3/5.6	57.2/5.40	530	18
6319	L-Ascorbate peroxidase	gil159488379	*C. reinhardtii*	32.7/6.0	36.5/9.23	208	10
Protein of miscellaneous functions							
1815	Binding protein 1	gil159487349	*C. reinhardtii*	91.7/4.8	72.7/4.99	597	14
2330	14-3-3-Like protein-related protein	gil74272601	*C. incerta*	34.2/5.0	29.7/4.90	65	4
3826	Binding protein 1	gil159487349	*C. reinhardtii*	92.8/5.3	72.7/4.99	73	1
4719	Iron–sulfur cluster assembly protein	gil159485362	*C. reinhardtii*	79.8/5.4	57.2/9.16	136	4
5416	Zygote-specific Zys3-like protein	gil124484343	*C. reinhardtii*	49.7/5.6	40.4/5.42	228	9
8318	Prohibitin	gil159477687	*C. reinhardtii*	34.8/6.6	31.2/6.37	459	33
8420	Adenosinetriphosphatase	gil1334356	*C. reinhardtii*	42.6/6.5	48.8/6.20	119	5
Unknown proteins							
1623	Hypothetical protein CHLREDRAFT_80907	gil159475896	*C. reinhardtii*	68.0/4.6	37.3/4.48	147	7
2329	Hypothetical protein CHLREDRAFT_179251	gil159486539	*C. reinhardtii*	32.6/4.9	33.2/6.08	493	18
3718	Predicted protein	gil159484662	*C. reinhardtii*	84.6/5.3	14.5/7.79	69	9
3828	Predicted protein	gil159472442	*C. reinhardtii*	94.6/5.3	58.6/8.62	224	7
4718	Predicted protein	gil159484464	*C. reinhardtii*	75.5/5.4	45.0/6.55	150	5
4820	Predicted protein	gil159463132	*C. reinhardtii*	90.9/5.4	76.2/5.31	306	6
4821	Predicted protein	gil159485022	*C. reinhardtii*	97.3/5.5	75.3/5.82	211	5
8222	Hypothetical protein CHLREDRAFT_205900	gil159470187	*C. reinhardtii*	26.0/6.7	28.9/8.92	307	18
8319	Hypothetical protein CHLREDRAFT_120516	gil159479888	*C. reinhardtii*	35.8/6.6	30.7/6.95	168	11
8624	Predicted protein	gil159468534	*C. reinhardtii*	63.8/6.6	42.7/6.28	751	37

Isolated proteins were resolved by 2-DE and subsequently identified by LC–MS/MS. Observed M_r and p*I* were calculated while the spot numbers were arbitrarily assigned by the PDQuest™ software. Mascot search score beyond 46 is considered as significant match. The identified spots are listed according to their cellular functions

3. Reverse-genetic approach to study function of CPN60 proteins

In this part of the work, which is the main original research proposal submitted to TRF, we tried to employ a reverse-genetic approach to down-regulate specific genes encoding for molecular chaperones found by the above-mentioned proteomic analyses to be key candidates for playing important roles in stress response. After a lot of attempts made on gene cloning, vector construction, algal transformation and screening, we could only succeed on creating transformants with down-regulated phenotype for *cpn60B1* and *cpn60B2* genes. Therefore, from this point onward, we will only report on the work on the CPN60 proteins.

3.1 Construction of artificial micro RNA vector for knocking down target gene

In order to down-regulate genes in *C. reinhardtii*, artificial microRNA (amiRNA) has been recognized as the most powerful tool. To design amiRNA target sequence for the genes

of interest, we used the web site http://wmd3.weigelworld.org/cgi-bin/webapp.cgi for analysis (Fig. 5).

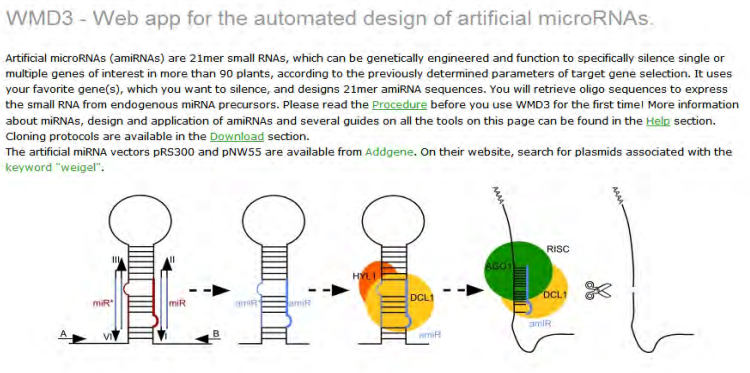

Figure 5. Online tool for designing artificial miRNA target for specific gene of interest.

After analysis, the miRNA target sequences of *cpn60B1* and *cpn60B2* were obtained as followings:

cpn60B1:

amiFor

5'ctagtAGGCCACACTACGGTTTCAAAtctcgctgatcggcaccatgggggtggtggtgatcagcgctaTTTGTAAC CGTAGTGTGGCCTg 3'

amiRev

5'ctagcAGGCCACACTACGGTTACAAAtagcgctgatcaccaccacccccatggtgccgatcagcgagaTTTGAAA CCGTAGTGTGGCCTa 3'

cpn60B2:

amiFor

5'ctagtCTGAGAACGCGCTGATGTTTAtctcgctgatcggcaccatgggggtggtggtgatcagcgctaTAAAGATC AGCGCGTTCTCAGg 3'

amiRev

5'ctagcCTGAGAACGCGCTGATCTTTAtagcgctgatcaccaccacccccatggtgccgatcagcgagaTAAACAT CAGCGCGTTCTCAGa 3'

The above sequences were custom-synthesized by commercial company before being subcloned into pChlamiRNA3int plasmid (obtained from *Chlamydomonas* Resource Center, USA). The protocol for constructing amiRNA vector was the same as that described by Molnar et al. (2009), illustrated in Fig. 6.

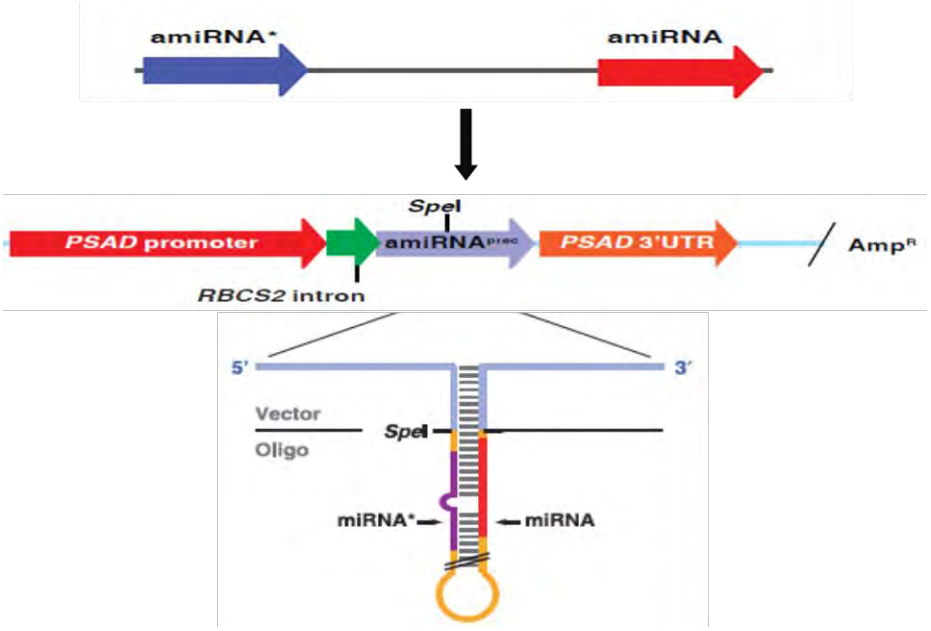

Figure 6. Diagram showing the construction of miRNA vector for transforming *C. reinhardtii*. The synthesized oligonucleotides will be inserted in between *psaD* promoter/rbcs2 intron and *psaD* terminator.

3.2 Transformation and screening for positive transformants

After obtaining all the vector constructs, each of the vectors was transformed into *C. reinhardtii* cells using standard glassbead method. Because every vector also harbored *aphVIII* genes conferring resistance to paromomycin, the transformed cells were spreaded onto agar medium containing 10 µg/ml of the antibiotic drug (TAP+paromomycin). After two weeks, single colonies of the positive transformants started to appear on the plates. Each of the colonies was transferred onto a new plate containing the same concentration of paromomycin to reaffirm their resistance to the drug. Several weeks later, we could obtain all the positive transformants for each of the amiRNA constructs. Figure 7 and 8 show the photographs of positive transformants of *C. reinhardtii* cells for each of the vector constructs after 2-3 generation of subculturing onto a fresh TAP+paromomycin

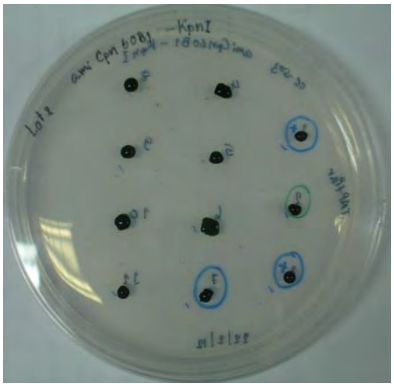

Figure 7. Photograph showing example transformant lines of *C. reinhardtii* after transformation with amiRNA vector for knocking down of *cpn60B1* gene. Positive primary transformants were subcultured onto a fresh TAP+paromomycin plate to validate their resistance to the antibiotic drug for 2-3 generations.

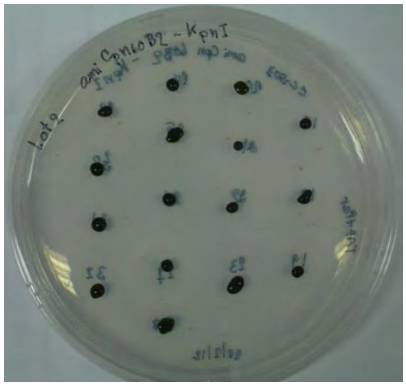

Figure 8. Photograph showing example transformant lines of *C. reinhardtii* after transformation with amiRNA vector for knocking down of *cpn60B2* gene. Positive primary transformants were subcultured onto a fresh TAP+paromomycin plate to validate their resistance to the antibiotic drug for 2-3 generations.

It is typical that a reverse genetic approach to knock down or enhance gene expression by transforming a vector construct into a host cell may not give rise to consistent results. Thus it was important to screen for the transformants that consistently manifest the phenotype according to the transforming vector. To do this, we inoculated each of the transformants into liquid medium and allowed them to grow until reaching logarithmic phase. Cells were harvested and total RNA was extracted using Trizol reagent. Expression of the target gene for each transformant was detected by semiquantitative RT-PCR.

Fig. 9 shows the semiquantitative RT-PCR detecting transcript levels of particular genes of the *cpn60B1* and *cpn60B2* knockdown transformants compared to the untransformed WT. From the figure, *cpn60A* as well as *actin* and *cblp* genes served as quantitative control as the abundance of those genes should not be affected by the knockdown of either *cpn60B1* or *cpn60B2*. As expected, transcript levels of *cpn60A*, *actin* and *cblp* were the same in WT and different knockdown lines of *cpn60B1* and *cpn60B2* (Fig. 9). Transcript level of *cpn60B1* in WT and *cpn60B2*-knockdown were pretty much the same but that of the *cpn60B1*-knockdown was markedly decreased. Transcript level of *cpn60B2*, on the other hands, was decrease in most transformants including that of the *cpn60B1* when compared to WT. It was clear from this figure that we successfully obtained knockdown transformants of either *cpn60B1* or *cpn60B2* or both transcripts.

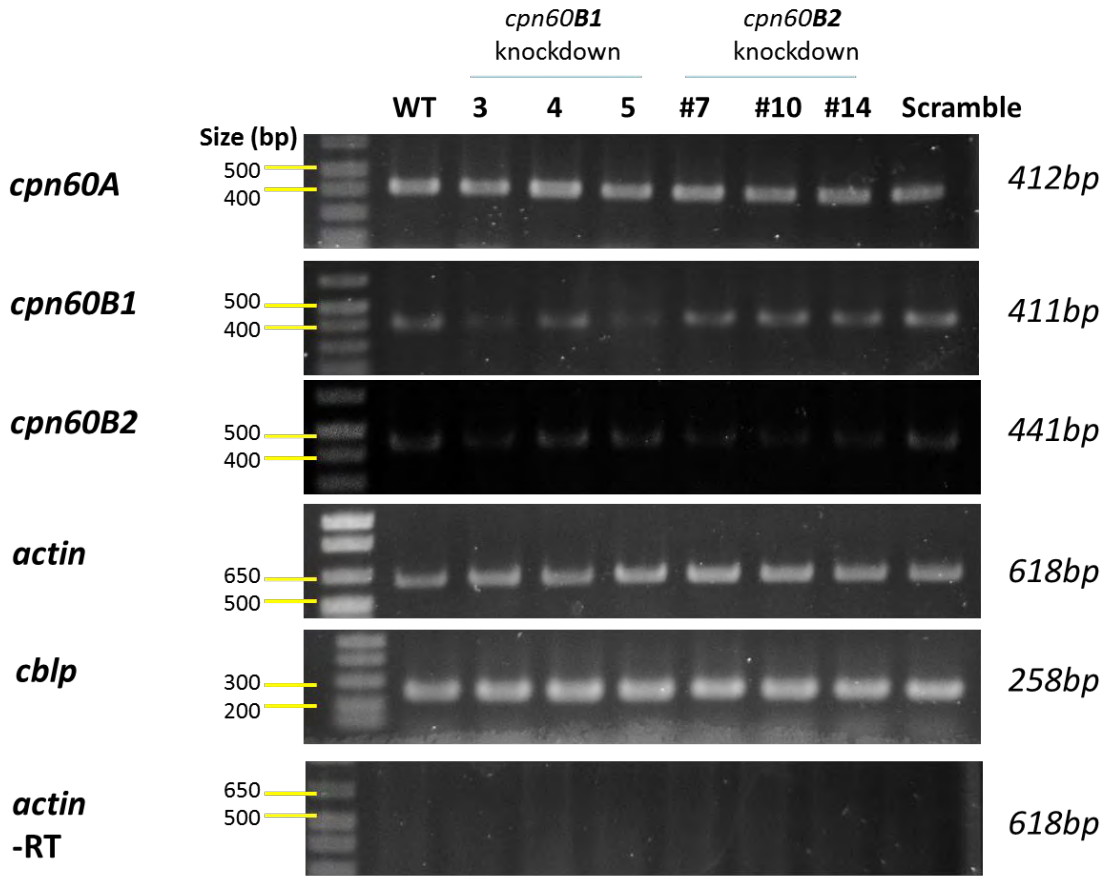

Figure 9. Semiquantitative RT-PCR showing transcript profiles of WT *C. reinhardtii* compared to 3 different lines each of *cpn60B1* and *cpn60B2* knockdown transformants.

3.3 Physiological analyses of the transformants

To explore the function of the chloroplast-localized chaperonin 60 beta subunits, we subjected the above transformants to various abiotic stress treatments and followed their physiological responses. First we grew the algae under optimal low light condition (50 µmol photons m^{-2} s^{-1}) in the TBP medium that only allow phototrophic growth. At the mid-logarithmic phase, the cultures were shifted to grow under high light (900 µmol photons m^{-2} s^{-1}) for 4 h. Cells were collected at different time intervals and subjected to measurement of maximum PSII quantum efficiency (F_v/F_m) using FMS-2 PAM fluorometer (Hansatech Instruments, UK). We expected that the transformants should exhibit more sensitivity to high irradiance and would manifest a more rapidly decline values of F_v/F_m. The overall results in Fig. 10 seems to support our hypothesis as all the transformants seemed to have faster decline kinetic of F_v/F_m values, especially at the first time point, when compared to WT. However, when we performed statistical analysis, these results turned out to have “no statistically significance” between each data set.

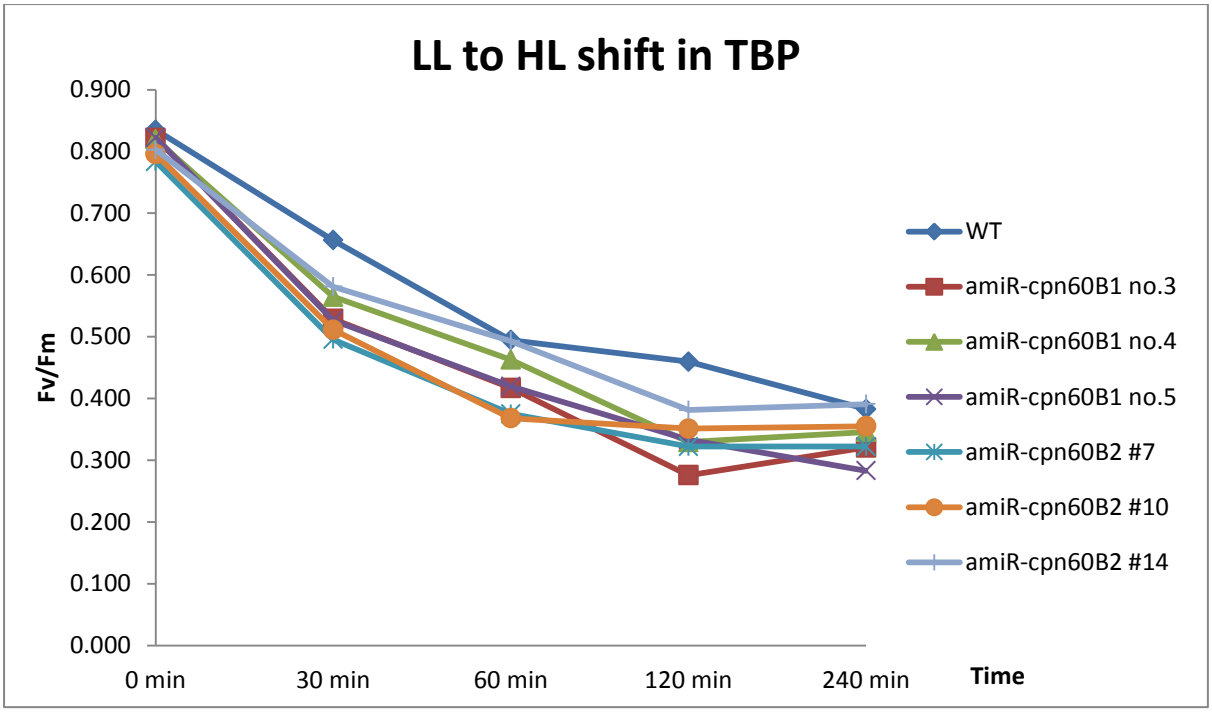

Figure 10. Decline kinetics of maximum PSII quantum efficiency as measured by chlorophyll fluorescence parameter F_v/F_m. *C. reinhardtii* cells (WT vs. different transformants as indicated in the graph) were grown under LL until mid-log phase before shifting to HL for 4 h. Cells were collected at different time intervals and the F_v/F_m values were measured. Each data point derived from 3 replicates.

In addition to the F_v/F_m values, we also measured maximum photosynthesis rates (Pmax), as determined by maximum rate of O_2 evolution per cells per min, of all the algae. The algal cultures were grown in TBP autotrophic growth medium under low light until mid-logarithmic phase before being shifted to high irradiance. Cell aliquots were taken at different time interval from 0 h (LL) to 2 h and were subjected to measurement of O_2 production rate at actinic illumination of 400 µmol photons m^{-2} s^{-1}, which is the saturation intensity. Rate of O_2 evolution at time 0 h for each algal strain was set as 1 and the rates at subsequent time after high light exposure were normalized accordingly. Consistent with the F_v/F_m parameter shown in Fig. 10, the Pmax of all transformants dropped more rapidly than the WT within the first 30 min after exposure to irradiance stress (see Fig. 11). At time longer than 30 min, the excessive light probably caused photodamage beyond any cell can cope and the final Pmax values were similar among all strains tested (Fig. 11). Again, these data did not have significant difference when subjected to statistical analysis.

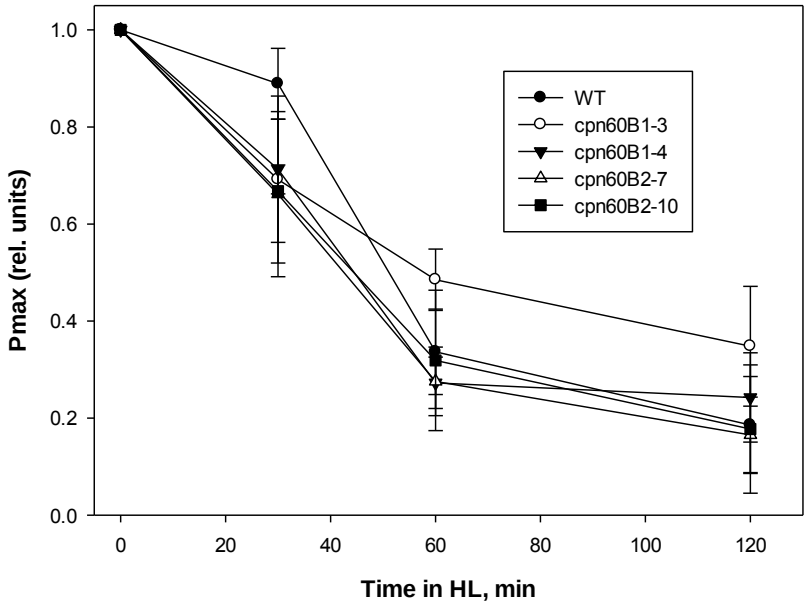

Figure 11. Decline kinetics of maximum photosynthesis rates (Pmax) as measured by maximum rate of O2 evolution per cells per min. *C. reinhardtii* cells (WT vs. different transformants as indicated in the graph) were grown under LL until mid-log phase before shifting to HL for 4 h. Cells were collected at different time intervals and the Pmax values were measured and normalized to the value at time 0 h. Each data point derived from 3 replicates.

We further stressed the algae with salinity shock to see if down regulation of the chaperonin 60B transcripts would result in poorer salt tolerance. All algal cells were grown in TAP mixotrophic growth medium until mid-logarithmic phase. Cells were then collected by gentle centrifugation and growth medium was replaced with TAP + 300 mM NaCl. It must be noted that NaCl concentration of 150 mM was already sufficient to inhibit growth of *C. reinhardtii*. Culture aliquots were removed to perform physiological analyses at different time intervals. Fig. 12 shows kinetics of the F_v/F_m values following the salt shock periods. It is interesting to note that such decline kinetics of the F_v/F_m parameters were virtually the same in all cells tested. This result plausibly suggested that the CPN60 protein may not have active role under salinity stress. This notion is consistent with the proteomic results presented above that the chaperonin was found to be associated with irradiance stress rather than salinity stress. We also performed measurement of the Pmax. However, presence of NaCl at the concentration of 300 mM completely inhibited photosynthesis as we could not detect any O_2 production after growth medium replacement.

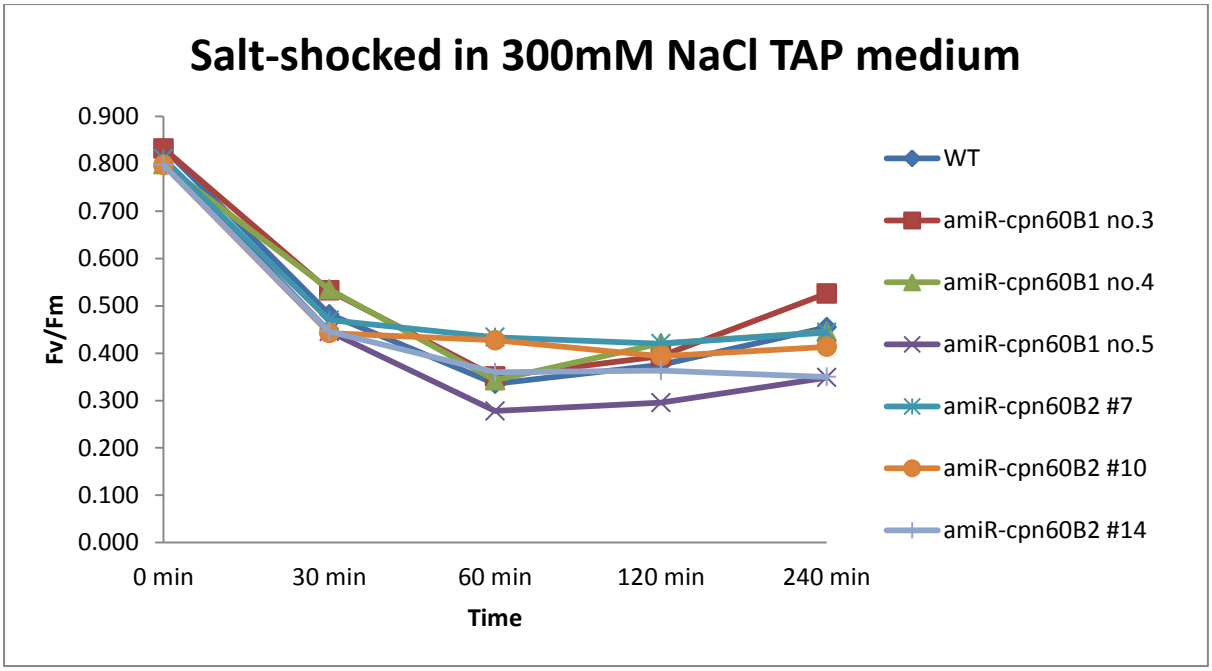

Figure 12. Decline kinetics of maximum PSII quantum efficiency as measured by chlorophyll fluorescence parameter F_v/F_m. *C. reinhardtii* cells (WT vs. different transformants as indicated in the graph) were grown in TAP medium under LL until mid-log phase before the growth medium was replaced with TAP + 300 mM NaCl. Cells were collected at different time intervals and the F_v/F_m values were measured. Each data point derived from 3 replicates.

To further assess the effect of CPN60B down regulation on photosynthetic performance, another set of analysis was conducted to determine the ability of the algal strains to dissipate excessive light energy as heat (termed nonphotochemical quenching or NPQ). The NPQ analysis was performed on cells grown under optimal condition. The method used was standard modulated chlorophyll fluorescence technique using the FMS2 fluorometer with parameters set as described by Thaipratum et al. (2009). Briefly, cuvettes containing ~3 ml of algal cells were dark-adapted for 5 min at room temperature prior to the Chl fluorescence measurements. Fo values were measured during the 5-min dark incubation. At the end of the 5-min dark adaptation, the algal cultures were subjected to a 1 second saturated light pulse to measure Fm and then illuminated with white actinic light (~2,000 µmol photons m^{-2} s^{-1}) for 10 min followed by a 10-min dark recovery period. During the 10-min actinic illumination and dark recovery periods, flashes of the saturated white light (~10,000 µmol photons m^{-2} s^{-1}) were given every 1 min to the cells for determination of Fm′. To avoid interference of state transition quenching, weak illuminations of far-red light (735 nm) were be applied to the cells during the dark adaptation periods before and after the actinic illumination. It was clear from our results in Fig. 13 that down regulation of the *cpn60B1* and *cpn60B2* transcripts did not result in NPQ induction kinetics when compared to wild type and another scramble amiRNA transformant.

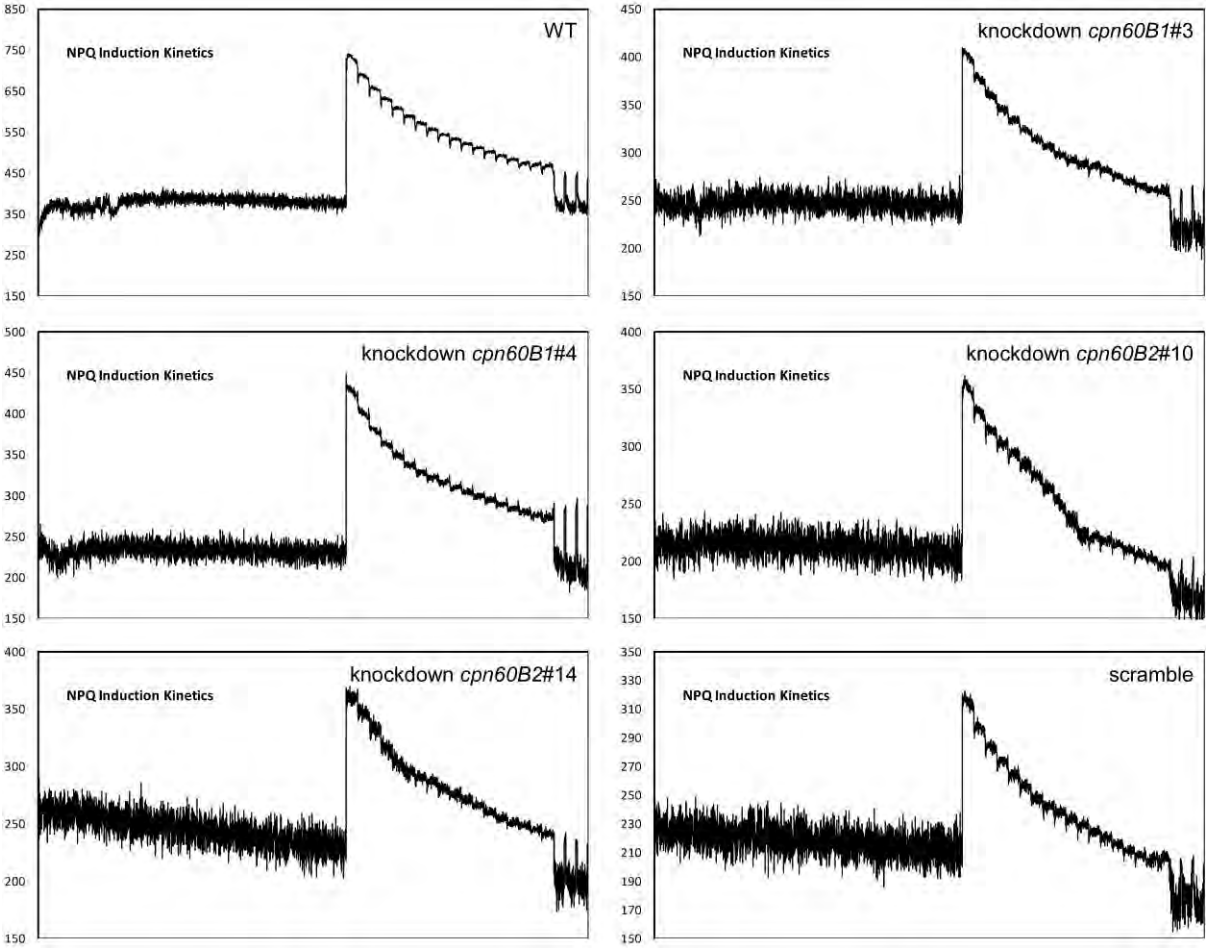

Figure 13. NPQ induction kinetics of WT *C. reinhardtii* compared to representative knockdown transformants of cpn60B1 and cpn60B2 as well as another amiRNA scramble control (as indicated).

Discussion

1. Comparative proteomic analysis of *C. reinhardtii* subjected to irradiance stress

Although the overall responses of plants to irradiance stress are somewhat conserved among different photosynthetic organisms, the molecular mechanisms underlying such process are complex. Proteomic analysis of the model green alga, *C. reinhardtii*, in this study revealed changes in proteins of many different functions ranging from photosynthetic light energy conversion, enzymes in metabolic pathways, cell structure and movement, signal transduction, protein translation, molecular chaperones and unknown proteins. As the number of the differentially–expressed protein spots are large (99 total), specific discussion made on every protein is impossible. We, therefore, will only discuss on the key finding that might be interpreted in a sensible way. The early changes we observed were rearrangements of the light–harvesting antenna proteins, manifested by the up– and down–regulation of several protein spots identified as the LHC–II polypeptides (Table 2 and 3). Since many of the

enhanced spots matched with the stress–related LHC, these proteins might have pivotal roles in handling of the greater ensuing photon flux density of irradiance stress. We also found increased expressions of the proteins involved in carbohydrate metabolisms at 1.5 h after transition to HL. The higher rate of carbohydrate metabolism could also help accelerate the utilization of electrons generated by the photosynthetic light reactions, minimizing the risk of superoxide formation. Another response of *C. reinhardtii* to irradiance stress observed in this study is the increase in spot intensities of the phytoene desaturase (PDS) and ChlI subunit of the Mg–chelatase enzyme (Table 3). PDS is one of the important enzymes in carotenoid biosynthesis pathway catalyzing a conversion of phytoene to ζ–carotene via 2 successive dehydrogenations. As carotenoid accumulation is one of the typical plant responses to HL, the elevation of PDS is foreseeable and is commonly observed (Steinbrenner and Linden 2003; Schäfer et al. 2006). It has been reported in the literature that Chl biosynthesis is suppressed under HL condition due to inhibition of ALA synthesis (Aarti et al 2007). As the Chl biosynthesis is slowed down at the upstream part of the pathway, plant cells may respond to the lack of Chl by up–regulate expression of the downstream components. Hence, it is possible that enhanced expression of ChlI protein discerned in our study may just be a side effect of HL instead of the elevated rate of Chl biosynthesis.

To our surprise was the finding that several important molecular chaperones were down–regulated in *Chlamydomonas* exposed to excessive growth irradiance for up to 6 h. In the literature, primary functions of the molecular chaperones are thought to be for assisting protein folding/refolding. However, as molecular chaperones are the housekeeping proteins, they could as well have many other specialized functions, including translation, protein trafficking, proteolytic cleavage, etc. The first evidence supporting the active role of molecular chaperones during plant adaption to irradiance stress came from the work from Schroda and his colleagues in Germany. Using *C. reinhardtii* as a model, this group of scientists discovered that down-regulation of a chloroplast-localized heat-shock protein 70 (HSP70B) by antisense technique makes the transformants more susceptible to photo-oxidative damage than wild type (Schroda et al. 1999). On the contrary, the transformants overexpressing such protein are more resistant to high light compared to the wild type counterpart (Schroda et al. 1999). Yokthongwattana et al. (2001) further demonstrated that HSP70B could be part of the PSII repair intermediate complex. Thus, it has been proposed that HSP70B plays important roles in the PSII repair process (Schroda et al. 2001; Yokthongwattana et al. 2009). In this study, the increasing level of HSP70B after 3 h of transition to HL is consistent with the previous evidence in the literature regarding its functions. However, CPN60, ClpC, HSP70A and HSP70E were

found to be underexpressed. HSP70 is a large protein family found in all living organisms. Although HSP70 chaperones have been reported to carry out a wide range of specialized cellular functions, including the PSII repair process, their predominant role is thought to be for helping renature the unfolded or misfolded proteins during stresses. HSP70A is a well–known cytosolic protein (Müller et al. 1992) believed to function as a typical chaperonin. HSP70E, on the other hand, was identified during the *C. reinhardtii* genome sequencing as an ORF that shares some degree of homology to the HSP70 and HSP110 protein family (Schroda 2004). It is predicted to encode for a cytosolic protein of about 87 kDa, the function of which has not been characterized. It is possible that both HSP70A and 70E may function in facilitating the transport/trafficking of nuclear-encoded proteins important for HL acclimation. Down regulation of these two proteins might results in the alga unable to cope with the excessive irradiance.

CPN60 or HSP60, which is a plastid homologue of bacterial GroEL (Viitanen et al. 1995), was suggested to help refold the denatured proteins by the same mechanism as that of the famous bacterial GroES/GroEL system. The primary substrate for the CPN60 could be Rubisco large subunit (RbcL) proteins (Schroda 2004). Decreasing level of the CPN60 may perhaps lead to accumulation of the Rubisco enzyme in the inactive form. Lacking of the active Rubisco leads to an imbalance between the rate of CO_2 assimilation and the rate of photon absorption and electron transport events. Therefore, lowering in the amount of the CPN60 could well explain the lower threshold of irradiance in *C. reinhardtii*.

HSP100 or Clp is also a large protein family found in both prokaryotes and eukaryotic organisms (Schirmer et al. 1996). The renowned function of Clp chaperones, especially ClpB, is their ability to dissociate protein aggregates and help them refold (Goloubinoff et al. 1999). In the chloroplast stroma of plants and green algae, ClpC and ClpD are the two homologues of the HSP100 protein family (Zheng et al. 2002). So far, the only reported function of ClpC is believed to facilitate protein import into the chloroplast (Nielsen et al. 1997).

Considering the fact that these molecular chaperones are housekeeping proteins normally expressed constitutively in the cell, reduction in their abundance even a small proportion could result in a drastic effects. Such down regulation of the abovementioned chaperones and heat-shock proteins in response to irradiance stress could partially explain the light-sensitive nature of *C. reinhardtii*. Lower amount of these key chaperones could lead to accumulation of denatured proteins in both chloroplast stroma and cytosol causing cell death. Presumably, this alga does not down regulate these important proteins on purpose but rather the cell may not be able to keep up the rate of their biosynthesis with the rapid rate of

reduction under high light. Further in-depth research on these molecular chaperones could provide better understanding on their expression pattern and functions.

2. Comparative proteomic analysis between *C. reinhardtii* cells grown under normal condition vs. cells subjected to short-term salinity stress

In complementary to the existing few reports on aquatic microalgae, we report here another proteomic study on the salinity-stress response of the model freshwater unicellular green alga *C. reinhardtii*. From our results, the overall changes in the proteome profiles upon treating the algal cells with 300 mM NaCl for 2 h seem to be similar with the previous proteomic reports in both higher plants and cyanobacteria, particularly in terms of the differential expression of enzymes or polypeptides involved in carbohydrate metabolism, energy production, protein translation as well as stress-related proteins (Kosová et al. 2011; Sobhanian et al. 2011). According to these changes, simple interpretations can be made as following: under salinity stress, (a) the *Chlamydomonas* cells require a lot of energy to maintain ion homeostasis, which can be obtained via glycolytic and other energy-producing metabolic pathways, (b) scavenging of the ROS is carried out by the antioxidant enzymes, and (c) heat-shock proteins and molecular chaperones help renature the misfolded and/or aggregated proteins. These observations and interpretations have commonly been reported in higher plants subjected to NaCl stress (Kosová et al. 2011; Sobhanian et al. 2011).

However, it is important to note that according to our proteomic comparison criterion, the spots corresponding to the proteins listed in Table 4 only appeared in the proteome of the control but not in the salt-shocked cells. Likewise, the proteins in Table 5 were detectable only in the 2-DE profile of the salt-stressed but not in the control cultures. The exclusive appearance of any protein spot in one sample but not in another suggests that such protein could either originate from de novo translation or it could be modified by PTM in a way that changes its p*I* and M_r, leading to a shift of the spot position on 2-DE or else the protein is completely degraded and disappear from the gel. In case of the proteins in the control culture as shown in Table 4, most of which did not show significant deviation between the observed and theoretical p*I* and M_r values. This observation entails that these proteins existed under normal growth condition to perform their normal function but excessive NaCl imposed on the alga led to their complete disappearance. Disappearance of the proteins in Table 4 under salt stress could result from complete degradation or that they were modified and the corresponding spots shifted away from the original location.

For the proteins in the salt-shocked cultures (Table 5), if they originated from de novo biosynthesis, it implies that the important housekeeping proteins like molecular chaperones and the translation machineries were not expressed under normal growth condition but instead were induced upon NaCl treatment. This notion is very unlikely because molecular chaperones/heat-shock proteins as well as translational apparatus are known constitutively-expressed proteins important for cell survival. Indeed, a previously published article from our group already showed that these housekeeping proteins existed in the proteome of *C. reinhardtii* cells grown under normal growth condition (Mahong et al. 2012). The data in this study, thus, suggests that the salt-stress-specific proteins presented in Table 5 could originate from PTM of the existing polypeptide pool rather than from de novo translation under salinity stress. Additionally, many of the proteins in Table 5 also have the observed p*I* and M_r significantly deviated than the theoretical values, insinuating the PTM notion. For example, we found the protein spot #2613 (mitochondrial ATP synthase β subunit, accession number gi|159466892) in Table 4 which has the observed p*I* and M_r well within the range of the theoretical values disappeared from the proteome of the salt-shocked cells. In parallel, the protein spot #2729 identified as the same protein emerged with significant shift in the observed p*I* and M_r (see Table 5). Such modification(s) must also be specific and unique to salt stress as the irradiance stress imposed to *C. reinhardtii* did not result in the exclusive occurrence of any protein spot similar to those presented in Table 2 (Mahong et al. 2012).

There are various types of PTM existing in living organisms. The most common PTMs include protein phosphorylation, acetylation, acylation, methylation, myristoylation, sumoylation, ubiquitination, etc. Certain modifications activate protein functions while some others have inhibitory effects. Since our mass spectrometric data could not distinguish the type of PTM for each protein spot, we desist from making speculation on specific roles of individual modification. Regardless of which PTM type, however, there are two possible explanations for the presence of salt-exclusive proteins in Table 5. In the first scenario, under salt stress condition, these proteins could possibly be modified and activated to perform specific and exclusive function in counteracting the drastic effects of excessive NaCl. Activation of such proteins, in this case, then fits with the functional interpretations commonly made to these groups of proteins under salt stress (Kosová et al. 2011; Sobhanian et al. 2011). In the second hypothesis, functions of the salt-specific proteins in Table 5 might be suppressed by the NaCl-responsive protein PTM. Losing the function of these important proteins under salinity stress in this case, even a small amount, may possibly make *C. reinhardtii* cells vulnerable to salt stress. This notion could perhaps explain the salt-sensitive nature of this model alga.

When comparing our results with the previously published proteomic works on *Synechcystis* and *Dunaliella*, it is interesting to note that in those halotolerant algae, expression of the stress-related proteins and translation machineries were found to be enhanced under salinity stress over the control baseline instead of being found as exclusive spots (Liska et al. 2004; Fulda et al. 2006). This observation together with the two possible hypotheses made above suggest that (a) the salt-sensitive *C. reinhardtii* may have unique mechanisms, via PTM, to turn on protein functions for counteracting salinity stress or (b) alternatively the algal cells might not be able to sustain the toxicity of such high NaCl concentration within the 2 h period and, by way of PTM, loses the function of these important proteins.

In summary, our work presents here the identification of proteins exclusively appeared in the proteome of *C. reinhardtii* subjected to short-term salinity stress. Most of the differentially expressed proteins are constitutive and essential proteins important for normal cellular processes as well as for stress response. As these protein spots are not present in the proteome of the control cells grown under normal TAP recipe, we suggest that these proteins may originate from salt-specific PTM. Whether the salt-exclusive proteins in *Chlamydomonas* detected in this work are modified to play an active role in salt-adaptation or are inactivated as an aftereffect of salt toxicity is open for further investigations.

3. Reverse-genetic approach to study function of CPN60 proteins

To follow up on the proteomic observation regarding the possible role of the chloroplast-localized chaperonin 60 protein during high light acclimation, we created *C. reinhardtii* transformants with down-regulation phenotype of the transcript level of *cpn60B1* and *cpn60B2*. Physiological analyses of these transformants compared to the wild type control showed supporting evidence for such claim. When subjected to irradiance stress, all transformants manifested a more rapid decline in photosynthetic performance in terms of PSII quantum efficiency (determined as the F_v/F_m parameters) and Pmax. Without NPQ interference, the F_v/F_m values would signify the amount of active photosystem II reaction centers. The typical value for healthy cells is around 0.8. Under stresses and when the PSII undergo photodamage, the F_v/F_m parameters can drop down to as low as 0.1. In our study, the NPQ induction kinetics was almost the same for both WT and transformants (see Fig. 13). Therefore, the decreasing F_v/F_m values under irradiance stress condition in Fig. 10 would imply that PSII in the transformants undergo faster photodamage than the WT in the initial period (time 30 min). At time longer than 30 min, the damaging effect of the excessive light was probably beyond the cells to cope. Thus, all algal cells ended up with similar F_v/F_m values.

Similar notion could be made when consider the Pmax parameter. Pmax is the measurement of whole-chain photosynthesis that begins with water oxidation at the PSII. As PSI photodamage is rarely seen at room temperature, the decline in Pmax would also indicate the PSII photodamage. Consistent with the F_v/F_m parameters, Pmax of the *cpn60B1* and *cpn60B2* transformants also dropped more rapidly than the WT in the first 30 min. The specific role of CPN60 chaperonin under irradiance stress was put forward by the results on salinity shock treatment (Fig. 12). Under salt stress, rate of the PSII photodamage as determined by the F_v/F_m ratios were similar among WT and transformants.

It must be note that although our results seemed to suggest the active role of the CPN60 protein under light stress of plants, the data can also be advocated for the statistical insignificance. There are obviously two possibilities regarding this argument. In the first case, the chaperone did not have any function and that our data originated from false positive experimental results. In the second scenario, the protein does have important function but our experiments were not sufficient to verify its involvement. As the CPN60 beta subunit has 2 isoforms B1 and B2, it is also possible that knocking down one isoform is not sufficient as another isoform could provide a bit of compensation. To prove this hypothesis, knocking down both isoform should be performed in the future research.

References

Aarti D, Tanaka R, Ito H, Tanaka A (2007) High light inhibits chlorophyll biosynthesis at the level of 5-aminolevulinate synthesis during de-etiolation in cucumber (*Cucumis sativus*) cotyledons. Photochem Photobiol 83: 171–176.

Aro E-M, Virgin I, Andersson B (1993) Photoinhibition of photosystem II. Inactivation, protein damage and turnover. Biochim Biophys Acta 1143: 113–134.

Baroli I, Gutman BL, Ledford HK, Shin JW, Chin BL, Havaux M, Niyogi KK (2004) Photo-oxidative stress in a xanthophyll-deficient mutant of *Chlamydomonas*. J Biol Chem 279: 6337–6344.

Drzymalla C, Schroda M, Beck CF (1996) Light-inducible gene *hsp70B* encodes a chloroplast-localized heat shock protein in *Chlamydomonas reinhardtii*. Plant Mol Biol 31: 1185–1194.

Fulda S, Mikkat S, Huang F, Huckauf J, Marin K, Norling B, Hagemann M (2006) Proteome analysis of salt stress response in the cyanobacterium *Synechocystis* sp. strain PCC 6803. Proteomics 6: 2733–2745.

Goloubinoff P, Mogk A, Ben Zvi AP, Tomoyasu T, Bukau B (1999) Sequential mechanism of solubilization and refolding of stable protein aggregates by a bichaperone network. Proc Natl Acad Sci USA 96: 13732–13737.

Harris EH (1988) The *Chlamydomonas* sourcebook – a comprehensive guide to biology and laboratory use. Academic Press, Inc.

Havaux M (1992) Stress tolerance of photosystem II in vivo: antagonistic effects of water, heat, and photoinhibition stresses. Plant Physiol 100: 424–432.

Horton P, Ruban A (2005) Molecular design of the photosystem II light-harvesting antenna: photosynthesis and photoprotection. J Exp Bot 56: 365–373.

Kok B (1956) On the inhibition of photosynthesis by intense light. Biochim Biophys Acta 21: 234–244.

Kosová K, Vítámvás P, Prásil T, Renaut J (2011) Plant proteome changes under abiotic stress – contribution of proteomics studies to understanding plant stress response. J Proteomics 74: 1301–1322.

Król M, Maxwell DP, Huner NPA (1997) Exposure of *Dunaliella salina* to low temperature mimics the high light-induced accumulation of carotenoids and the carotenoid binding protein (Cbr). Plant Cell Physiol 38: 213–216.

Liska AJ, Shevchenko A, Pick U, Katz A (2004) Enhanced photosynthesis and redox energy production contribute to salinity tolerance in *Dunaliella* as revealed by homology–based proteomics. Plant Physiol 136: 2806–2817.

Long SP, Humphries S, Falkowski PG (1994) Photoinhibition of photosynthesis in nature. Annu Rev Plant Physiol Plant Mol Biol 45: 633–662.

Mahong B, Roytrakul S, Phaonaklop N, Wongratana J, Yokthongwattana K (2012) Proteomic analysis of a model unicellular green alga, *Chlamydomonas reinhardtii*, during short-term exposure to irradiance stress reveals significant down regulation of several heat-shock proteins. Planta 235: 499–511.

Melis A (1999) Photosystem-II damage and repair cycle in chloroplasts: what modulates the rate of photodamage in vivo? Trends Plant Sci 4: 130–135.

Molnar A, Bassett A, Thuenemann E, Schwach F, Karkare S, Ossowski S, Weigel D, Baulcombe D (2009) Highly specific gene silencing by artificial microRNAs in the unicellular alga *Chlamydomonas reinhardtii*. Plant J 58: 165–174.

Müller FW, Igloi GL, Beck CF (1992) Structure of a gene encoding heat-shock protein HSP70 from the unicellular alga *Chlamydomonas reinhardtii*. Gene 111: 165–173.

Müller-Moule´ P, Havaux M, Niyogi KK (2003) Zeaxanthin deficiency enhances the high light sensitivity of an ascorbate-deficient mutant of *Arabidopsis*. Plant Physiol 133: 748–760.

Nielsen E, Akita M, Davila-Aponte J, Keegstra K (1997) Stable association of chloroplastic precursors with protein translocation complexes that contain proteins from both envelope membranes and a stromal Hsp100 molecular chaperone. EMBO J 16: 935–946.

Niyogi KK (1999) Photoprotection revisited: genetic and molecular approaches. Annu Rev Plant Physiol Plant Mol Biol 50: 333–359.

Niyogi KK (2000) Safety valves for photosynthesis. Curr Opin Plant Biol 3: 455–460.

Powles S (1984) Photoinhibition of photosynthesis induced by visible light. Annu Rev Plant Physiol 35: 15–44.

Schäfer L, Sandmann M, Woitsch S, Sandmann G (2006) Coordinate up-regulation of carotenoid biosynthesis as a response to light stress in *Synechococcus* PCC7942. Plant Cell Environ 29: 1349–1356.

Schirmer EC, Glover JR, Singer MA, Lindquist S (1996) HSP100/Clp proteins: a common mechanism explains diverse functions. Trends Biochem Sci 21: 289–296.

Schroda M (2004) The *Chlamydomonas* genome reveals its secrets: chaperone genes and the potential roles of their gene products in the chloroplast. Photosynth Res 82: 221–240.

Schroda M, Vallon O, Wollman F-A, Beck CF (1999) A chloroplast-targeted heat shock protein 70 (HSP70) contributes to the photoprotection and repair of photosystem II during and after photoinhibition. Plant Cell 11: 1165–1178.

Sobhanian H, Aghaei K, Komatsu S (2011) Changes in the plant proteome resulting from salt stress: toward the creation of salt-tolerant crops? J Proteomics 74: 1323–1337.

Steinbrenner J, Linden H (2003) Light induction of carotenoid biosynthesis genes in the green alga *Haematococcus pluvialis*: regulation by photosynthetic redox control. Plant Mol Biol 52: 343–356.

Stitt M (1986) Limitation of photosynthesis by carbon metabolism. 1. Evidence for excess electron transport capacity in leaves carrying out photosynthesis in saturating light and CO_2. Plant Physiol 81: 1115–1122.

Thaipratum R, Melis A, Svasti J, Yokthongwattana K (2009) Analysis of non-photochemical energy dissipating processes in wild type *Dunaliella salina* (green algae) and in zea1, a mutant constitutively accumulating zeaxanthin. J Plant Res 122: 465–476.

Vass I, Styring S, Hundal T, Koivuniemi A, Aro E-M, Andersson B (1992) Reversible and irreversible intermediates during photoinhibition of photosystem II. Stable reduced Q_A species promote chlorophyll triplet formation. Proc Natl Acad Sci USA 89: 1408–1412.

Viitanen PV, Schmidt M, Buchner J, Suzuki T, Vierling E, Dickson R, Lorimer G, Gatenby A, Soll J (1995) Functional characterization of the higher plant chloroplast chaperonins. J Biol Chem 270: 18158–18164.

Yokthongwattana K, Chrost B, Behrman S, Casper-Lindley C, Melis A (2001) Photosystem II damage and repair cycle in the green alga *Dunaliella salina*: involvement of a chloroplast-localized HSP70. Plant Cell Physiol. 42: 1389–1397.

Yokthongwattana K, Jine E, Melis A (2009) Chloroplast acclimation, photodamage and repair reactions of photosystem-II in the model green alga *Dunaliella salina*. In: Ben-Amotz A, Polle JEW, Rao DVS (eds) The alga *Dunaliella*: biodiversity, physiology, genomics and biotechnology. Science Publishers, New Hampshire, USA, pp. 273–299. ISBN 978–1–57808–545–3.

Yokthongwattana K, Melis A (2006) Photoinhibition and recovery in oxygenic photosynthesis: mechanism of a photosystem-II damage and repair cycle. In: Demmig-Adams B, Adams III WW, Mattoo AK (eds) Photoprotection, photoinhibition, gene regulation and environment. Advances in Photosynthesis Series, Springer, Dordrecht, The Netherlands, pp. 175–191. ISBN 1–4020–3564–0.

Zheng B, Halperin T, Hruskova-Heidingsfeldova O, Adam Z, Clarke AK (2002) Characterization of chloroplast Clp proteins in *Arabidopsis*: Localization, tissue specificity and stress responses. Physiol Plant 114: 92–101.

Output จากโครงการวิจัยที่ได้รับทุนจาก สกว.

1. ผลงานตีพิมพ์ในวารสารวิชาการนานาชาติ

1.1 Mahong B, Roytrakul S, Phaonaklop N, Wongratana J, Yokthongwattana K* (2012) Proteomic analysis of a model unicellular green alga, *Chlamydomonas reinhardtii*, during short-term exposure to irradiance stress reveals significant down regulation of several **heat-shock proteins**. Planta 235 (3): 499–511. (IF 2012 = 3.347)

1.2 Yokthongwattana C, Mahong B, Roytrakul S, Phaonaklop N, Narangajavana J, Yokthongwattana K* (2012) Proteomic analysis of salinity-stressed *Chlamydomonas reinhardtii* revealed differential suppression and induction of a large number of important housekeeping proteins. Planta 235 (3): 649–659. (IF 2012 = 3.347)

1.3 Wongratana J, Juntadech T, Sereeruk C, Angsuthanasombat C, Yokthongwattana K* (2013) Generation and characterization of His-tagged-PsbA-expressing transformants of *Chlamydomonas reinhardtii* that are capable of photoautotrophic growth. Journal of Applied Phycology, 25 (2): 445–452. (IF 2012 = 2. 326)[#]

* แสดงถึง corresponding author

[#] เงินงบประมาณบางส่วนของทุน สกว. ที่ได้รับมีส่วนสนับสนุนผลงานชิ้นนี้

2. การนำผลงานวิจัยไปใช้ประโยชน์

2.1 เชิงพาณิชย์

N/A

2.2 เชิงนโยบาย

N/A

2.3 เชิงสาธารณะ

N/A

2.4 เชิงวิชาการ

2.4.1 มีการผลิตนักศึกษาที่จบการศึกษาระดับปริญญาเอก 1 คนคือนายเจนวิทย์ วงศ์รัตน์

2.4.2 มีการนำเนื้อหางานวิจัยบางส่วนไปใช้ในการเรียนการสอน

3. อื่น ๆ

N/A

ภาคผนวก

ผนวก 1. Reprint ผลงานตีพิมพ์ หมายเลข 1.1

ผนวก 2. Reprint ผลงานตีพิมพ์ หมายเลข 1.2

ผนวก 3. Reprint ผลงานตีพิมพ์ หมายเลข 1.3

Planta (2012) 235:499–511
DOI 10.1007/s00425-011-1521-x

ORIGINAL ARTICLE

Proteomic analysis of a model unicellular green alga, *Chlamydomonas reinhardtii*, during short-term exposure to irradiance stress reveals significant down regulation of several heat-shock proteins

Bancha Mahong · Suttiruk Roytrakul · Narumon Phaonaklop · Janewit Wongratana · Kittisak Yokthongwattana

Received: 13 August 2011 / Accepted: 14 September 2011 / Published online: 29 September 2011

Abstract Oxygenic photosynthetic organisms often suffer from excessive irradiance, which cause harmful effects to the chloroplast proteins and lipids. Photoprotection and the photosystem II repair processes are the mechanisms that plants deploy to counteract the drastic effects from irradiance stress. Although the protective and repair mechanisms seemed to be similar in most plants, many species do confer different level of tolerance toward high light. Such diversity may originate from differences at the molecular level, i.e., perception of the light stress, signal transduction and expression of stress responsive genes. Comprehensive analysis of overall changes in the total pool of proteins in an organism can be performed using a proteomic approach. In this study, we employed 2-DE/LC–MS/MS-based comparative proteomic approach to analyze total proteins of the light sensitive model unicellular green alga *Chlamydomonas reinhardtii* in response to excessive irradiance. Results showed that among all the differentially expressed proteins, several heat-shock proteins and molecular chaperones were surprisingly down-regulated after 3–6 h of high light exposure. Discussions were made on the possible involvement of such down regulation and the light sensitive nature of this model alga.

Keywords 2-DE · *Chlamydomonas* · Irradiance stress · Heat-shock proteins · Molecular chaperones · Proteomics

Abbreviations

2-DE	Two-dimensional gel electrophoresis
Chl	Chlorophyll
HL	High light intensity
LL	Low light intensity

Introduction

Light is an essential driving force for photosynthesis, a process that generates primary food in the form of reduced-carbon compounds to sustain living organisms on this planet. Photosynthetic organisms respond to the changing growth irradiance in the ways to promote maximum efficiency of photosynthesis and to avoid harmful side effects. Whenever the photon flux density is beyond the maximum threshold for photosynthetic capacity, oxidative damage to the photosynthetic apparatus frequently occurs (Melis 1999). Singlet oxygen ($^1O_2$), formed in the vicinity of photosystem II (PSII), can attack and cause irreversible damage to the D1 reaction center protein (Yokthongwattana et al. 2009) whereas superoxide and hydroxyl radicals generated at the acceptor side of photosystem I (PSI) can also lead to oxidative damage of chloroplast proteins and lipids (Niyogi 1999).

To alleviate drastic effects under the excessive irradiance, plants have evolved protective and repair mechanisms to

B. Mahong · J. Wongratana · K. Yokthongwattana (✉)
Department of Biochemistry and Center for Excellence in Protein Structure and Function, Faculty of Science, Mahidol University, 272 Rama 6 Rd., Bangkok 10400, Thailand
e-mail: tekyw@mahidol.ac.th

Present Address:
B. Mahong
Crop Biotech Institute and Department of Plant Molecular Systems Biotechnology, Kyung Hee University, Yongin 446–701, Korea

S. Roytrakul · N. Phaonaklop
Genome Institute, National Center for Genetic Engineering and Biotechnology, 113 Thailand Science Park, Phahonyothin Rd., Pathumthani 12120, Thailand

counteract such stress. Photoprotection is a complex network of physiological responses to prevent oxidative damage from occurring (Niyogi 1999). The repair, on the other hand, is a mechanism to mend the damage that already takes place, especially the impairment of the PSII. Comparative studies on these two subject areas have been conducted in various plant species. Despite of the extensive research, detail mechanisms underlying such processes are far from being complete. Although the overall protective and repair systems are somewhat conserved among oxygenic photosynthetic organisms, different plants exhibit diverse level of tolerance to irradiance stress. Such diversity may originate from differences at the molecular level, i.e., perception of the light stress, signal transduction and expression of stress responsive genes. Probing the changes in global protein expression profiles, therefore, may provide crucial clues on the molecular understanding how particular plants respond to the excessive light.

Comprehensive analysis of a complex protein mixture in the proteome can be performed using a proteomic approach. To date, there are quite a number of published articles in the literature on *Chlamydomonas* proteomics (reviewed in Rolland et al. 2009). Among those, the only paper described comparative proteomic study on HL responses was published by Förster et al. (2006). However, that paper only compared the proteome profiles of HL-acclimated wild type and two very high light (VHL) resistant mutants after 24 h of transition from HL to VHL. In the real world situation, the chance that plants are exposed to excessive irradiance for more than 6 h is very rare. Therefore, information on the differentially expressed proteins during the initial few hours of plants exposed to HL can be a very useful piece of information for understanding of their molecular responses. In this work, another set of comparative proteomics was conducted to study changes in *Chlamydomonas* global protein expression during shorter term of HL response. As the model unicellular green alga *Chlamydomonas reinhardtii* is particularly sensitive to high light, the results obtained from this study provide complementary evidence to the existing work and may offer plausible explanation on the light sensitive nature of this alga.

Materials and methods

Algal strain and growth conditions

Chlamydomonas reinhardtii strain CC-503, obtained from the *Chlamydomonas* Culture Collection (http://www.chlamy.org), was grown photoautotrophically in a Tris-Bicarbonate-Phosphate (TBP) medium (Polle et al. 2000). Initially the algal cultures were grown under LL (50 μmol photons m^{-2} s^{-1}). When the cultures reached mid-logarithmic phase, they were shifted to HL (1,200 photons m^{-2} s^{-1}). Cells were collected at time 0 (LL), 1.5, 3, and 6 h after the LL → HL shift for further analyses.

Chlorophyll fluorescence measurement

Maximum quantum efficiency of the PSII in intact cells was measured as the F_v/F_m ratio using a standard pulse–amplitude modulated (PAM) fluorometer model FMS–2 (Hansatech Instruments, UK).

Protein isolation and separation by 2-DE

Cell aliquots were subjected to centrifugation at 2,000×*g* for 2 min at room temperature and the supernatant was discarded. The pellet was washed twice with distilled water before lysis with buffer containing 8 M urea, 4% CHAPS, 2% thiourea. Cell debris and unsolubilized materials were separated by centrifugation at 10,000×*g* for 5 min; the resulting green supernatant was transferred to a new microcentrifuge tube while the pellet was discarded. To eliminate photosynthetic pigments and other hydrophobic compounds that may interfere with 2-DE, the supernatant was added with three to four volumes of ice-cold acetone and kept at –20°C overnight. The precipitated material was harvested by centrifugation at 10,000×*g* for 5 min and was resuspended in rehydration buffer containing 8 M urea, 4% CHAPS, 2% thiourea, 0.002% bromophenol blue, and 2% IPG buffer. Protein concentration of the extract was determined using Bradford protein assay kit (Bio-Rad Laboratory). Approximately 500 μg of protein samples were subjected to the 1st dimension IEF separation on 13 cm Immobiline dry strip pH 4–7 (GE Healthcare) using Ettan IPGphor 3 (GE Healthcare) with running condition set according to the protocol recommended by the manufacturer. The 2nd dimension of electrophoresis was carried out using standard SDS-PAGE on a 12.5% acrylamide concentration (Laemmli 1970). Protein spots were visualized upon staining the resolved 2-DE gel with colloidal Coomassie blue G. Proteins from at least three independent biological replicates of each time interval of LL → HL shift were isolated. For each of the biological replicate, the isolated proteins were resolved on at least three or four 2-DE gels, called sample replicates.

Image analysis and spot comparison

Gel images were scanned and analyzed electronically with computer software PDQuest™ (Bio-Rad Laboratory) similar to the protocol previously described (Mitprasat et al. 2011). Briefly protein spot patterns from independent

biological replicates of the same time point were compared. The spots that 'consistently' appeared on every biological replicate of each time were marked by the software for construction of a master image and the spot intensities were averaged. Any protein spot 'inconsistently' appears in different biological samples was not included in the master image and was also ignored from the subsequent cross-comparison with the spot patterns from other time points. Master images of 2-DE from different time intervals were compared and spot density data from all three different biological replicates of each time point were statistically analyzed by pair-wise *t* test for significant difference (P value <0.05). The spots that showed significant up- or down-regulation pattern were subjected to subsequent tryptic digestion and protein identification by mass spectrometry.

In-gel tryptic digestion of protein spots

Protein spots of interest were excised from the gel. The gel slices were dehydrated with 100% acetonitrile (ACN), reduced with 10 mM DTT in 10 mM ammonium bicarbonate at room temperature for 1 h and alkylated at room temperature for 1 h in the dark in the presence of 100 mM iodoacetamide (IAA) in 10 mM ammonium bicarbonate. After alkylation, the gel pieces were dehydrated twice with 100% ACN for 5 min. To perform in-gel digestion of proteins, 10 µl of trypsin solution (10 ng/µl trypsin in 50% ACN/10 mM ammonium bicarbonate) was added to the gels followed by incubation at room temperature for 20 min, and then 20 µl of 30% ACN was added to keep the gels immersed throughout digestion. The gels were incubated at 37°C overnight. To extract peptide digestion products, 30 µl of 50% ACN in 0.1% formic acid (FA) was added into the gels and incubated at room temperature for 10 min with shaking. Peptides extracted were collected and pooled together into a new tube. The pool of extracted peptides were dried by vacuum centrifuge and kept at –80°C until ready for mass spectrometric analysis.

Protein identification by mass spectrometry

Peptide solutions were analyzed using an HCTultra PTM Discovery System (Bruker Daltonics Ltd., UK) coupled to an UltiMate 3000 LC System (Dionex Ltd., UK). Peptides were separated on a nanocolumn (Acclaim PepMap 100 C18, 3 mm, 100A, 75 mm id × 150 mm). Eluent A was 0.1% formic acid and eluent B was 80% acetonitrile in water containing 0.1% formic acid. Peptide separation was achieved with a linear gradient from 10 to 70% of eluent B for 13 min at a flow rate of 300 nl/min. Including the regeneration step at 90% B and the equilibration step at 10% B, one run took about 20 min. Peptide fragment mass spectra were acquired in data-dependent AutoMS mode with a scan range of 300−1500 *m/z*, 3 averages, and up to 5 precursor ions selected from the MS scan 50−3000 *m/z*.

Peptide peaks were detected and deconvoluted automatically using DataAnalysis version 4.0 (Bruker Daltonics Ltd., UK). Mass lists in the form of Mascot generic files were created automatically and used as the input for Mascot MS/MS Ions searches of the National Center for Biotechnology Information nonredundant (NCBI nr) database (http://www.matrixscience.com). Default search parameters used were the following: Enzyme = trypsin, max. missed cleavages = 1; fixed modifications = carbamidomethyl (C); variable modifications = oxidation (M); peptide tolerance ±1.2 Da; MS/MS tolerance ±0.6 Da; peptide charge = 1+, 2+ and 3+; instrument = ESI–TRAP.

Statistical analysis

Averaged protein spot intensities among samples at different time points were subjected to statistical analysis by pair-wise *t* test with 95% significance level (P value <0.05).

Results

Irradiance stress in *C. reinhardtii*

Irradiance stress was imposed on the cells of *C. reinhardtii* by shifting the cultures from LL growth intensity to HL. Under this experimental condition, photo-oxidative damage was manifested as the lowering of the PSII photochemical efficiency (F_v/F_m). The F_v/F_m ratio declined from ~0.85 to a value of ~0.50 within 2 h and was retained at this number during the subsequent 2–6 h of HL exposure (Fig. 1). This result affirmed that our HL condition was sufficient to elicit irradiance-stress responses for the subsequent proteomic analysis.

Proteomic analysis

Total proteins extracted from cell aliquots of *C. reinhardtii*, which include both soluble and membrane polypeptides, were resolved on 2-DE and stained with colloidal Coomassie Brilliant Blue G. We opted for the use of colloidal Coomassie as the intensity of the protein spots stained by this type of dye is more consistent and is quantifiable. Although many of the low-abundant proteins might be undetectable by the Coomassie staining, we could already discern a large number of polypeptide spots in this study. Figure 2 shows representatives of the 2-DE-resolved gels of the samples collected at time 0 (LL), 1.5, 3 and 6 h after HL exposure. Initially a broader range of pH gradient

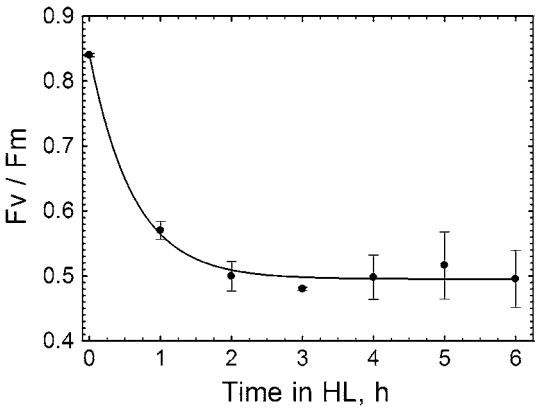

Fig. 1 PSII quantum efficiency as determined by the F_v/F_m ratio. *Chlamydomonas* cultures were grown under LL at time 0 and then shifted to HL for 6 h. Cell aliquots were taken at every h and subjected to analysis using PAM fluorometer. *Error bars* represent SD

(pH 3–10) was employed for the 1st dimension. However, as most of the proteins scattered between pH 4–7 (data not shown), we therefore used the latter narrow pH range for better resolution. In the 4–7 pH range, we could detect approximately 514 protein spots 'consistently' present in all 3 independent biological replicates of the LL samples (Fig. 2a). Using the same comparative criteria, proteome of *C. reinhardtii* cultures exposed to photoinhibitory condition for 1.5 h contained ~526 protein spots (Fig. 2b). At 3 h after the transition to HL, ~530 proteins could be detected in our study (Fig. 2c). After *C. reinhardtii* was exposed to irradiance stress for 6 h, about 527 total protein spots were consistently observed (Fig. 2d).

Stringent cross-comparison (see "Materials and methods") of the proteome profiles between that of the LL-grown alga and of the cells harvested at time 1.5, 3, and 6 h after the LL → HL shift revealed that totally 99 proteins, at any point in time, showed statistically significant up- or down-regulation pattern. Those proteins (numbered in Fig. 2) were subjected to identification by LC–MS/MS. After mass spectrometry and database search, their identities are presented in Table 1 with the relative spot intensities at different time intervals listed in Tables 2 and 3. Table 2 shows the averaged spot densities of proteins that were down-regulated while Table 3 presents those that were up-regulated during the 6 h exposure of *C. reinhardtii* to irradiance stress. The italicised values (Tables 2, 3) signify the time point where the averaged spot intensity of the corresponding proteins became 'statistically significant' different from that of the control LL values.

At 1.5 h after transition from LL to HL, we observed significant down-regulation pattern of 19 proteins (Table 2) while the intensities of 18 spots were enhanced (Table 3). Among the proteins that their expression deviates from the pattern under LL at this time point, we could detect up- and down-regulation of LHC-II proteins, several of which were identified as the same proteins with different p*I* values. It is interesting to note the increasing LHC-II tended to have lower p*I* values than those underexpressed, suggesting that the proteins could undergo posttranslational modification that results in lowering of the p*I*. Protein phosphorylation is one of such modifications. However, as our data could not provide proof on such modification, we refrain from claiming that phosphorylation is the cause of such lower p*I* values. Besides the light-harvesting proteins, expression of several other proteins involved in metabolic pathways as well as proteins involved in translation and degradation also changed (Tables 2, 3). Of particular remark, we observed enhanced expression of the oxygen evolution enhancer (OEE) proteins. However, as the corresponding spot of this protein had much lower observed M_r than the calculated values, it is most likely that they are degradation fragments of the OEE polypeptides. Several amino acid biosynthesis enzymes were found to be down-regulated in response to HL, whereas expressions of proteins involved in carbohydrate metabolism were enhanced. Abundance of two spots corresponding to triose phosphate isomerase and a spot each of phytoene desaturase and ChlI subunit of Mg-chelatase were also found to be elevated at this period.

When the alga was exposed to HL for 3 h, the expressions of 27 proteins were decreased when compared to the LL profile (Table 2), several of which were already found to be down-regulated at time 1.5 h. On the other hand, 30 protein spots showed significant increase in spot densities from the control values, 12 of which were non-redundant with those observed at the time 1.5 h in HL. At this time point, we could still observe up- and down- regulation of the Chl antenna proteins, particularly the minor LHC, as well as the increase in the abundance of the OEE fragments. Proteins involved in cytoskeleton, flagella structure and general cellular metabolism were also down-regulated. A notable up-regulated protein observed after 3 h of HL exposure is the chloroplast-localized heat-shock protein 70 (HSP70B). Expression of HSP70B, at both transcript and protein levels, has been reported to be enhanced under HL (Drzymalla et al. 1996; Schroda et al. 1999; Yokthongwattana et al. 2001). Therefore, the finding that protein level of HSP70B was enhanced after exposure of *C. reinhardtii* to irradiance stress for 3 h can, as well, serve as an internal validation of our experiment. To our surprise was the observation that level of the chaperonin 60 B1 subunit (CPN60) was decreased after 3 h of the LL → HL shift. As CPN60 is one of the molecular chaperones that help the denatured proteins to regain their proper conformation during stresses (Schroda 2004), its expression was rather expected to be the opposite.

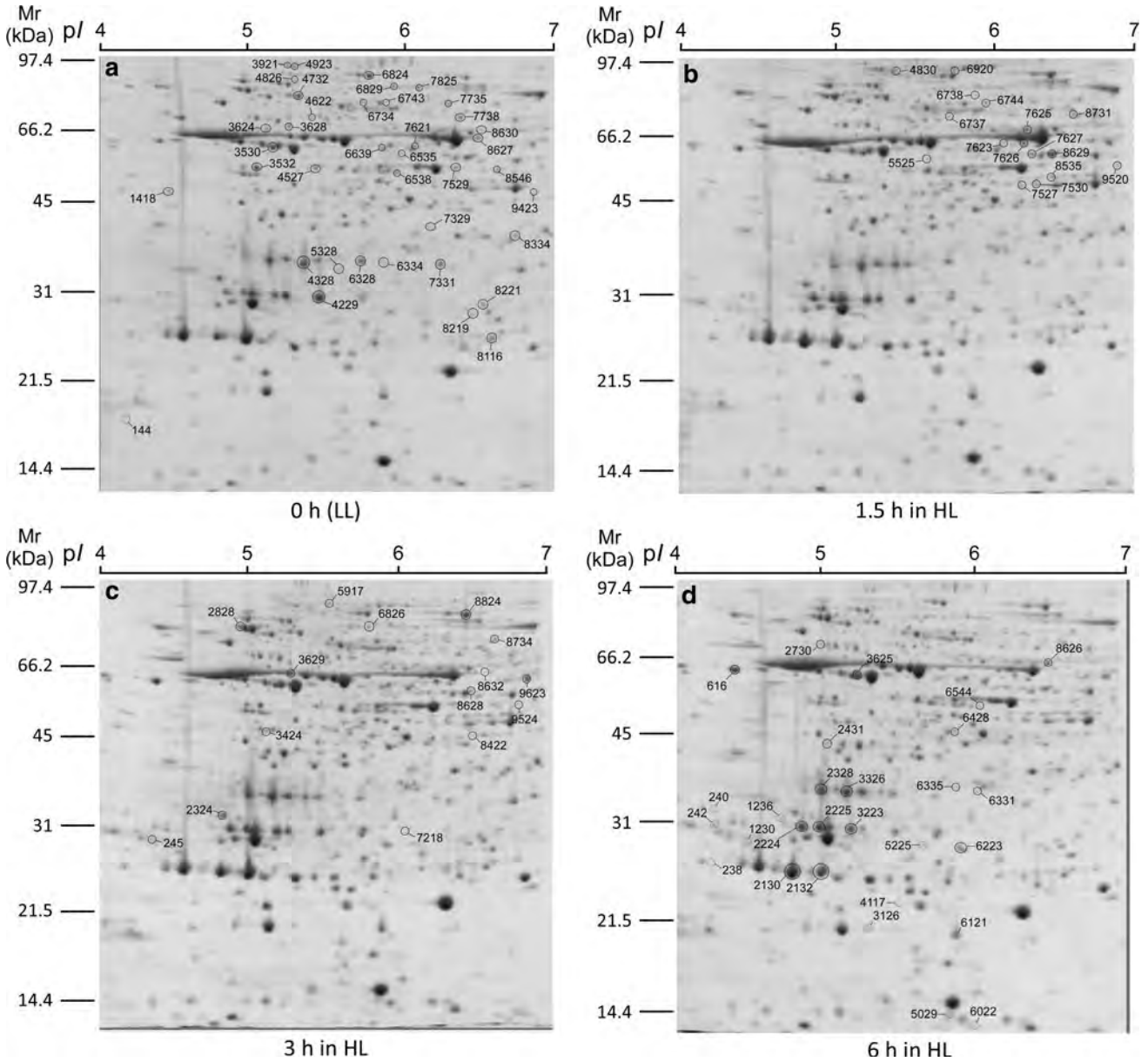

Fig. 2 Gel images showing total proteins of *C. reinhardtii* resolved by 2-dimensional gel electrophoresis. Immobilized strips with pH gradient 4–7 were used for the 1st dimension. The 2nd dimension separation was performed using 12.5% acrylamide gels. Protein spots were visualized by staining with colloidal Coomassie Blue G. Proteomes of LL-grown cells (**a**), and cells after shifted from LL → HL for 1.5 h (**b**), 3 h (**c**) and 6 h (**d**) are presented. *Numbered spots* indicates proteins whose abundance showed significant change during the transition from LL to HL

After prolonged exposure of *C. reinhardtii* cultures to irradiance stress for 6 h, 67 proteins were underexpressed while the levels of 29 proteins were elevated (Tables 2, 3). Within the set of down-regulated proteins at this period, 32 spots were not redundant with those found at time 1.5 and 3 h of HL exposure. In contrast, spot# 7530 (phosphoglycerate kinase) was the only unique protein up-regulated at 6 h of irradiance stress response in *C. reinhardtii*. Of those down-regulated, most are proteins involved in wide range of general cellular processes, such as amino acid and carbohydrate metabolisms, cytoskeleton and cell movement, etc. We also noticed the decline in the amount of the antenna proteins without concomitant increase of other isoforms. This observation suggested that at 6 h of HL exposure, the Chl antenna size may start to be truncated in response to the excessive irradiance. Furthermore, our proteomic analysis (see Table 2) also revealed a remarkable down-regulation of several other molecular chaperones beside the CPN60. Such chaperones include HSP70A, HSP70E, and ClpC (HSP100 family).

Table 1 List of identified protein spots that the expression level showed significant deviation during the 6 h transition from LL → HL

Spot #	Matched protein	Organism	NCBI Accession #	Observed MW/p*I*	Theoretical MW/p*I*	MOWSE score	# Of matched peptide	% Sequence coverage
Photosynthetic proteins								
240	LI818r-1	*C. reinhardtii*	gil1865771	33.2/4.3	21.7/4.53	58	1	7
242	Stress-related chlorophyll *a*/*b* binding protein 2	*C. reinhardtii*	gil159475924	31.0/4.4	28.2/4.88	227	4	24
1230	Stress-related chlorophyll *a*/*b* binding protein 1	*C. reinhardtii*	gil159476046	28.9/4.6	27.5/4.94	108	2	12
1236	Major light-harvesting complex II protein m3	*C. reinhardtii*	gil159491492	31.9/4.8	27.4/5.68	152	1	6
2130	Major light-harvesting complex II protein m1	*C. reinhardtii*	gil20269804	25.8/4.8	27.6/5.96	271	9	17
2132	Major light-harvesting complex II protein m1	*C. reinhardtii*	gil20269804	25.4/5.1	27.6/5.96	252	8	17
2224	Major light-harvesting complex II protein m3	*C. reinhardtii*	gil159491492	30.9/4.9	27.4/5.68	103	1	6
2228	Chlorophyll *a*-*b* binding protein of LHCII type I	*C. reinhardtii*	gil115827	31.1/5.0	27.0/5.96	73	1	5
2328	Minor chlorophyll *a*-*b* binding protein of PSII	*C. reinhardtii*	gil159475641	35.9/5.1	30.7/5.38	245	3	12
2730	RuBisCO large subunit-binding protein subunit alpha	*C. reinhardtii*	gil2493647	71.6/5.0	62.0/5.57	760	12	23
3126	Oxygen-evolving enhancer protein 2	*C. reinhardtii*	gil131389	19.6/5.3	25.9/9.14	361	8	30
3223	Chlorophyll *a*-*b* binding protein of LHCII type I	*C. reinhardtii*	gil115827	30.5/5.3	27.0/5.96	301	1	4
3326	Minor chlorophyll *a*-*b* binding protein of PSII	*C. reinhardtii*	gil159475641	35.2/5.2	30.7/5.38	182	2	8
4117	Oxygen-evolving enhancer protein 2	*C. reinhardtii*	gil131389	21.7/5.5	25.9/9.14	437	8	35
4328	Chlorophyll *a*/*b* binding protein Lhcb5	*C. incerta*	gil87313239	35.2/5.4	27.6/4.66	54	1	3
5029	Oxygen evolving enhancer protein 3	*C. reinhardtii*	gil159486609	13.5/5.9	21.8/9.58	312	7	25
6022	Photosystem I reaction center subunit XI	*C. reinhardtii*	gil159465747	13.0/6.0	20.4/9.37	53	1	4
6121	Chlorophyll *a*/*b*-binding protein	*C. reinhardtii*	gil19421770	19.1/5.9	23.9/9.41	249	7	35
6328	Chlorophyll *a*-*b* binding protein of PSII	*C. reinhardtii*	gil159478202	35.0/5.8	30.1/6.22	294	7	20
6334	Chlorophyll *a*-*b* binding protein of PSII	*C. reinhardtii*	gil159478202	34.5/5.9	30.1/6.22	93	2	6
7331	Chlorophyll *a*-*b* binding protein of PSII	*C. reinhardtii*	gil159478202	35.5/6.3	30.1/6.22	219	7	25
7529	RuBisCO large subunit	*C. reinhardtii*	gil41179049	55.7/6.4	53.2/6.14	420	10	21
8116	Chlorophyll *a*/*b* binding protein Lhca3	*C. reinhardtii*	gil87313217	26.0/6.6	27.1/8.14	117	2	10
8219	Chlorophyll *a*-*b* binding protein of LHCII	*C. reinhardtii*	gil159478875	29.0/6.5	28.7/7.79	69	2	7
8627	RuBisCO large subunit	*C. reinhardtii*	gil41179049	65.9/6.5	53.2/6.14	471	2	18
Stress proteins								
2828	Heat shock protein 70B	*C. reinhardtii*	gil159476666	83.2/5.0	72.1/5.31	99	2	2
3624	T-complex protein, theta subunit	*C. reinhardtii*	gil159490756	66.4/5.2	58.0/5.16	265	4	8
3921	Heat shock protein 70E	*C. reinhardtii*	gil159475503	93.3/5.3	88.1/5.22	1133	26	28
4622	Chaperonin 60B1	*C. reinhardtii*	gil159486163	70.7/5.5	62.3/6.38	583	6	19
4732	Heat shock protein 70A	*C. reinhardtii*	gil159486599	80.1/5.4	71.5/5.25	1466	30	40
4923	Heat shock protein 70E	*C. reinhardtii*	gil159475503	93.5/5.4	88.1/5.22	663	13	17
6824	Chaperone, Hsp100 family, ClpC-type	*O. lucimarinus*	gil145356586	89.1/5.8	92.7/5.27	517	9	11
8630	Ascorbate peroxidase	*C. reinhardtii*	gil159487873	68.6/6.5	36.0/8.67	174	2	8
Pigment biosynthesis								
3424	Magnesium chelatase subunit chlI	*C. reinhardtii*	gil20137882	47.6/5.2	45.5/6.22	411	9	21

Table 1 continued

Spot #	Matched protein	Organism	NCBI Accession #	Observed MW/p*I*	Theoretical MW/p*I*	MOWSE score	# Of matched peptide	% Sequence coverage
6535	4-Hydroxy-3-methylbut-2-enyl diphosphate reductase	*C. reinhardtii*	gil159486551	58.1/6.0	51.9/6.19	392	7	16
8535	Delta-aminolevulinic acid dehydratase	*C. reinhardtii*	gil159487537	52.3/6.4	43.1/7.72	340	6	20
8632	Phytoene desaturase	*C. reinhardtii*	gil159465297	66.1/6.6	63.0/7.68	106	1	2
Carbohydrate metabolism								
2431	Sedoheptulose-1,7-bisphosphatase	*C. reinhardtii*	gil159467635	43.8/5.1	42.4/8.59	607	15	36
3532	Fructose-1,6-bisphosphatase	*C. reinhardtii*	gil159465323	53.9/5.1	44.9/5.61	86	2	5
3628	Galactose kinase	*C. reinhardtii*	gil159487006	67.7/5.3	55.9/6.17	141	3	5
4229	Ribose-5-phosphate isomerase	*C. reinhardtii*	gil159467673	30.0/5.5	29.0/7.63	95	3	14
5225	Triose phosphate isomerase	*C. reinhardtii*	gil159463610	28.5/5.7	30.4/7.56	272	4	18
6223	Triose phosphate isomerase	*C. reinhardtii*	gil159463610	28.5/6.0	30.4/7.56	540	8	32
6538	Sugar nucleotide epimerase	*C. reinhardtii*	gil159462534	52.4/6.0	43.8/5.78	186	2	6
6428	Phosphoribulokinase	*C. reinhardtii*	gil159471788	46.4/5.9	42.1/8.11	310	6	17
6639	ADP-glucose pyrophosphorylase small subunit	*C. reinhardtii*	gil159467349	59.9/5.9	55.9/8.38	736	12	31
6743	Phosphoglucomutase	*C. reinhardtii*	gil159479834	76.9/6.0	64.8/7.12	238	3	6
7527	Phosphoglycerate kinase	*C. reinhardtii*	gil159482940	49.8/6.2	49.2/8.92	304	6	15
7530	Phosphoglycerate kinase	*C. reinhardtii*	gil1172455	49.8/6.3	49.3/8.84	250	4	11
8731	6-Phosphogluconate dehydrogenase	*C. reinhardtii*	gil159477567	73.1/6.6	61.3/8.35	516	9	20
Amino acid metabolism								
5328	Diaminopimelate epimerase	*C. reinhardtii*	gil159479426	33.8/5.6	34.8/6.95	366	6	21
7738	Acetohydroxyacid dehydratase	*C. reinhardtii*	gil159470063	72.9/6.4	64.8/7.51	335	7	11
8546	LL-Diaminopimelate aminotransferase	*C. reinhardtii*	gil159469820	55.4/6.6	48.3/8.29	763	13	38
8626	Acetohydroxy acid isomeroreductase	*C. reinhardtii*	gil159489328	67.6/6.5	60.6/8.29	75	2	2
8824	Cobalamin-independent methionine synthase	*C. reinhardtii*	gil159489910	89.6/6.5	87.3/5.94	1265	24	29
9520	LL-Diaminopimelate aminotransferase	*C. reinhardtii*	gil159469820	56.2/6.8	48.3/8.29	943	18	36
9623	Serine hydroxymethyltransferase 2	*C. reinhardtii*	gil159487140	63.0/6.7	52.2/6.25	1095	21	44
9524	Agmatine iminohydrolase	*C. reinhardtii*	gil159484436	57.3/6.7	46.1/6.50	173	4	9
Energy metabolism								
3625	ATP synthase CF1 beta subunit	*C. reinhardtii*	gil41179057	60.3/5.3	53.2/5.21	298	5	14
6734	Vacuolar ATP synthase, subunit A	*C. reinhardtii*	gil159480680	76.4/5.8	68.9/5.68	636	13	25
6744	Vacuolar ATP synthase, subunit A	*C. reinhardtii*	gil159480680	76.9/6.0	68.9/5.68	198	4	6
7735	Succinate dehydrogenase subunit A	*C. reinhardtii*	gil159463224	77.8/6.3	69.5/6.25	160	2	5
Signal transduction								
616	Calreticulin 2, calcium-binding protein	*C. reinhardtii*	gil159462862	63.6/4.5	47.4/4.54	384	9	21
1418	Protein phosphatase 2C	*C. reinhardtii*	gil159477373	49.0/4.6	39.1/4.67	201	4	10
8221	4 Ran-like small GTPase	*C. reinhardtii*	gil159467397	30.2/6.5	25.7/6.25	184	4	15
Cytoskeleton/trafficking/cell movement								
3530	Alpha tubulin 1	*C. reinhardtii*	gil159467393	59.9/5.3	50.2/5.01	687	16	34
4830	Flagellar associated protein	*C. reinhardtii*	gil159476808	92.2/5.4	90.9/5.29	61	1	1
6738	*N*-ethylmaleimide sensitive fusion protein	*C. reinhardtii*	gil159480686	79.9/5.9	78.7/5.68	54	1	1
8734	Dynamin-related GTPase	*C. reinhardtii*	gil159485798	78.5/6.6	67.8/6.50	73	1	1
9423	Flagellar associated protein	*C. reinhardtii*	gil159475749	49.2/6.7	41.4/6.34	549	9	28
Transcription/translation								
4527	Eukaryotic initiation factor 4A-like protein	*C. reinhardtii*	gil159466510	53.4/5.5	47.3/5.50	703	14	30

Table 1 continued

Spot #	Matched protein	Organism	NCBI Accession #	Observed MW/p*I*	Theoretical MW/p*I*	MOWSE score	# Of matched peptide	% Sequence coverage
6737	Aspartyl-tRNA synthetase	*C. reinhardtii*	gil159474374	70.2/5.8	60.7/5.61	385	6	11
6920	Elongation factor 2	*C. reinhardtii*	gil159490505	91.9/5.8	95.0/5.63	139	4	4
7621	Subunit of exon junction complex	*C. reinhardtii*	gil159491657	61.0/6.1	49.4/5.77	205	4	8
7625	Chloroplast polyprotein of elongation factor Ts precursor	*C. reinhardtii*	gil53794015	67.2/6.3	109.2/4.53	329	5	5
8334	Acidic ribosomal protein P0	*C. reinhardtii*	gil159477927	34.7/6.1	34.7/6.07	64	1	3
8422	Plastid-specific ribosomal protein 1	*C. reinhardtii*	gil159479306	47.4/6.5	31.9/9.18	412	11	29
Proteins of miscellaneous functions								
2324	14-3-3-Like protein-related protein	*C. reinhardtii*	gil74272601	32.9/4.9	29.7/4.90	114	2	9
3629	Selenium binding protein	*C. reinhardtii*	gil159490794	64.1/5.3	52.5/5.18	504	13	24
6335	Phosphoglycolate phosphatase	*C. reinhardtii*	gil159464681	36.4/5.9	33.5/5.42	48	1	3
6826	Arsenite translocating ATPase-like protein	*C. reinhardtii*	gil159488560	83.1/5.8	54.4/8.68	333	5	11
7329	26S Proteasome regulatory subunit	*C. reinhardtii*	gil159479806	41.5/6.2	37.1/5.75	143	3	12
7623	*S*-Adenosylmethionine synthetase	*C. reinhardtii*	gil159477124	62.4/6.1	43.1/6.03	271	5	15
7626	*S*-Adenosylmethionine synthetase	*C. reinhardtii*	gil159477124	62.7/6.3	43.1/6.03	412	8	17
7627	*S*-Adenosylmethionine synthetase	*C. reinhardtii*	gil159477124	59.3/6.3	43.1/6.03	416	5	11
7825	Putative chloroplast 1-hydroxy-2-methyl-2-(E)-butenyl-4-diphosphate synthase precursor	*C. reinhardtii*	gil61742128	83.8/6.1	75.2/5.76	239	5	6
8628	Isopropylmalate dehydratase, large subunit	*C. reinhardtii*	gil159488260	60.0/6.5	53.6/7.04	385	7	17
8629	*S*-Adenosylmethionine synthetase	*C. reinhardtii*	gil159477124	59.3/6.5	43.1/6.03	1039	23	47
Unknown proteins								
144	Hypothetical protein	*C. reinhardtii*	gil159465102	17.9/4.2	14.2/8.66	61	1	13
238	Putative membrane protein	*C. reinhardtii*	gil159488214	26.6/4.3	30.0/5.02	288	5	20
245	Hypothetical protein	*C. reinhardtii*	gil159475228	29.6/4.5	27.9/4.94	356	5	25
4826	Hypothetical protein CHLREDRAFT_192147	*C. reinhardtii*	gil159477457	88.1/5.4	73.7/5.29	67	1	1
5525	Predicted protein	*C. reinhardtii*	gil159487851	56.7/5.7	53.9/6.36	232	4	8
5917	Hypothetical protein CHLREDRAFT_120875	*C. reinhardtii*	gil159481287	93.8/5.6	12.3/9.17	80	1	9
6331	Predicted protein	*C. reinhardtii*	gil159463656	36.1/6.0	40.1/9.31	201	4	11
6544	Hypothetical protein CHLREDRAFT_132041	*C. reinhardtii*	gil159482705	52.5/6.0	47.0/6.42	144	4	11
6829	Hypothetical protein CHLREDRAFT_82920	*C. reinhardtii*	gil159488381	84.0/6.0	77.2/5.73	188	3	4
7218	Predicted protein	*C. reinhardtii*	gil159470065	30.6/6.1	31.3/8.18	177	4	14

Proteins were tryptic digested and identified by LC–MS/MS as described in the "Materials and methods" section. Spot numbers were assigned arbitrarily by the analysis software. MOWSE search scores of 47 or more are considered as significant match

Discussion

Although the overall responses of plants to irradiance stress are somewhat conserved among different photosynthetic organisms, the molecular mechanisms underlying such process are complex. Proteomic analysis of the model green alga, *C. reinhardtii*, in this study revealed changes in proteins of many different functions ranging from photosynthetic light energy conversion, enzymes in metabolic pathways, cell structure and movement, signal transduction, protein translation, molecular chaperones and unknown proteins. As the number of the differentially-expressed protein spots are large (99 total), specific discussion made on every protein is impossible. We,

Table 2 Relative spot intensities of *Chlamydomonas reinhardtii* proteins of which the expression levels were down-regulated during the 6 h HL exposure period

Spot #	Protein	Averaged spot density at time following LL → HL shift			
		Control (LL)	1.5 h	3 h	6 h
2132	Major light-harvesting complex II protein m1	15071 ± 3995	*11437 ± 3031*	*11057 ± 3270*	*7105 ± 949*
4527	Eukaryotic initiation factor 4A-like protein	1209 ± 180	*618 ± 87*	*705 ± 133*	*781 ± 125*
5328	Diaminopimelate epimerase	903 ± 113	*742 ± 82*	*662 ± 57*	*542 ± 102*
6334	Chlorophyll *a-b* binding protein of PSII	452 ± 192	*214 ± 85*	*165 ± 119*	*149 ± 38*
6538	Sugar nucleotide epimerase	891 ± 58	*753 ± 30*	*720 ± 59*	*540 ± 80*
7329	26S Proteasome regulatory subunit	1310 ± 206	*872 ± 192*	*814 ± 22*	*793 ± 124*
7331	Chlorophyll *a-b* binding protein of PSII	1856 ± 230	*1127 ± 218*	*804 ± 159*	*594 ± 240*
7623	S-Adenosylmethionine synthetase	916 ± 16	*663 ± 157*	*561 ± 76*	*465 ± 138*
7625	Chloroplast polyprotein of elongation factor Ts precursor	1382 ± 265	*1032 ± 252*	*963 ± 74*	*807 ± 164*
7738	Acetohydroxyacid dehydratase	1632 ± 121	*1242 ± 109*	*1119 ± 136*	*722 ± 142*
8628	Isopropylmalate dehydratase, large subunit	1192 ± 139	*743 ± 58*	*693 ± 25*	*547 ± 58*
8630	Ascorbate peroxidase	648 ± 39	*401 ± 53*	*414 ± 19*	*326 ± 48*
8731	6-Phosphogluconate dehydrogenase	631 ± 108	*516 ± 101*	*451 ± 103*	*325 ± 55*
9524	Agmatine iminohydrolase	718 ± 29	*570 ± 90*	*622 ± 31*	*459 ± 65*
5917	Hypothetical protein CHLREDRAFT_120875	748 ± 49	*653 ± 26*	632 ± 192	*442 ± 34*
6639	ADP-glucose pyrophosphorylase small subunit	1149 ± 217	*906 ± 216*	936 ± 57	*701 ± 86*
6744	Vacuolar ATP synthase, subunit A	771 ± 106	*552 ± 69*	617 ± 57	*389 ± 136*
7627	*S*-Adenosylmethionine synthetase	1159 ± 192	*880 ± 176*	852 ± 230	*663 ± 58*
7735	Succinate dehydrogenase subunit A	917 ± 95	*760 ± 112*	707 ± 105	*554 ± 72*
2324	14-3-3-Like protein-related protein	2742 ± 452	2388 ± 105	*2228 ± 403*	*1759 ± 192*
3530	Alpha tubulin 1	1715 ± 288	1478 ± 279	*1283 ± 272*	*1027 ± 158*
4328	Chlorophyll *a/b* binding protein Lhcb5	3591 ± 671	2334 ± 645	*1874 ± 191*	*1016 ± 299*
4622	Chaperonin 60B1	548 ± 22	514 ± 207	*367 ± 56*	*427 ± 67*
4826	Hypothetical protein CHLREDRAFT_192147	662 ± 41	599 ± 114	*473 ± 42*	*418 ± 34*
6121	Chlorophyll *a/b*-binding protein	3631 ± 647	3313 ± 421	*2908 ± 269*	*1868 ± 305*
6328	Chlorophyll *a-b* binding protein of PSII	2374 ± 774	1856 ± 426	*1407 ± 196*	*834 ± 56*
6826	Arsenite translocating ATPase-like protein	864 ± 24	703 ± 186	*616 ± 60*	*527 ± 89*
6920	Elongation factor 2	457 ± 39	528 ± 131	*343 ± 58*	*332 ± 58*
7626	*S*-Adenosylmethionine synthetase	2112 ± 585	1332 ± 536	*1202 ± 283*	*846 ± 213*
7825	Putative chloroplast 1-hydroxy-2-methyl-2-(E)-butenyl-4-diphosphate synthase	1016 ± 146	689 ± 330	*467 ± 306*	*55 ± 10*
8116	Chlorophyll *a/b* binding protein Lhca3	1919 ± 376	1676 ± 155	*1378 ± 141*	*1200 ± 175*
9423	Flagellar associated protein	839 ± 155	710 ± 59	*517 ± 41*	513 ± 145
144	Hypothetical protein	1344 ± 821	1264 ± 25	1024 ± 245	*612 ± 58*
1418	Protein phosphatase 2C	1310 ± 186	1031 ± 225	827 ± 160	*765 ± 141*
3532	Fructose-1,6-bisphosphatase	2562 ± 540	2068 ± 154	1985 ± 52	*1587 ± 176*
3624	T-complex protein, theta subunit	908 ± 94	739 ± 134	691 ± 103	*607 ± 61*
3628	Galactose kinase	774 ± 151	749 ± 90	742 ± 93	*471 ± 50*
3629	Selenium binding protein	1930 ± 279	1392 ± 320	1601 ± 32	*1039 ± 296*
3921	Heat shock protein 70E	949 ± 40	933 ± 261	798 ± 250	*603 ± 80*
4732	Heat shock protein 70A	2370 ± 133	2627 ± 386	2837 ± 603	*1719 ± 155*
4830	Flagellar associated protein	872 ± 63	734 ± 301	703 ± 175	*284 ± 22*
4923	Heat shock protein 70E	1264 ± 206	1129 ± 204	1213 ± 306	*641 ± 148*
5525	Predicted protein	410 ± 140	343 ± 37	320 ± 6	*188 ± 113*
6022	Photosystem I reaction center subunit XI	1652 ± 298	1487 ± 187	1194 ± 130	*1062 ± 207*
6535	4-Hydroxy-3-methylbut-2-enyl diphosphate reductase	501 ± 81	385 ± 85	338 ± 59	*315 ± 3*

Table 2 continued

Spot #	Protein	Averaged spot density at time following LL → HL shift			
		Control (LL)	1.5 h	3 h	6 h
6734	Vacuolar ATP synthase, subunit A	614 ± 118	571 ± 153	511 ± 25	*370 ± 35*
6737	Aspartyl-tRNA synthetase	469 ± 115	353 ± 78	318 ± 14	*239 ± 29*
6738	*N*-ethylmaleimide sensitive fusion protein	425 ± 55	375 ± 93	351 ± 55	*235 ± 39*
6743	Phosphoglucomutase	442 ± 89	377 ± 112	343 ± 17	*185 ± 62*
6824	Chaperone, Hsp100 family, ClpC-type	2941 ± 135	2344 ± 595	2639 ± 547	*1773 ± 143*
6829	Hypothetical protein CHLREDRAFT_82920	772 ± 53	598 ± 193	676 ± 136	*474 ± 62*
7218	Predicted protein	796 ± 77	589 ± 155	610 ± 111	*528 ± 58*
7527	Phosphoglycerate kinase	971 ± 144	780 ± 129	668 ± 119	*630 ± 46*
7529	RuBisCO large subunit	1116 ± 192	856 ± 103	937 ± 205	*699 ± 80*
7621	Subunit of exon junction complex	866 ± 112	721 ± 230	702 ± 172	*330 ± 70*
8219	Chlorophyll *a-b* binding protein of LHCII	1044 ± 128	1163 ± 301	968 ± 233	*639 ± 21*
8221	4 Ran-like small GTPase	1415 ± 234	1249 ± 209	1131 ± 222	*715 ± 197*
8334	Acidic ribosomal protein P0	816 ± 355	424 ± 185	859 ± 372	*337 ± 126*
8535	Delta-aminolevulinic acid dehydratase	950 ± 203	774 ± 96	692 ± 179	*575 ± 21*
8546	LL-Diaminopimelate aminotransferase	980 ± 217	835 ± 167	665 ± 159	*587 ± 108*
8626	Acetohydroxy acid isomeroreductase	1942 ± 83	1612 ± 264	1714 ± 145	*1155 ± 131*
8627	RuBisCO large subunit	1631 ± 210	996 ± 371	1084 ± 443	*567 ± 103*
8629	*S*-Adenosylmethionine synthetase	1764 ± 323	1683 ± 630	1984 ± 202	*837 ± 121*
8734	Dynamin-related GTPase	960 ± 8	861 ± 147	881 ± 131	*516 ± 69*

Averaged spot densities of proteins (3 biological replicates each ± SD) at time 1.5, 3 and 6 h after the transition from LL → HL were subjected to pair-wise *t* test statistical analysis against the respective values of the LL control. The *italicised* values indicates the time points where the expression level of that particular protein was significantly different from the control level. *P* values of all samples were less than 0.05

therefore, will only discuss on the key finding that might be interpreted in a sensible way. The early changes we observed were rearrangements of the light-harvesting antenna proteins, manifested by the up- and down-regulation of several protein spots identified as the LHC-II polypeptides (Tables 2, 3). Since many of the enhanced spots matched with the stress-related LHC, these proteins might have pivotal roles in handling of the greater ensuing photon flux density of irradiance stress. We also found increased expressions of the proteins involved in carbohydrate metabolisms at 1.5 h after transition to HL. The higher rate of carbohydrate metabolism could also help accelerate the utilization of electrons generated by the photosynthetic light reactions, minimizing the risk of superoxide formation. Another response of *C. reinhardtii* to irradiance stress observed in this study is the increase in spot intensities of the phytoene desaturase (PDS) and ChlI subunit of the Mg-chelatase enzyme (Table 3). PDS is one of the important enzymes in carotenoid biosynthesis pathway catalyzing a conversion of phytoene to ζ-carotene via two successive dehydrogenations. As carotenoid accumulation is one of the typical plant responses to HL, the elevation of PDS is foreseeable and is commonly observed (Steinbrenner and Linden 2003; Schäfer et al. 2006). It has been reported in the literature that Chl biosynthesis is suppressed under HL condition due to inhibition of ALA synthesis (Aarti et al. 2007). As the Chl biosynthesis is slowed down at the upstream part of the pathway, plant cells may respond to the lack of Chl by up-regulate expression of the downstream components. Hence, it is possible that enhanced expression of ChlI protein discerned in our study may just be a side effect of HL instead of the elevated rate of Chl biosynthesis.

To our surprise was the finding that several important molecular chaperones were down-regulated in *Chlamydomonas* exposed to excessive growth irradiance for up to 6 h. In the literature, primary functions of the molecular chaperones are thought to be for assisting protein folding/refolding. However, as molecular chaperones are the housekeeping proteins, they could as well have many other specialized functions, including translation, protein trafficking, proteolytic cleavage, etc. The first evidence supporting the active role of molecular chaperones during plant adaption to irradiance stress came from the work from Schroda and his colleagues in Germany. Using *C. reinhardtii* as a model, this group of scientists discovered that down-regulation of a chloroplast-localized heat-shock protein 70 (HSP70B) by antisense technique makes the transformants more susceptible to photo-oxidative damage than wild type (Schroda et al. 1999). On the contrary, the

Table 3 Averaged spot densities of proteins that were up-regulated during transition of *C. reinhardtii* from LL to HL

Spot #	Matched protein	Averaged spot density at time following LL → HL shift			
		Control (LL)	1.5 h	3 h	6 h
238	Putative membrane protein	n/d	*883 ± 281*	*624 ± 78*	*677 ± 197*
242	Stress-related chlorophyll *a/b* binding protein 2	n/d	*795 ± 306*	*861 ± 264*	*920 ± 118*
1230	Stress-related chlorophyll *a/b* binding protein 1	n/d	*1030 ± 253*	*899 ± 101*	*829 ± 139*
1236	Major light-harvesting complex II protein m3	79 ± 5	*1099 ± 239*	*1002 ± 86*	*953 ± 64*
2130	Major light-harvesting complex II protein m1	5510 ± 1424	*14242 ± 596*	*10195 ± 2322*	*12561 ± 2012*
2224	Major light-harvesting complex II protein m3	2441 ± 695	*4029 ± 97*	*4131 ± 213*	*4316 ± 1081*
2431	Sedoheptulose-1,7-bisphosphatase	n/d	*1108 ± 162*	*1092 ± 202*	*1148 ± 198*
2730	RbcL-binding protein subunit alpha	n/d	*688 ± 145*	*675 ± 111*	*886 ± 187*
3126	Oxygen-evolving enhancer protein 2	693 ± 77	*1400 ± 188*	*1379 ± 53*	*1454 ± 442*
3223	Chlorophyll *a-b* binding protein of LHCII type I	2254 ± 439	*4081 ± 509*	*3814 ± 642*	*3499 ± 304*
3424	Magnesium chelatase subunit chlI	n/d	*392 ± 63*	*422 ± 50*	*452 ± 58*
5225	Triose phosphate isomerase	n/d	*751 ± 193*	*728 ± 98*	*871 ± 196*
6223	Triose phosphate isomerase	1441 ± 97	*2455 ± 483*	*2033 ± 251*	*2127 ± 264*
6428	Phosphoribulokinase	n/d	*605 ± 68*	*620 ± 37*	*690 ± 92*
6544	Hypothetical protein CHLREDRAFT_132041	n/d	*688 ± 204*	*689 ± 69*	*449 ± 56*
8422	Plastid-specific ribosomal protein 1	n/d	*431 ± 68*	*477 ± 135*	*437 ± 80*
8632	Phytoene desaturase	n/d	*345 ± 106*	*274 ± 66*	*291 ± 47*
2228	Chlorophyll *a-b* binding protein of LHCII type I	2620 ± 453	*4737 ± 611*	3954 ± 508	*5216 ± 633*
9623	Serine hydroxymethyltransferase 2	1325 ± 156	*1645 ± 110*	*1710 ± 178*	1162 ± 306
240	LI818r-1	n/d	n/d	*746 ± 134*	*854 ± 206*
245	Hypothetical protein	n/d	n/d	*968 ± 147*	*949 ± 82*
616	Calreticulin 2, calcium-binding protein	1777 ± 165	2260 ± 248	*2722 ± 367*	*2780 ± 128*
2328	Minor chlorophyll *a-b* binding protein of PSII	1920 ± 112	3274 ± 1076	*4790 ± 1157*	*5496 ± 570*
2828	Heat shock protein 70B	731 ± 117	1114 ± 308	*1289 ± 143*	*1515 ± 299*
3625	ATP synthase CF1 beta subunit	2298 ± 554	2568 ± 231	*3110 ± 299*	*3780 ± 385*
4117	Oxygen-evolving enhancer protein 2	n/d	n/d	*946 ± 181*	*956 ± 79*
5029	Oxygen evolving enhancer protein 3	n/d	n/d	*1821 ± 341*	*2506 ± 278*
6331	Predicted protein	n/d	n/d	*630 ± 56*	*721 ± 128*
6335	Phosphoglycolate phosphatase	182 ± 16	212 ± 22	*290 ± 36*	*272 ± 19*
3326	Minor chlorophyll *a-b* binding protein of PSII	4576 ± 227	5060 ± 366	*5895 ± 147*	4934 ± 868
8824	Cobalamin-independent methionine synthase	1929 ± 549	2778 ± 1110	*3322 ± 814*	2088 ± 436
7530	Phosphoglycerate kinase	662 ± 70	780 ± 147	1104 ± 334	*1281 ± 80*

Averaged spot densities of proteins (3 biological replicates each ± SD) at time 1.5, 3 and 6 h after the transition from LL → HL were subjected to pair-wise *t* test statistical analysis against the respective values of the LL control. The *italicised* values indicates the time points where the expression level of that particular protein was significantly different from the control level

n/d the protein could not be detected at that time point

P values of all samples were less than 0.05

transformants overexpressing such protein are more resistant to high light compared to the wild type counterpart (Schroda et al. 1999). Yokthongwattana et al. (2001) further demonstrated that HSP70B could be part of the PSII repair intermediate complex. Thus, it has been proposed that HSP70B plays important roles in the PSII repair process (Schroda et al. 2001; Yokthongwattana et al. 2009). In this study, the increasing level of HSP70B after 3 h of transition to HL is consistent with the previous evidence in the literature regarding its functions. However, CPN60, ClpC, HSP70A and HSP70E were found to be underexpressed. HSP70 is a large protein family found in all living organisms. Although HSP70 chaperones have been reported to carry out a wide range of specialized cellular functions, including the PSII repair process, their predominant role is thought to be for helping renature the unfolded or misfolded proteins during stresses. HSP70A is a well-known cytosolic protein (Müller et al. 1992) believed to

function as a typical chaperonin. HSP70E, on the other hand, was identified during the *C. reinhardtii* genome sequencing as an ORF that shares some degree of homology to the HSP70 and HSP110 protein family (Schroda 2004). It is predicted to encode for a cytosolic protein of about 87 kDa, the function of which has not been characterized. It is possible that both HSP70A and 70E may function in facilitating the transport/trafficking of nuclear-encoded proteins important for HL acclimation. Down regulation of these two proteins might results in the alga unable to cope with the excessive irradiance.

CPN60 or HSP60, which is a plastid homologue of bacterial GroEL (Viitanen et al. 1995), was suggested to help refold the denatured proteins by the same mechanism as that of the famous bacterial GroES/GroEL system. The primary substrate for the CPN60 could be Rubisco large subunit (RbcL) proteins (Schroda 2004). Decreasing level of the CPN60 may perhaps lead to accumulation of the Rubisco enzyme in the inactive form. The lack of the active Rubisco leads to an imbalance between the rate of CO_2 assimilation and the rate of photon absorption and electron transport events. Therefore, lowering in the amount of the CPN60 could well explain the lower threshold of irradiance in *C. reinhardtii*.

HSP100 or Clp is also a large protein family found in both prokaryotes and eukaryotic organisms (Schirmer et al. 1996). The renowned function of Clp chaperones, especially ClpB, is their ability to dissociate protein aggregates and help them refold (Goloubinoff et al. 1999). In the chloroplast stroma of plants and green algae, ClpC and ClpD are the two homologues of the HSP100 protein family (Zheng et al. 2002). So far, the only reported function of ClpC is believed to facilitate protein import into the chloroplast (Nielsen et al. 1997).

Considering the fact that these molecular chaperones are housekeeping proteins normally expressed constitutively in the cell, reduction in their abundance even a small proportion could result in drastic effects. Such down regulation of the abovementioned chaperones and heat-shock proteins in response to irradiance stress could partially explain the light-sensitive nature of *C. reinhardtii*. Lower amount of these key chaperones could lead to accumulation of denatured proteins in both chloroplast stroma and cytosol causing cell death. Presumably, this alga does not down regulate these important proteins on purpose but rather the cell may not be able to keep up the rate of their biosynthesis with the rapid rate of reduction under high light. Further in-depth research on these molecular chaperones could provide better understanding on their expression pattern and functions.

Acknowledgments This work was financially supported in part by funding from Mahidol University and Thailand Research Fund.

References

Aarti D, Tanaka R, Ito H, Tanaka A (2007) High light inhibits chlorophyll biosynthesis at the level of 5-aminolevulinate synthesis during de-etiolation in cucumber (*Cucumis sativus*) cotyledons. Photochem Photobiol 83:171–176

Drzymalla C, Schroda M, Beck CF (1996) Light-inducible gene *hsp70B* encodes a chloroplast-localized heat shock protein in *Chlamydomonas reinhardtii*. Plant Mol Biol 31:1185–1194

Förster B, Mathesius U, Pogson BJ (2006) Comparative proteomics of high light stress in the model alga *Chlamydomonas reinhardtii*. Proteomics 6:4309–4320

Goloubinoff P, Mogk A, Ben Zvi AP, Tomoyasu T, Bukau B (1999) Sequential mechanism of solubilization and refolding of stable protein aggregates by a bichaperone network. Proc Natl Acad Sci USA 96:13732–13737

Laemmli UK (1970) Cleavage of structural proteins during the assembly of the head of bacteriophage T4. Nature 227:680–685

Melis A (1999) Photosystem-II damage and repair cycle in chloroplasts: what modulates the rate of photodamage in vivo? Trends Plant Sci 4:130–135

Mitprasat M, Roytrakul S, Jiemsup S, Boonseng O, Yokthongwattana K (2011) Leaf proteomic analysis in cassava (*Manihot esculenta*, Crantz) during plant development, from planting of stem cutting to storage root formation. Planta 233:1209–1221

Müller FW, Igloi GL, Beck CF (1992) Structure of a gene encoding heat-shock protein HSP70 from the unicellular alga *Chlamydomonas reinhardtii*. Gene 111:165–173

Nielsen E, Akita M, Davila-Aponte J, Keegstra K (1997) Stable association of chloroplastic precursors with protein translocation complexes that contain proteins from both envelope membranes and a stromal Hsp100 molecular chaperone. EMBO J 16:935–946

Niyogi KK (1999) Photoprotection revisited: genetic and molecular approaches. Annu Rev Plant Physiol Plant Mol Biol 50:333–359

Polle JEW, Benemann JR, Tanaka A, Melis A (2000) Photosynthetic apparatus organization and function in the wild type and a chlorophyll *b*-less mutant of *Chlamydomonas reinhardtii*. Dependence on carbon source. Planta 211:335–344

Rolland N, Atteia A, Decottignies P, Garin J, Hippler M, Kreimer G, Lemaire SD, Mittag M, Vagner V (2009) Chlamydomonas proteomics. Curr Opin Microbiol 12:285–291

Schäfer L, Sandmann M, Woitsch S, Sandmann G (2006) Coordinate up-regulation of carotenoid biosynthesis as a response to light stress in *Synechococcus* PCC7942. Plant Cell Environ 29:1349–1356

Schirmer EC, Glover JR, Singer MA, Lindquist S (1996) HSP100/Clp proteins: a common mechanism explains diverse functions. Trends Biochem Sci 21:289–296

Schroda M (2004) The *Chlamydomonas* genome reveals its secrets: chaperone genes and the potential roles of their gene products in the chloroplast. Photosynth Res 82:221–240

Schroda M, Kropat J, Oster U, Rüdiger W, Vallon O, Wollman F-A, Beck CF (2001) Possible role for molecular chaperones in assembly and repair of photosystem II. Biochem Soc Trans 29:413–418

Schroda M, Vallon O, Wollman FA, Beck CF (1999) A chloroplast-targetedheat shock protein 70 (HSP70) contributes to the photoprotection and repair of photosystem II during and after photoinhibition. Plant Cell 11:1165–1178

Steinbrenner J, Linden H (2003) Light induction of carotenoid biosynthesis genes in the green alga *Haematococcus pluvialis*: regulation by photosynthetic redox control. Plant Mol Biol 52:343–356

Viitanen PV, Schmidt M, Buchner J, Suzuki T, Vierling E, Dickson R, Lorimer G, Gatenby A, Soll J (1995) Functional characterization of the higher plant chloroplast chaperonins. J Biol Chem 270:18158–18164

Yokthongwattana K, Chrost B, Behrman S, Casper-Lindley C, Melis A (2001) Photosystem II damage and repair cycle in the green alga *Dunaliella salina*: involvement of a chloroplast-localized HSP70. Plant Cell Physiol 42:1389–1397

Yokthongwattana K, Jin E, Melis A (2009) Chloroplast acclimation, photodamage and repair reactions of photosystem-II in the model green alga *Dunaliella salina*. In: Ben-Amotz A, Polle JEW, Rao DVS (eds) The alga *Dunaliella*: biodiversity physiology genomics and biotechnology. Science Publishers, New Hampshire, pp 273–299

Zheng B, Halperin T, Hruskova-Heidingsfeldova O, Adam Z, Clarke AK (2002) Characterization of chloroplast Clp proteins in Arabidopsis: localization, tissue specificity and stress responses. Physiol Plant 114:92–101

Planta (2012) 235:649–659
DOI 10.1007/s00425-012-1594-1

RAPID COMMUNICATION

Proteomic analysis of salinity-stressed *Chlamydomonas reinhardtii* revealed differential suppression and induction of a large number of important housekeeping proteins

Chotika Yokthongwattana · Bancha Mahong · Sittiruk Roytrakul · Narumon Phaonaklop · Jarunya Narangajavana · Kittisak Yokthongwattana

Received: 19 December 2011 / Accepted: 11 January 2012 / Published online: 26 January 2012

Abstract Salinity stress is one of the most common abiotic stresses that hamper plant productivity worldwide. Successful plant adaptations to salt stress require substantial changes in cellular protein expression. In this work, we present a 2-DE-based proteomic analysis of a model unicellular green alga, *Chlamydomonas reinhardtii*, subjected to 300 mM NaCl for 2 h. Results showed that, in addition to the protein spots that showed partial up- or down-regulation patterns, a number of proteins were exclusively present in the proteome of the control cells, but were absent from the salinity-stressed samples. Conversely, a large number of proteins exclusively appeared in the proteome of the salinity-stressed samples. Of those exclusive proteins, we could successfully identify, via LC–MS/MS, 18 spots uniquely present in the control cells and 99 spots specific to NaCl-treated cells. Interestingly, among the salt-exclusive protein spots, we identified several important housekeeping proteins like molecular chaperones and proteins of the translation machinery, suggesting that they may originate from post-translational modifications rather than from de novo biosynthesis. The possible role and the salt-specific modification of these proteins by salinity stress are discussed.

Keywords Abiotic stress · *Chlamydomonas* · NaCl · Proteomics · Salt-specific proteins · Salt stress

Abbreviations

2-DE	Two-dimensional gel electrophoresis
LC–MS/MS	Liquid chromatography couple with tandem mass spectrometry
PTM	Post-translational modification
ROS	Reactive oxygen species

C. Yokthongwattana
Department of Biochemistry, Faculty of Science, Kasetsart University, 50 Phahonyothin Rd., Bangkok 10900, Thailand

B. Mahong · K. Yokthongwattana (✉)
Department of Biochemistry, Center for Excellence in Protein Structure and Function, Faculty of Science, Mahidol University, 272 Rama 6 Rd., Bangkok 10400, Thailand
e-mail: tekyw@mahidol.ac.th

Present Address:
B. Mahong
Department of Plant Molecular Systems Biotechnology, Crop Biotech Institute, Kyung Hee University, Yongin 446–701, Korea

S. Roytrakul · N. Phaonaklop
Genome Institute, National Center for Genetic Engineering and Biotechnology, 113 Thailand Science Park, Phahonyothin Rd., Pathumthani 12120, Thailand

J. Narangajavana
Department of Biotechnology, Faculty of Science, Mahidol University, 272 Rama 6 Rd., Bangkok 10400, Thailand

Introduction

Salinity stress is one of the major abiotic stresses that encumber plant productivity (Boyer 1982). Increasing salt concentration, especially of NaCl, in the environment affects plants in many different ways. Such effects can be as small as lower photosynthetic productivity or as harsh as causing plant death. Hypertonic concentration of NaCl in the surrounding environment results in osmotic stress, which ultimately leads to water loss from plant cells. Excessive concentration of Na^+ outside the cell that could leak into plant cytoplasm can also cause toxicity (Munns et al. 2006). For survival, plants must respond to salt stress

in different manners from turning on or off gene expression to biochemical and physiological adaptations (Taji et al. 2004). In general, the common strategies that plants counteract hyperosmotic stress induced by excessive salinity are (a) to prevent water loss by synthesizing and accumulating counter-osmolytes and (b) to maintain internal concentration of Na^+ by regulating the corresponding transporters or pump (Bohnert et al. 1999). Albeit sharing the common responses to salt stress, different plants exhibit diverse level of tolerance toward salinity. As the aforementioned responses are commenced from a complex network of cellular events, such diversity in salt tolerance may originate from minor differences at the molecular level. Thus, comparative studies of how different plant species respond to salt stress may provide a better understanding of how certain plants can successfully adapt to high saline environment while others cannot.

Physiological and biochemical studies of plant responses to salt stress have been extensively conducted. Increasing salt concentration in the soil leads to water loss, which in turn results in closure of stomata via the effect of abscisic acid (Mahajan and Tuteja 2005). Excessive NaCl also has both direct and indirect negative effects on photosynthesis (Shama and Hall 1991; Lawlor and Cornic 2002; Vega et al. 2006). Limited availability of CO_2 as a result of stomatal closure leads to imbalance between photosynthetic electron transport and carbon assimilation reactions (Chaves et al. 2009). Such disturbance on photosynthesis leads to oxidative stress, generating toxic level of ROS (Abogadallah 2010). Moreover, it has been reported that salt stress exacerbates the rate of photosystem II (PSII) photoinactivation (Neale and Melis 1989; Shama and Hall 1991) by the suppression of D1 protein turnover at both transcriptional and translational level (Allakhverdiev et al. 2002). Not only the PSII is primary target of salinity stress, but structural organization and electron transport reaction at photosystem I (PSI) have also been reported to be affected. In a model unicellular green alga *Chlamydomonas reinhardtii*, hyperosmotic stress caused by NaCl led to the suppression of electron transfer between plastocyanin and P_{700}^+ (Cruz et al. 2007) as well as structural damage to the PSI-LHCI (Subramanyam et al. 2010). Oxidation and degradation of Rubisco enzyme have also been reported to be a consequence of saline stress (Marín-Navarro and Moreno 2006). Thus, proper adjustment of photosynthetic apparatus and detoxification of the ROS are the important plant responses toward salt stress. In addition to photosynthesis, it was reported that NaCl stress elicits phospholipid signaling pathways via activation of phospholipase A_2 (Arisz and Munnik 2011). Salinity stress imposed on *C. reinhardtii* also triggers the cells to release volatile organic compounds and to accumulate oil (Siaut et al. 2011; Zuo et al. 2012).

Plant adaptations to stresses often require substantial changes in protein expression. Analysis of the proteome profile of an organism can, therefore, provide useful information of complex protein mixtures that are being expressed in the cell under any particular stress condition. Proteomic studies of salt stress response have been frequently reported in many land plant species, including in *Arabidopsis* (Ndimba et al. 2005; Pang et al. 2010), maize (Zörb et al. 2009), potato (Aghaei et al. 2008), rice (Abbasi and Komatsu 2004; Dooki et al. 2006; Chitteti and Peng 2007), etc. The most common patterns of proteome changes manifested under salt stress are enhanced expressions of enzymes involved in carbohydrate catabolism, enzymes in the pathway for biosynthesis of compatible solutes, antioxidant enzymes, molecular chaperones, etc. (Abbasi and Komatsu 2004; Ndimba et al. 2005; Dooki et al. 2006; Wang et al. 2008). Those observations led to the suggestion that under salinity stress, plants require huge amount of energy for maintaining intracellular ion homeostasis and counter-osmolytes to balance osmotic pressure. Up-regulation of antioxidant enzymes and various heat-shock proteins could also be important for getting rid of ROS as well as for renaturing the denatured proteins. However, higher plants are complex organisms comprise different tissues and cell types, each responding differently to salt stress. As proteomic analyses are often performed on one particular cell or tissue type, multiple studies on different parts of the plant body are important for accurate interpretation of the protein expressions in relation to the physiological responses.

Aquatic unicellular microalgae, on the other hand, lack the complication of tissues and cell types. As the single-cell algae are always in contact with the environment, high salt concentration in the surrounding water is directly and uniformly responded by individual cells. Hence, the microalgae can serve as good models for investigation of plant salinity stress response at the cellular and molecular level. To date, there have been very few proteomic reports on salinity stress of aquatic microalgae, most of which were carried out on the cyanobacterium *Synechocystis* (Fulda et al. 2006; Huang et al. 2006; Pandhal et al. 2008, 2009). The only proteomic paper describing salt stress response of eukaryotic microalgae was on a halophilic green alga *Dunaliella* sp. (Liska et al. 2004). As both *Synechocystis* and *Dunaliella* are rather halotolerant, additional complementary proteomic analysis on a salt-sensitive alga could provide useful data for comparison with those tolerant species. In this study, a comparative proteomic analysis was performed in a model unicellular green alga *Chlamydomonas reinhardtii* challenged with a short-term exposure to 300 mM NaCl versus cells grown in normal TAP medium. Results showed that a number of proteins could be exclusively detected in one sample but not in the other.

Discussions were made on the possible roles of these proteins in salt stress response.

Materials and methods

Plant material and growth conditions

Unicellular green alga *Chlamydomonas reinhardtii* strain CC-503 was grown mixotrophically in TAP medium (Harris 1989) under 50 μmol photons m^{-2} s^{-1} of constant illumination. When the cultures reached mid-logarithmic phase, cells were pelleted down by centrifugation at $\sim 1{,}000 \times g$. The cell pellets were either resuspended back in the TAP medium (control) or in TAP medium containing 300 mM NaCl (TAP-NaCl, salt-shocked). In the previous proteomic report on salt-stressed *Synechocystis*, the analysis was conducted after the cells were challenged with high salinity for 2 h (Fulda et al. 2006). For comparative purpose, *C. reinhardtii* cells in this study were also allowed to grow in the new media (in the presence or absence of 300 mM NaCl) for another 2 h before harvesting by centrifugation at $1{,}000 \times g$ for the subsequent protein extraction.

Protein isolation and 2-DE separation

Isolation of total proteins from *Chlamydomonas* cells were conducted as previously described in Mahong et al. (2012). The protein samples were separated according to the p*I* in the 1st dimension on 13-cm immobilized pH gradient (4–7) strips (GE Healthcare) using IPGphor3 machine (GE Healthcare) with standard running condition as suggested by the manufacturer's manual. In the 2nd dimension, the IEF-resolved proteins were separated according to their molecular size by standard Tris–glycine SDS-PAGE using 13-cm 12.5% acrylamide gel. The resolved 2-DE gels were stained by colloidal Coomassie blue G for visualization.

Gel image analysis

Gels were scanned and protein spot profiles were analyzed by computer software PDQuest™ (Bio-Rad Laboratory). Protein spots that "consistently" appeared on every gel image of different biological replicates for the same type of cultures (control or salt shocked) were marked by the software and used for construction of master virtual images. For spots that were missing from any of the biological replicates within the same set of cultures were excluded from the subsequence cross-comparison between control and salt-stressed samples. Only protein spots that showed "exclusive expression" i.e., only appeared in the control but not in the salt stress sample, and vice versa, were marked as differentially expressed proteins and were subjected to identification by LC–MS/MS.

Protein identification by mass spectrometry

In-gel tryptic digestion of the protein spots and subsequent tandem mass spectrometric analysis for identification of the protein spots were performed as described previously (Mahong et al. 2012).

Results

At first, total proteins of control *C. reinhardtii* culture grown under normal TAP medium and the salt-shocked cells were subjected to 2-DE separation using strips of pH 3–10. However, as more than 80% of the proteins scattered in the middle of the gel (results not shown), strips with narrower pH gradient range of 4–7 were used for better visibility and resolution. Representative of the 2-DE-based proteome profiles of the control cells is presented in Fig. 1a, while that of the salt-shocked samples is illustrated in Fig. 1b. Cross comparison of the proteome profiles between the two sets of samples revealed a large number of differentially expressed protein spots. As there have already been a lot of proteomic studies reporting on plant proteins that are partially up- or down-regulated under salt stress, we opted for a more stringent criterion of analysis. In this study, the protein spots that their expressions exclusively appeared in one group of samples (either in the control- or salt-shocked cells) but not in another group were picked for subsequent identification by tandem mass spectrometry. Even with this strict criterion, we could distinguish more than 100 proteins matched with our screening. Of these, we could elucidate the identities of only 18 spots from the population of proteins that exclusively appeared in *C. reinhardtii* cells grown under normal TAP medium and 99 proteins that are solely discernible in the salt-shocked cells.

Table 1 lists all the 18 proteins that uniquely appeared in the control *Chlamydomonas* cells. Most of the polypeptides in this group are enzymes involved in general metabolic pathways. We found four proteins in the group of TCA cycle and energy metabolism including ATP synthase beta (spot #2613) and gamma (#416) subunits and its associated protein (#9214) as well as isocitrate lyase (#5311). Two spots each of proteins involved in carbohydrate metabolisms (#9209 and 9612) and photosynthesis (#1615 and 2131) were not observed in the salt-shocked cells. There was only one spot each of enzyme in the amino acid and fatty acid metabolism (spot #1022 and 9614, respectively), protein folding (#141), and protein translation (#140). The notable proteins in this group are the

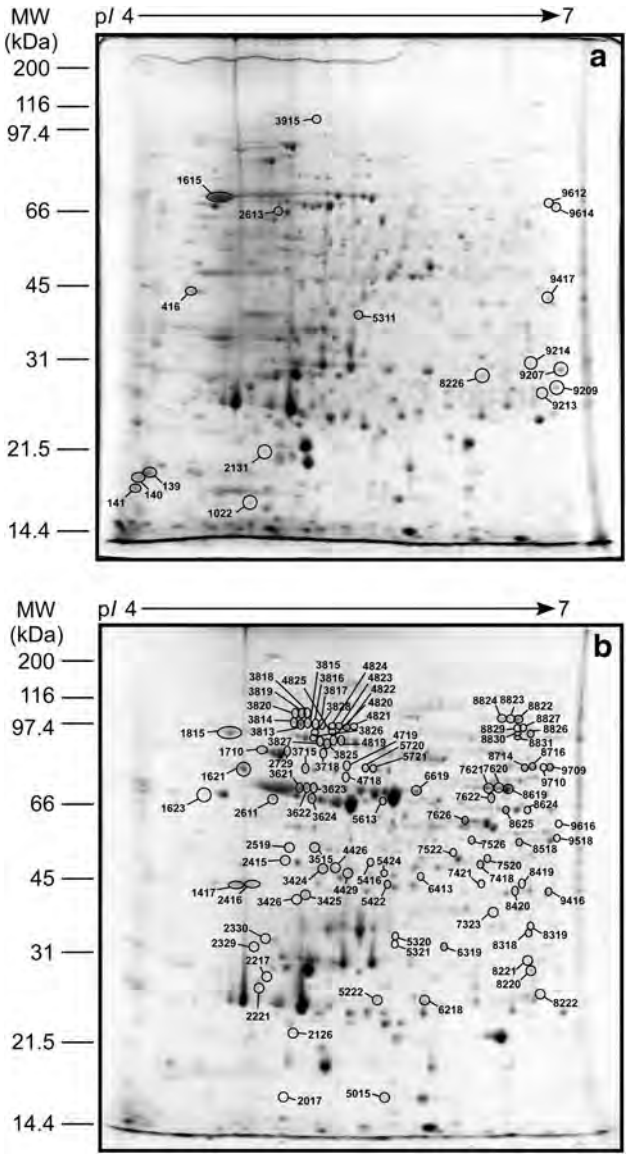

Fig. 1 Representative images of 2-DE-resolved protein spot profiles of control *C. reinhardtii* cells grown under normal TAP medium (**a**) and 2 h salt-shocked cultures (**b**). Proteins were separated according to their p*I* in the first dimension using 13 cm strip with pH gradient range of 4–7. Separations in the 2nd dimension were carried out using standard SDS-PAGE with 12.5% acrylamide gels. Protein spots were visualized by staining with colloidal Coomassie blue G. Numbered spots correspond to the identified spot # in Tables 1 and 2

telomere-binding proteins (spot #8226, 9207, 9213 in Fig. 1a). The absence of these telomere-binding proteins in the salt-shocked cells may suggest possible alteration in the chromatin structure under salinity stress condition. Functions of the remaining three spots could not be postulated as they were identified as unknown proteins (spot #139, 3915 and 9417).

Particularly remarkable was the identification of the 99 protein spots that were found only in the salt-shocked but not in the control cells of *C. reinhardtii*. Table 2 shows identities of those proteins as determined by LC–MS/MS, which can be classified into 11 groups based on their cellular functions. Figure 2 illustrates the proportions of proteins in each group, which include: carbohydrate (11%) and amino acid (12%) metabolisms, metabolism of vitamin and cofactors (4%), metabolism of terpenoids and polyketides (1%), TCA cycle and energy metabolism (10%), photosynthesis (8%), stress-related proteins (~15%), protein translation (13%), protein folding/sorting/degradation (9%), protein of miscellaneous functions (7%) and unknown proteins (10%). Among the 99 proteins, 11 of which are enzymes involved in carbohydrate metabolism. We found three spots (#8714, 9709, 9710) matched with splice variant of PEP carboxykinase enzymes, 2 each of phosphoribulokinase (#6218, 7522) and glyceraldehyde-3-phosphate dehydrogenase (#3424, 4426) and one spot each of pyruvate dehydrogenase E1 beta subunit (#3425), pyruvate dehydrogenase (#7520), phosphoglycerate kinase (#8518) and succinate-CoA ligase beta chain (#9518).

Twelve proteins that showed exclusive expression in the salt-shocked samples belong to the group of amino acid metabolism. Pyruvate–formate lyase (#8826, 8827, 8829, 8830) and cobalamin-independent methionine synthase (#8822, 8823, 8824) occupy the majority of the protein spots found in this group. Ten polypeptides fall into the group of TCA cycle and energy metabolism, most of which (8 spots) were identified as subunits of ATP synthase enzyme both mitochondrial and chloroplast version (#1417, 1710, 2416, 2729, 3624, 5613, 6619) and its associated protein (#7323). For photosynthetic proteins that appeared only under salinity stress, six out of eight spots were identified as chain A subunit of the Rubisco enzyme (#3621, 3622, 3623, 7620, 7621, 8619) while two others are LHC-II and a subunit of cytochrome b_6f complex (#2221 and 5015, respectively). We also found specific appearance of membrane AAA-metalloprotease (#3825, 3827), chloroplast membrane translocon 7 (#3816, 3817), cyclophilin-type peptidyl-prolyl cis–trans isomerase (#2415, 5424), and one spot each of protein disulfide isomerase (#1621), translocon component Tic40-related protein (#2611) and ubiquitin conjugating enzyme E2 (#2017) in the salt-shocked cells of *C. reinhardtii*.

Protein translation and stress-related proteins (Table 2) are the two largest groups of proteins, the corresponding spots of which could only be discerned in the short-term exposure of *Chlamydomonas* to 300 mM NaCl. Protein spots distinguished as translation machineries including ribosomal proteins (#2217, 7421, 8220, 9416), initiation (#2126, 2519, 8419) and elongation (#4822, 4823, 4824, 7626) factors occupy the majority population in the former group. To our surprise was the finding that in the group of stress proteins, 11 out of 14 spots could be identified as

Table 1 List of identified protein spots that are solely detectable in the cells of *C. reinhardtii* grown in TAP medium but not present in the proteome of the salt-shock cultures

Spot #	Identified as	NCBI accession #	Organism	Observed MW (kDa)/p*I*	Theoretical MW (kDa)/p*I*	Search score	% Sequence coverage
Carbohydrate metabolism							
9209	Phosphoenolpyruvate carboxykinase	gil74272695	*C. incerta*	27.1/7.0	24.5/8.65	70	4
9612	Dihydrolipoamide dehydrogenase	gil159463380	*C. reinhardtii*	68.4/7.0	60.1/8.73	103	4
Amino acid metabolism							
1022	Homocysteine methyltransferase	gil3334258	*C. reinhardtii*	18.0/4.9	87.2/6.02	80	1
Fatty acid metabolism							
9614	Biotin carboxylase, acetyl-CoA carboxylase component	gil159488652	*C. reinhardtii*	67.7/7.0	52.3/8.96	222	9
TCA cycle and energy metabolism							
416	ATP synthase, gamma subunit	gil228698	*C. reinhardtii*	44.1/4.6	39.1/9.08	150	6
2613	Mitochondrial ATP synthase beta subunit	gil159466892	*C. reinhardtii*	65.8/5.1	62.0/5.00	241	8
5311	Isocitrate lyase	gil619932	*C. reinhardtii*	39.5/5.7	45.8/5.78	73	2
9214	Mitochondrial ATP synthase-associated 31.2-kDa protein	gil159470863	*C. reinhardtii*	30.7/6.9	34.1/6.86	77	3
Photosynthesis							
1615	Rubisco, chain A	gil16975080	*C. reinhardtii*	70.7/4.8	53.1/6.04	174	10
2131	Light-harvesting complex protein I-20	gil18125	*C. reinhardtii*	21.3/5.0	23.5/7.98	63	4
Protein folding, sorting, degradation							
141	Peptidyl-prolyl cis–trans isomerase, cyclophilin-type	gil159484660	*C. reinhardtii*	19.1/4.0	18.6/7.66	48	6
Chromatin structure							
8226	G strand-binding protein 1/telomere-binding protein	gil74272657	*C. incerta*	29.6/6.5	24.5/6.78	132	7
9207	G strand-binding protein 1/telomere-binding protein	gil74272657	*C. incerta*	29.6/7.0	24.5/6.78	393	20
9213	G strand-binding protein 1/telomere-binding protein	gil74272657	*C. incerta*	26.6/6.9	24.5/6.78	212	9
Protein translation							
140	Ribosomal protein L12	gil159477751	*C. reinhardtii*	19.7/4.0	17.8/9.19	222	25
Unknown proteins							
139	Predicted protein	gil159463270	*C. reinhardtii*	20.2/4.0	20.7/5.10	129	13
3915	Predicted protein	gil159471910	*C. reinhardtii*	103.7/5.6	67.6/6.41	156	4
9417	Predicted protein	gil159487124	*C. reinhardtii*	43.7/7.0	31.0/8.50	65	3

Spots were resolved by 2-DE and identified by LC–MS/MS. Observed M_r and p*I* were calculated while the spot numbers were arbitrarily assigned by the PDQuest™ software. Mascot search score beyond 46 is considered as significant match. The identified proteins are listed according to their functional relevance

heat-shock proteins or molecular chaperones. We detected three spots corresponding to HSP90A (#3813, 3814, 3815), four spots to HSP90C (#3818, 3819, 3820, 4825), two spots matched with chaperonin 60C (#5720, 5721), one spot each of chaperonin 60A and HSP70A (#3715 and 4819, respectively). Three other protein spots in the group of stress-related proteins are antioxidant enzyme ascorbate peroxidase (#5321, 6329) and NADPH-dependent thioredoxin reductase (#4429). The remaining 22 protein spots exclusively expressed in the salt-shocked were classified as enzymes involved in metabolism of vitamin, cofactors, terpenoids and polyketides as well as proteins of miscellaneous function and unknown proteins.

Discussion

In complementary to the existing few reports on aquatic microalgae, we report here another proteomic study on the salinity stress response of the model freshwater unicellular green alga *C. reinhardtii*. From our results, the overall changes in the proteome profiles upon treating the algal

Table 2 List of proteins exclusively present in the 2-h salt-shocked cells but not in the control cultures of *C. reinhardtii*

Spot #	Protein	NCBI accession #	Organism	Observed M_r (kDa)/p*I*	Theoretical MW (kDa)/p*I*	Search score	% Sequence coverage
Carbohydrate metabolism							
3424	Glyceraldehyde-3-phosphate dehydrogenase	gil159463282	*C. reinhardtii*	48.3/5.3	40.5/9.17	290	17
3425	Pyruvate dehydrogenase E1 beta subunit	gil159482300	*C. reinhardtii*	41.9/5.2	38.5/5.53	500	23
4426	Chloroplast glyceraldehyde-3-phosphate dehydrogenase	gil74272659	*C. incerta*	48.0/5.4	40.0/9.08	207	10
6218	Phosphoribulokinase	gil159471788	*C. reinhardtii*	25.3/5.9	42.1/8.11	108	3
7520	Pyruvate dehydrogenase	gil15223294	*A. thaliana*	50.5/6.3	47.6/7.16	67	2
7522	Phosphoribulokinase	gil159471788	*C. reinhardtii*	51.5/6.1	42.1/8.11	316	17
8518	Phosphoglycerate kinase	gil1172455	*C. reinhardtii*	55.0/6.5	49.3/8.84	358	15
8714	Phosphoenolpyruvate carboxykinase, splice variant	gil159473683	*C. reinhardtii*	78.8/6.6	62.4/6.23	471	17
9518	Succinate-CoA ligase beta chain	gil159466790	*C. reinhardtii*	54.9/6.9	44.7/8.10	313	14
9709	Phosphoenolpyruvate carboxykinase, splice variant	gil159473683	*C. reinhardtii*	77.9/6.9	62.4/6.23	506	23
9710	Phosphoenolpyruvate carboxykinase, splice variant	gil159473683	*C. reinhardtii*	78.0/6.8	62.4/6.23	493	19
Amino acid metabolism							
7418	Glutamine synthetase	gil159469782	*C. reinhardtii*	48.7/6.3	41.7/7.14	368	22
7622	Acetolactate synthase, small subunit	gil159484278	*C. reinhardtii*	68.0/6.3	52.8/8.90	105	6
8625	Argininosuccinate synthase	gil159477301	*C. reinhardtii*	62.9/6.4	49.2/8.41	382	17
8716	Acetohydroxyacid dehydratase	gil159470063	*C. reinhardtii*	79.6/6.7	64.7/7.51	228	9
8822	Cobalamin-independent methionine synthase	gil159489910	*C. reinhardtii*	100.2/6.7	87.3/5.94	689	16
8823	Cobalamin-independent methionine synthase	gil159489910	*C. reinhardtii*	100.4/6.5	87.3/5.94	540	11
8824	Cobalamin-independent methionine synthase	gil159489910	*C. reinhardtii*	100.7/6.4	87.3/5.94	628	16
8826	Pyruvate–formate lyase	gil92084842	*C. reinhardtii*	93.3/6.7	93.7/6.40	512	12
8827	Pyruvate–formate lyase	gil159462978	*C. reinhardtii*	95.8/6.6	91.4/6.49	306	7
8829	Pyruvate–formate lyase	gil159462978	*C. reinhardtii*	96.1/6.6	91.4/6.49	278	7
8830	Pyruvate–formate lyase	gil159462978	*C. reinhardtii*	93.7/6.6	91.4/6.49	434	11
9616	Cystathionine gamma synthase	gil159475262	*C. reinhardtii*	59.3/6.9	51.1/7.28	90	2
Metabolism of vitamins and cofactors							
3426	Gamma glutamyl hydrolase	gil159476168	*C. reinhardtii*	41.1/5.2	41.4/5.34	210	10
3515	Magnesium chelatase subunit chlI	gil20137882	*C. reinhardtii*	53.0/5.3	45.5/6.22	463	22
5422	Thiazole biosynthetic enzyme	gil159481205	*C. reinhardtii*	44.8/5.7	37.0/6.72	112	7
6413	3,8-Divinyl protochlorophyllide *a* 8-vinyl reductase	gil159463876	*C. reinhardtii*	46.1/5.9	44.8/9.01	627	26
Metabolism of terpenoids and polyketides							
8831	1-Deoxy-D-xylulose-5-phosphate synthase	gil4185881	*C. reinhardtii*	91.4/6.5	79.3/7.07	375	9
TCA cycle and energy metabolism							
1417	Chloroplast ATP synthase, gamma chain	gil159476472	*C. reinhardtii*	44.0/4.9	39.1/9.08	336	18
1710	Mitochondrial ATP synthase, beta subunit	gil159466892	*C. reinhardtii*	84.2/5.0	62.0/4.99	783	28
2416	Chloroplast ATP synthase, gamma chain	gil159476472	*C. reinhardtii*	44.1/5.0	39.1/9.08	551	30
2729	Mitochondrial ATP synthase, beta subunit	gil159466892	*C. reinhardtii*	84.6/5.1	62.0/4.99	205	6
3624	ATP synthase CF1, beta subunit	gil41179057	*C. reinhardtii*	67.4/5.3	53.2/5.21	516	19
5222	Soluble inorganic pyrophosphatase	gil159473581	*C. reinhardtii*	25.1/5.6	22.4/5.49	108	13
5613	ATP synthase CF1, beta subunit	gil41179057	*C. reinhardtii*	66.8/5.7	53.2/5.21	390	16
6619	ATP synthase CF1, alpha subunit	gil41179050	*C. reinhardtii*	70.5/5.9	54.8/5.44	531	21

Table 2 continued

Spot #	Protein	NCBI accession #	Organism	Observed M_r (kDa)/p*I*	Theoretical MW (kDa)/p*I*	Search score	% Sequence coverage
7323	Mitochondrial ATP synthase-associated 31.2-kDa protein	gil159470863	*C. reinhardtii*	38.2/6.4	34.1/6.86	369	23
7526	NADP-malate dehydrogenase	gil159477375	*C. reinhardtii*	54.7/6.2	45.3/8.04	458	19
Photosynthesis							
2221	Major light-harvesting complex II protein m1	gil20269804	*C. reinhardtii*	26.9/4.9	27.6/5.96	69	4
3621	Rubisco, chain A	gil16975080	*C. reinhardtii*	70.4/5.2	53.0/6.04	473	17
3622	Rubisco, chain A	gil16975080	*C. reinhardtii*	70.6/5.2	53.0/6.04	450	14
3623	Rubisco, chain A	gil16975080	*C. reinhardtii*	70.9/5.3	53.0/6.04	531	18
5015	Cytochrome b_6f chain C	gil40889430	*C. reinhardtii*	18.6/5.6	13.9/5.74	97	12
7620	Rubisco, chain A	gil16975080	*C. reinhardtii*	71.1/6.4	53.1/6.04	441	16
7621	Rubisco, chain A	gil16975080	*C. reinhardtii*	70.9/6.3	53.1/6.04	508	17
8619	Rubisco, chain A	gil16975080	*C. reinhardtii*	70.9/6.5	53.1/6.04	494	17
Protein folding, sorting, degradation							
1621	Protein disulfide isomerase 1	gil159487489	*C. reinhardtii*	76.5/4.8	58.4/4.80	1,130	36
2017	Ubiquitin conjugating enzyme E2	gil121077798	*V. carteri*	18.5/5.1	17.0/5.04	67	10
2415	Peptidyl-prolyl cis–trans isomerase, cyclophilin-type	gil159467709	*C. reinhardtii*	49.9/5.1	44.8/5.37	283	15
2611	Translocon component Tic40-related protein	gil159465627	*C. reinhardtii*	66.9/5.0	50.0/5.61	434	20
3816	Chloroplast membrane translocon 7	gil159490640	*C. reinhardtii*	97.9/5.3	87.7/5.55	290	7
3817	Chloroplast membrane translocon 7	gil159490640	*C. reinhardtii*	97.7/5.3	87.7/5.55	256	8
3825	Membrane AAA-metalloprotease	gil159465357	*C. reinhardtii*	88.8/5.3	77.7/5.70	429	12
3827	Membrane AAA-metalloprotease	gil159465357	*C. reinhardtii*	89.3/5.3	77.7/5.70	722	20
5424	Peptidyl-prolyl cis–trans isomerase, cyclophilin-type	gil159466422	*C. reinhardtii*	47.0/5.7	42.3/5.69	346	15
Protein translation							
2126	Eukaryotic initiation factor	gil159483583	*C. reinhardtii*	22.4/5.2	18.2/4.97	130	19
2217	Plastid ribosomal protein L3	gil159485314	*C. reinhardtii*	28.6/5.0	27.9/10.26	136	10
2519	Eukaryotic initiation factor	gil159482426	*C. reinhardtii*	53.0/5.1	37.7/4.96	212	12
4822	Chloroplast elongation factor G	gil159487669	*C. reinhardtii*	97.0/5.4	79.9/5.23	767	19
4823	Chloroplast elongation factor G	gil159487669	*C. reinhardtii*	97.8/5.4	79.9/5.23	480	13
4824	Chloroplast elongation factor G	gil159487669	*C. reinhardtii*	97.8/5.4	79.9/5.23	255	8
5320	Heterogeneous nuclear ribonucleoprotein	gil159486121	*C. reinhardtii*	34.2/5.7	31.3/5.79	165	10
7421	Acidic ribosomal protein P0	gil159477927	*C. reinhardtii*	44.0/6.3	34.6/6.07	260	15
7626	Elongation factor Tu	gil226818	*C. reinhardtii*	60.0/6.2	45.7/5.84	242	9
8220	Plastid-specific ribosomal protein 1	gil159479306	*C. reinhardtii*	29.5/6.6	31.9/9.18	501	29
8221	Ran-like small GTPase	gil159467397	*C. reinhardtii*	30.1/6.6	25.7/6.24	252	21
8419	Eukaryotic initiation factor	gil159470237	*C. reinhardtii*	44.0/6.6	36.8/6.01	73	4
9416	Acidic ribosomal protein P0	gil159477927	*C. reinhardtii*	42.8/6.8	34.6/6.07	466	28
Stress-related proteins							
3715	Chaperonin 60A	gil159491478	*C. reinhardtii*	78.0/5.2	61.9/5.49	944	31
3813	Heat-shock protein 90A	gil159474294	*C. reinhardtii*	97.9/5.2	81.0/4.99	643	17
3814	Heat-shock protein 90A	gil159474294	*C. reinhardtii*	97.7/5.2	81.0/4.99	643	14
3815	Heat-shock protein 90A	gil159474294	*C. reinhardtii*	98.2/5.2	81.0/4.99	281	7
3818	Heat-shock protein 90C	gil159490014	*C. reinhardtii*	102.6/5.2	89.5/5.24	574	12
3819	Heat-shock protein 90C	gil159490014	*C. reinhardtii*	103.0/5.2	89.5/5.24	743	15
3820	Heat-shock protein 90C	gil159490014	*C. reinhardtii*	102.7/5.2	89.5/5.24	765	17

Table 2 continued

Spot #	Protein	NCBI accession #	Organism	Observed M_r (kDa)/p*I*	Theoretical MW (kDa)/p*I*	Search score	% Sequence coverage
4429	NADPH-dependent thioredoxin reductase	gil159488145	*C. reinhardtii*	46.9/5.5	37.0/5.26	241	14
4819	Heat-shock protein 70A	gil159486599	*C. reinhardtii*	90.9/5.4	71.5/5.25	980	30
4825	Heat-shock protein 90C	gil159490014	*C. reinhardtii*	95.2/5.4	89.5/5.24	134	3
5321	L-Ascorbate peroxidase	gil159488379	*C. reinhardtii*	32.8/5.7	36.5/9.23	149	7
5720	Chaperonin 60C	gil159466312	*C. reinhardtii*	79.4/5.6	57.2/5.40	482	18
5721	Chaperonin 60C	gil159466312	*C. reinhardtii*	79.3/5.6	57.2/5.40	530	18
6319	L-Ascorbate peroxidase	gil159488379	*C. reinhardtii*	32.7/6.0	36.5/9.23	208	10
Protein of miscellaneous functions							
1815	Binding protein 1	gil159487349	*C. reinhardtii*	91.7/4.8	72.7/4.99	597	14
2330	14-3-3-Like protein-related protein	gil74272601	*C. incerta*	34.2/5.0	29.7/4.90	65	4
3826	Binding protein 1	gil159487349	*C. reinhardtii*	92.8/5.3	72.7/4.99	73	1
4719	Iron–sulfur cluster assembly protein	gil159485362	*C. reinhardtii*	79.8/5.4	57.2/9.16	136	4
5416	Zygote-specific Zys3-like protein	gil124484343	*C. reinhardtii*	49.7/5.6	40.4/5.42	228	9
8318	Prohibitin	gil159477687	*C. reinhardtii*	34.8/6.6	31.2/6.37	459	33
8420	Adenosinetriphosphatase	gil1334356	*C. reinhardtii*	42.6/6.5	48.8/6.20	119	5
Unknown proteins							
1623	Hypothetical protein CHLREDRAFT_80907	gil159475896	*C. reinhardtii*	68.0/4.6	37.3/4.48	147	7
2329	Hypothetical protein CHLREDRAFT_179251	gil159486539	*C. reinhardtii*	32.6/4.9	33.2/6.08	493	18
3718	Predicted protein	gil159484662	*C. reinhardtii*	84.6/5.3	14.5/7.79	69	9
3828	Predicted protein	gil159472442	*C. reinhardtii*	94.6/5.3	58.6/8.62	224	7
4718	Predicted protein	gil159484464	*C. reinhardtii*	75.5/5.4	45.0/6.55	150	5
4820	Predicted protein	gil159463132	*C. reinhardtii*	90.9/5.4	76.2/5.31	306	6
4821	Predicted protein	gil159485022	*C. reinhardtii*	97.3/5.5	75.3/5.82	211	5
8222	Hypothetical protein CHLREDRAFT_205900	gil159470187	*C. reinhardtii*	26.0/6.7	28.9/8.92	307	18
8319	Hypothetical protein CHLREDRAFT_120516	gil159479888	*C. reinhardtii*	35.8/6.6	30.7/6.95	168	11
8624	Predicted protein	gil159468534	*C. reinhardtii*	63.8/6.6	42.7/6.28	751	37

Isolated proteins were resolved by 2-DE and subsequently identified by LC–MS/MS. Observed M_r and p*I* were calculated while the spot numbers were arbitrarily assigned by the PDQuest™ software. Mascot search score beyond 46 is considered as significant match. The identified spots are listed according to their cellular functions

cells with 300 mM NaCl for 2 h seem to be similar with the previous proteomic reports in both higher plants and cyanobacteria, particularly in terms of the differential expression of enzymes or polypeptides involved in carbohydrate metabolism, energy production, protein translation as well as stress-related proteins (Kosová et al. 2011; Sobhanian et al. 2011). According to these changes, simple interpretations can be made as following: under salinity stress, (a) the *Chlamydomonas* cells require a lot of energy to maintain ion homeostasis, which can be obtained via glycolytic and other energy-producing metabolic pathways, (b) scavenging of the ROS is carried out by the antioxidant enzymes, and (c) heat-shock proteins and molecular chaperones help renature the misfolded and/or aggregated proteins. These observations and interpretations have commonly been reported in higher plants subjected to NaCl stress (Kosová et al. 2011; Sobhanian et al. 2011).

However, it is important to note that according to our proteomic comparison criterion, the spots corresponding to the proteins listed in Table 1 only appeared in the proteome of the control but not in the salt-shocked cells. Likewise, the proteins in Table 2 were detectable only in the 2-DE profile of the salt-stressed but not in the control cultures. The exclusive appearance of any protein spot in one sample but not in another suggests that such protein could either originate from de novo translation or it could be modified by PTM in a way that changes its p*I* and M_r, leading to a shift of the spot position on 2-DE or else the protein is

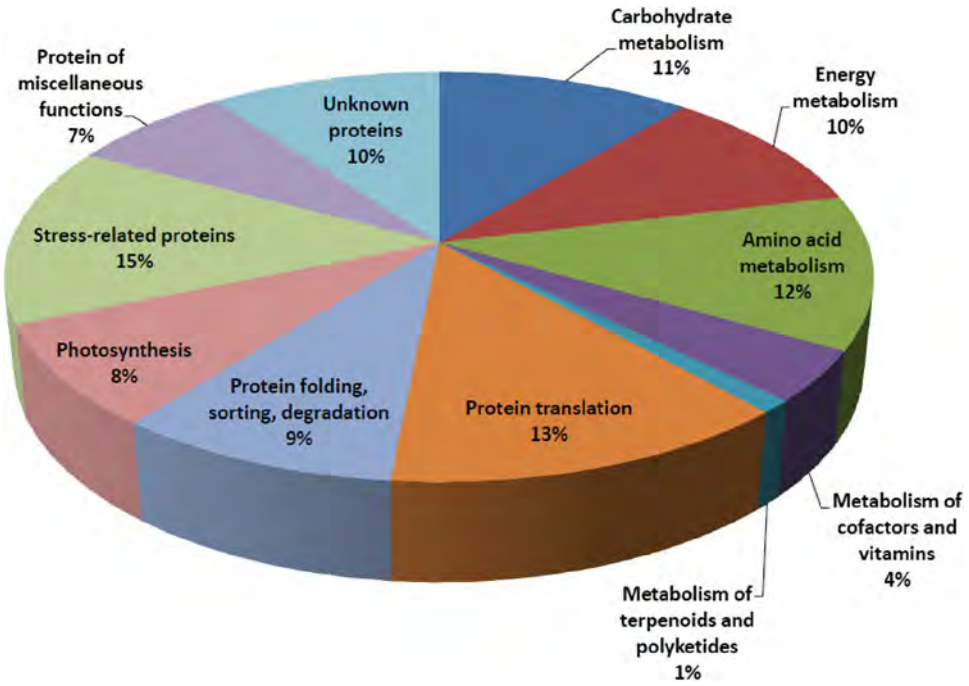

Fig. 2 A pie chart showing relative proportions of individual functional groups of the salt-specific proteins from Table 2. The percentage values were rounded to the nearest integer by the computer software

completely degraded and disappear from the gel. In case of the proteins in the control culture as shown in Table 1, most of which did not show significant deviation between the observed and theoretical p*I* and M_r values. This observation entails that these proteins existed under normal growth condition to perform their normal function but excessive NaCl imposed on the alga led to their complete disappearance. Disappearance of the proteins in Table 1 under salt stress could result from complete degradation or that they were modified and the corresponding spots shifted away from the original location.

For the proteins in the salt-shocked cultures (Table 2), if they originated from de novo biosynthesis, it implies that the important housekeeping proteins like molecular chaperones and the translation machineries were not expressed under normal growth condition but instead were induced upon NaCl treatment. This notion is very unlikely because molecular chaperones/heat-shock proteins as well as translational apparatus are known to be constitutively expressed proteins important for cell survival. Indeed, a previously published article from our group already showed that these housekeeping proteins existed in the proteome of *C. reinhardtii* cells grown under normal growth condition (Mahong et al. 2012). The data in this study, thus, suggests that the salt-stress-specific proteins presented in Table 2 could originate from PTM of the existing polypeptide pool rather than from de novo translation under salinity stress. Additionally, many of the proteins in Table 2 also have the observed p*I* and M_r significantly deviated than the theoretical values, insinuating the PTM notion. For example, we found the protein spot #2613 (mitochondrial ATP synthase β subunit, accession number gi|159466892) in Table 1 which has the observed p*I* and Mr well within the range of the theoretical values disappeared from the proteome of the salt-shocked cells. In parallel, the protein spot #2729 identified as the same protein emerged with significant shift in the observed p*I* and M_r (see Table 2). Such modification(s) must also be specific and unique to salt stress as the irradiance stress imposed to *C. reinhardtii* did not result in the exclusive occurrence of any protein spot similar to those presented in Table 2 (Mahong et al. 2012).

There are various types of PTM existing in living organisms. The most common PTMs include protein phosphorylation, acetylation, acylation, methylation, myristoylation, sumoylation, ubiquitination, etc. Certain modifications activate protein functions while some others have inhibitory effects. Since our mass spectrometric data could not distinguish the type of PTM for each protein spot, we desist from making speculation on specific roles of individual modification. Regardless of which PTM type, however, there are two possible explanations for the presence of salt-exclusive proteins in Table 2. In the first scenario, under salt stress condition, these proteins could possibly be modified and activated to perform specific and exclusive function in counteracting the drastic effects of excessive NaCl. Activation of such proteins, in this case, then fits with the functional interpretations commonly

made to these groups of proteins under salt stress (Kosová et al. 2011; Sobhanian et al. 2011). In the second hypothesis, functions of the salt-specific proteins in Table 2 might be suppressed by the NaCl-responsive protein PTM. Losing the function of these important proteins under salinity stress in this case, even a small amount, may possibly make *C. reinhardtii* cells vulnerable to salt stress. This notion could perhaps explain the salt-sensitive nature of this model alga.

When comparing our results with the previously published proteomic works on *Synechcystis* and *Dunaliella*, it is interesting to note that in those halotolerant algae, expression of the stress-related proteins and translation machineries were found to be enhanced under salinity stress over the control baseline instead of being found as exclusive spots (Liska et al. 2004; Fulda et al. 2006). This observation together with the two possible hypotheses made above suggest that (a) the salt-sensitive *C. reinhardtii* may have unique mechanisms, via PTM, to turn on protein functions for counteracting salinity stress or (b) alternatively the algal cells might not be able to sustain the toxicity of such high NaCl concentration within the 2-h period and, by way of PTM, loses the function of these important proteins.

In summary, our work presents here the identification of proteins exclusively appeared in the proteome of *C. reinhardtii* subjected to short-term salinity stress. Most of the differentially expressed proteins are constitutive and essential proteins important for normal cellular processes as well as for stress response. As these protein spots are not present in the proteome of the control cells grown under normal TAP recipe, we suggest that these proteins may originate from salt-specific PTM. Whether the salt-exclusive proteins in *Chlamydomonas* detected in this work are modified to play an active role in salt adaptation or are inactivated as an aftereffect of salt toxicity is open for further investigations.

Acknowledgments This work was conducted with funding in part from KURDI, Faculty of Science, Kasetsart University, Office of the Higher Education Commission and Thailand Research Fund grant # MRG5280035 to CY. KY thanks Thailand Research Fund, Office of the Higher Education Commission and Mahidol University for financial support.

References

Abbasi FM, Komatsu S (2004) A proteomic approach to analyze salt-responsive proteins in rice sheath. Proteomics 4:2072–2081

Abogadallah GM (2010) Antioxidative defense under salt stress. Plant Signal Behav 5:369–374

Aghaei K, Ehsanpour AA, Komatsu S (2008) Proteome analysis of potato under salt stress. J Proteome Res 7:4858–4868

Allakhverdiev SI, Nishiyama Y, Miyairi S, Yamamoto H, Inagaki N, Kanesaki Y, Murata N (2002) Salt stress inhibits the repair of photodamaged photosystem II by suppressing the transcription and translation of *psbA* genes in *Synechocystis*. Plant Physiol 130:1443–1453

Arisz SA, Munnik T (2011) The salt stress-induced LPA response in *Chlamydomonas* is produced via PLA_2 hydrolysis of DGK-generated phosphatidic acid. J Lipid Res 52:2012–2020

Bohnert HJ, Su H, Shen B (1999) Molecular mechanisms of salinity tolerance. In: Shinozaki K, Yamaguchi-Shinozaki K (eds) Molecular responses to cold, drought, heat and salt stress in higher plants. RG Landes Company, Austin, pp 29–60

Boyer JS (1982) Plant productivity and environments. Science 218:443–448

Chaves MM, Flexas J, Pinheiro C (2009) Photosynthesis under drought and salt stress: regulation mechanisms from whole plant to cell. Ann Bot 103:551–560

Chitteti BR, Peng Z (2007) Proteome and phosphoproteome differential expression under salinity stress in rice (*Oryza sativa*) roots. J Proteome Res 6:1718–1727

Cruz JA, Salbilla BA, Kanazawa A, Kramer DM (2007) Inhibition of plastocyanin to P700+ electron transfer in *Chlamydomonas reinhardtii* by hyperosmotic stress. Plant Physiol 127:1167–1179

Dooki AD, Mayer-Posner FJ, Askari H, Zaiee AA, Salekdeh GH (2006) Proteomic responses of rice young panicles to salinity. Proteomics 6:6498–6507

Fulda S, Mikkat S, Huang F, Huckauf J, Marin K, Norling B, Hagemann M (2006) Proteome analysis of salt stress response in the cyanobacterium *Synechocystis* sp. strain PCC 6803. Proteomics 6:2733–2745

Harris EH (1989) The Chlamydomonas sourcebook—a comprehensive guide to biology and laboratory use. Academic Press, San Diego

Huang F, Fulda S, Hagemann M, Norling B (2006) Proteomic screening of salt stress-induced changes in plasma membranes of *Synechocystis* sp. strain PCC 6803. Proteomics 6:910–920

Kosová K, Vítámvás P, Prásil T, Renaut J (2011) Plant proteome changes under abiotic stress—contribution of proteomics studies to understanding plant stress response. J Proteomics 74:1301–1322

Lawlor DW, Cornic G (2002) Photosynthetic carbon assimilation and associated metabolism in relation to water deficits in higher plants. Plant Cell Environ 25:275–294

Liska AJ, Shevchenko A, Pick U, Katz A (2004) Enhanced photosynthesis and redox energy production contribute to salinity tolerance in *Dunaliella* as revealed by homology-based proteomics. Plant Physiol 136:2806–2817

Mahajan S, Tuteja N (2005) Cold, salinity and drought stresses: an overview. Arch Biochem Biophys 444:139–158

Mahong B, Roytrakul S, Phaonaklop N, Wongratana J, Yokthongwattana K (2012) Proteomic analysis of a model unicellular green alga, *Chlamydomonas reinhardtii*, during short-term exposure to irradiance stress reveals significant down regulation of several heat-shock proteins. Planta. doi 10.1007/s00425-011-1521-x (in press)

Marín-Navarro J, Moreno J (2006) Cysteins 449 and 459 modulate the reduction-oxidation conformational changes of ribulose 1,5-bisphosphate carboxylase/oxygenase and the translocation of the enzyme to membranes during stress. Plant Cell Environ 29:898–908

Munns R, James RA, Läuchli A (2006) Approaches to increasing the salt tolerance of wheat and other cereals. J Exp Bot 57:1025–1043

Ndimba BK, Chivasa S, Simon WJ, Slabas AR (2005) Identification of *Arabidopsis* salt and osmotic stress responsive proteins using two-dimensional difference gel electrophoresis and mass spectrometry. Proteomics 5:4185–4196

Neale PJ, Melis A (1989) Salinity-stress enhances photoinhibition of photosystem II in *Chlamydomonas reinhardtii*. J Plant Physiol 134:619–622

Pandhal J, Wright PC, Biggs CA (2008) Proteomics with a pinch of salt: a cyanobacterial perspective. Saline Systems 4:1. doi: 10.1186/1746-1448-4-1

Pandhal J, Ow SY, Wright PC, Biggs CA (2009) Comparative proteomics study of salt tolerance between a nonsequenced extremely halotolerant cyanobacterium and its mildly halotolerant relative using in vivo metabolic labeling and in vitro isobaric labeling. J Proteome Res 8:818–828

Pang Q, Chen S, Dai S, Chen Y, Wang Y, Yan X (2010) Comparative Proteomics of Salt Tolerance in *Arabidopsis thaliana* and *Thellungiella halophile*. J Proteome Res 9:2584–2599

Shama PK, Hall DO (1991) Interaction of salt stress and photoinhibition on photosynthesis in barley and sorghum. J Plant Physiol 138:614–619

Siaut M, Cuiné S, Cagnon C, Fessler B, Nguyen M, Carrier P, Beyly A, Beisson F, Triantaphylidès C, Li-Beisson Y, Peltier G (2011) Oil accumulation in the model green alga Chlamydomonas reinhardtii: characterization, variability between common laboratory strains and relationship with starch reserves. BMC Biotechnol 11:7 (http://www.biomedcentral.com/1472-6750/11/7)

Sobhanian H, Aghaei K, Komatsu S (2011) Changes in the plant proteome resulting from salt stress: toward the creation of salt-tolerant crops? J Proteomics 74:1323–1337

Subramanyam R, Jolley C, Thangaraj B, Nellaepalli S, Webber AN, Fromme P (2010) Structural and functional changes of PSI–LHCI supercomplexes of *Chlamydomonas reinhardtii* cells grown under high salt conditions. Planta 231:913–922

Taji T, Seki M, Satou M, Sakurai T, Kobayashi M, Ishiyama K, Narusaka Y, Narusaka M, Zhu Y-K, Shinozaki K (2004) Comparative genomics in salt tolerance between Arabidopsis and Arabidopsis-related halophyte salt cress using Arabidopsis microarray. Plant Physiol 135:1697–1709

Vega JM, Garbayo I, Domínguez MJ, Vigara J (2006) Effects of abiotic stress on photosynthesis and respiration in *Chlamydomonas reinhardtii*: induction of oxidative stress. Enzyme Microb Tech 40:163–167

Wang MC, Peng ZY, Li CL, Li F, Liu C, Xia GM (2008) Proteomic analysis on a high salt tolerance introgression strain of *Triticum aestivum*/*Thinopyrum ponticum*. Proteomics 8:1470–1489

Zörb C, Herbst R, Forreiter C, Schubert S (2009) Short-term effects of salt exposure on the maize chloroplast protein pattern. Proteomics 9:4209–4220

Zuo Z-J, Zhu Y-R, Bai Y-L, Wang Y (2012) Volatile communication between *Chlamydomonas reinhardtii* cells under salt stress. Biochem Syst Ecol 40:19–24

J Appl Phycol (2013) 25:445–452
DOI 10.1007/s10811-012-9878-1

Generation and characterization of His-tagged-PsbA-expressing transformants of *Chlamydomonas reinhardtii* that are capable of photoautotrophic growth

Janewit Wongratana · Thanate Juntadech · Chutima Sereeruk · Chanan Angsuthanasombat · Kittisak Yokthongwattana

Received: 12 May 2012 / Revised and accepted: 15 July 2012 / Published online: 31 July 2012

Abstract Histidine tags attached to subunits of photosystem II (PSII) have proven to be very useful tools for isolation and purification of the complex for investigation of its components. However, it has been reported that *Chlamydomonas reinhardtii* transformants carrying N-terminal histidine-tagged version of the PSII D1 reaction center protein could not grow photoautotrophically. We report here a successful generation of *C. reinhardtii* transformants expressing histidine-tagged version of the PsbA protein that are capable of photoautotrophic growth. Biochemical and physiological analyses revealed that the histidine tag present at the N terminus of the D1 subunit did not cause total instability to the PSII complex as assessed by their phototrophic growth and oxygen evolution capability. Simple one-step affinity column chromatography also revealed that the histidine-tagged D1 subunit as well as its associated proteins could be effectively purified. These transformants could potentially serve as very good tools for the study of the PSII complex particularly the D1 protein.

J. Wongratana · C. Sereeruk · K. Yokthongwattana (✉)
Department of Biochemistry and Center for Excellence in Protein Structure and Function, Faculty of Science,
Mahidol University,
272 Rama 6 Rd,
Bangkok 10400, Thailand
e-mail: kittisak.yok@mahidol.ac.th

T. Juntadech · C. Angsuthanasombat
Institute of Molecular Biosciences, Mahidol University,
Salaya Campus,
Nakhon Pathom 73170, Thailand

Keywords *Chlamydomonas reinhardtii* · D1 protein · Histidine tag · Photosynthesis · Photosystem II · PsbA

Introduction

The photosystem II reaction center (PSII) catalyzes the initial steps of photosynthesis, a process that transforms light energy into chemical energy when the energy from sunlight is absorbed and used by PSII to drive electron transfer from H_2O to plastoquinone and eventually, via cytochrome b_6f complex and photosystem I, to $NADP^+$. The reduced form of the latter, NADPH, together with ATP generated by photophosphorylation is subsequently used for CO_2 assimilation reactions. Biochemically, PSII is a large integral membrane protein complex residing in the chloroplast thylakoid membranes. Among all the PSII subunits, the 32/34-kDa D1/D2 reaction center proteins (*psbA* and *psbD* gene products, respectively) can be considered as the most important components. The two subunits bind all essential cofactors required for photosynthetic electron transport reactions within the PSII (Yokthongwattana and Melis 2006).

The D1 reaction center protein of PSII has a unique feature in that it undergoes frequent and rapid turnover (Melis 1999; Takahashi and Badger 2011). Excessive irradiance primarily brings about photo-oxidative damage to the PsbA protein, causing inactivation of the PSII activity. Plants have a repair mechanism to mend this problem and return the damaged PSII to its functional form. The repair mechanism entails a series of biochemical processes. Briefly, the repair process begins by partial disassembly of the inactivated PSII (Guenther and Melis 1990) into a

putative PSII repair intermediate (Yokthongwattana et al. 2001, 2009), which travels from grana thylakoids to stroma-exposed membranes. At the stroma lamellae, the damaged D1 protein is selectively degraded via specific proteases (Lindahl et al. 2000; Haußuhl et al. 2001; Kato and Sakamoto 2009; Nixon et al. 2010) and replaced with a de novo synthesized copy (Mulo et al. 2008; Nixon et al. 2010). The already repaired PSII core moves back to the grana, reintegrates with the remaining subunits, and regains its activity. Although being the subject of intensive research, knowledge of the PSII damage and repair cycle is far from complete; specifically, little is known regarding the intermediates in the process.

A tagged version of the PSII can be a very useful tool for isolation and purification of the PSII complex for various studies. There have been a number of papers reporting on successful generation and purification of histidine-tagged PSII subunits including D2 (Sugiura et al. 1998), CP43 (Sugiura and Inoue 1999), CP47 (Suzuki et al. 2003), Cyt b_{559} (Fey et al. 2008), and PsbH (Bumba et al. 2005; Cullen et al. 2007). To date, only one case of successful engineering a histidine tag on the D1 protein has been reported in the unicellular green alga *Chlamydomonas reinhardtii* (Sugiura et al. 1998). However, the transformant expressing the N-terminally His-tagged D1 subunit reported in that paper could not grow photoautotrophically and manifested a very low photosynthetic activity when compared to the wild-type (WT) control (Sugiura et al. 1998). More importantly, this transformant line has been lost due to heavy contamination (Minagawa, personal communication). As PsbA is the only PSII subunit that encounters the rapid turnover, transformants expressing the His-tagged D1 protein could prove beneficial for tracking its fates over the course of the PSII damage and repair cycle. In an attempt to create such a tool, we present here another successful construction of *C. reinhardtii* transformants carrying the histidine-tagged D1 protein. Analyses of their physiology, photosynthetic performances and simple biochemical purification of the tagged subunit as well as its associated proteins are reported. Results showed that our transformants can confer phototrophic growth as well as having better physiology and higher PSII activity than the original one reported by Sugiura et al. (1998). These transformants could potentially serve as very good tools for scientists studying the PSII complex.

Materials and methods

The model unicellular green alga *Chlamydomonas reinhardtii* strains CC-400 (*cw-15* mt+, serving as a reference WT control) and CC-744 (FUD7 or ac-u-β *psbA*-deletion mutant) were obtained from the Chlamydomonas Resource Center (http://chlamycollection.org). The two algae and the transformants generated in this work were grown in either standard TAP medium for mixotrophic or in a modified TBP medium (Polle et al. 2000) for photoautotrophic growth under low-light (LL ~50 μmol photons m^{-2} s^{-1}) provided by fluorescent lamps. Temperature was maintained at 25–28 °C. Culture cell density was monitored by light scattering at OD_{720nm} using a U-1900 UV spectrometer (Hitachi).

Construction of transformation vector

Expression cassettes of the 6× histidine-tagged *psbA* cDNA and the spectinomycin resistant *aadA* gene were subcloned from pBAH158 (Minagawa and Crofts 1994). The bacterial *cry4Ba* expression cassette was constructed by subcloning the corresponding cDNA into the plasmid p546 (chloroplast expression vector, http://chlamycollection.org). The backbone pBluescriptII KS + (Invitrogen) was employed to harbor the three expression cassettes located in between left- and right-recombination fragments (RF and LF, respectively) corresponding to the NCBI reference NC_005353 (bases 137761 to 138969 and 146986 to 148500, respectively). The *psbA* promoter/5′-UTR and 3′-UTR were employed as an expression cassette to individually control *cry4Ba* and the His-tagged *psbA* genes, while gene expression of *aadA* gene was driven by *atpA* promoter/5′-UTR and *rbcL* 3′-UTR. The RF was amplified from *C. reinhardtii* chloroplast genome using RF-f [5′-GGCCGTCGACGCTAGCAATATCTGATGGTAC-3′] and RF-r [5′-GGCCGGGCCCGAATCTCAGTTCTA GTGCTAG-3′] primers and the PCR product was inserted into the backbone as a *Sal*I-*Apa*I fragment. Subsequently, the *cry4Ba* expression cassette was introduced into the backbone at the unique *Sal*I restriction site adjacent to the RF. Finally, a fragment in combination of LF and both *His-psbA* and *aadA* expression cassettes was amplified from pBAH158 using LF-f [5′-GCCCCGCGGACGTTAGTCGATATTTATACAC-3′] and *rbcL*/3′-UTR-r [5′-CCCCGCGGTGGCGGCCGCTC-3′] primers prior to delivery into the backbone as a *Not*I-*Sac*II fragment. The final chloroplast transformation vector is depicted in Fig. 1.

Chloroplast transformation and transformant screening

The FUD7 mutant (CC-744) was grown in TAP medium until late-log phase and was collected by centrifugation. The cell pellet was resuspended in a small aliquot of the growth medium to reach an approximate cell concentration of 10^7 cells mL^{-1}. About 5 mL of the concentrated cells were spread onto a TAP agar plate containing spectinomycin (Sigma) at the final concentration of 100 μg mL^{-1}. Chloroplast transformations were performed by particle

bombardment with the vector-coated gold particles (Bio-Rad) under 25 in. Hg vacuum chamber, 9 cm target distance and 900 psi helium pressure. After screening for spectinomycin resistance conferred by the *aadA* expression cassette (Goldschmidt-Clermont 1991), the chloroplast transformant lines were subsequently verified for the recovery of photosynthetic capability by transferring them onto HSM plates (Sueoka 1960). Survivors of the stringent double screens were subjected to further verifications and characterizations.

Analytical methods

Chl was extracted using 80 % acetone. Cell debris and unsolubilized materials were removed by centrifugation at 10,000×*g* for 5 min at room temperature. The Chl concentration and Chl *a*/*b* ratio were analyzed spectrophotometrically according to the method of Arnon (1949) with the corrected equation described by Melis et al. (1987).

Rates of whole cell O_2 evolution as a function of irradiance were determined using a Clark-type electrode model OX1LP Dissolved O_2 Package (Qubit Systems, Canada). Before measurement, $NaHCO_3$ was additionally supplied to the cells at the final concentration of 15 mM to ensure sufficient availability of C during analysis. O_2 evolution rates were monitored for 2 min each at individual irradiance from 0–1,000 μmol photons m^{-2} s^{-1}.

For analysis of PSII quantum efficiency cell aliquots were taken from the algal cultures and incubated in the dark for 10 min before analysis. PSII quantum efficiency as determined by the F_v/F_m ratio was determined using manufacturer's built-in scripts of a PAM fluorometer model FMS-2 (Hansatech Instruments, UK).

To isolate total proteins, cells were harvested by centrifugation at 1,000×*g* for 5 min at room temperature. The cell pellet was resuspended in solubilization buffer containing 250 mM Tris pH 6.8, 2 M urea, 7 % SDS, 20 % glycerol and 10 % β-mercaptoethanol. Removal of cell debris and unsolubilized materials was performed by centrifugation at 16,200×*g* for 5 min at room temperature. Thylakoid membranes were isolated and purified using the protocol described by Kim et al. (1993). The thylakoid membrane pellet was solubilized with buffer containing 25 mM Hepes-KOH pH 7.5, 100 mM NaCl, 15 mM imidazole, and 2 % NP-40 for subsequent purification of the His-tagged PsbA subunit and its associated proteins.

SDS-PAGE and Western blot analyses

Standard SDS-PAGE and Western blot analyses were as described by Kim et al. (1993), with the exception of the primary antibodies used. In this work, polyclonal antibodies specific to the PsbA subunit of the PSII and LHC-II proteins as well as monoclonal antibody raised against 6× histidine tag were employed.

Purification of the His-tagged D1 subunit and its associated proteins

The NP-40-solubilized thylakoid membranes as described above were loaded to a pre-pack nickel resin column (HisTrap™ FF Crude, GE Healthcare) equilibrated with binding buffer containing 25 mM Hepes-KOH pH 7.5, 100 mM NaCl, 15 mM imidazole, and 2 % NP-40. After sample loading, the column was washed excessively with the binding buffer to remove as many nonspecific proteins as possible. After several washes (approximately five-column volume), the tagged proteins were eluted from the column using elution buffer (40 mM Tris–HCl pH 6, 10 mM NaCl, 0.5 % NP-40, 200 mM imidazole). The eluted proteins and wash fractions were concentrated by centrifugation with AMICON™ (Millipore) tubes and were examined by SDS-PAGE followed by standard silver staining.

Results

Our original aim was to create *C. reinhardtii* transformants expressing the mosquito larvicidal protein from *Bacillus thuringiensis*, Cry4Ba, in the chloroplast. By using both antibiotic resistance and photosynthetic complementation, we imposed very stringent screening criteria for positive transformants. As the CC-744 *psbA*-less mutant was already a weak host growing very slowly even in the TAP medium, only three transformant lines passed our strict double screens on both TAP+spectinomycin and HSM plates. After investigations, it turned out that none of the transformants expressed the bacterial toxin we introduced into their chloroplast genomes (Juntadech et al. 2012). However, all of the transformants grew well photoautotrophically on both HSM and TBP media, indicating that the PSII activity was successfully restored via the 6×His *psbA* cDNA cassette present in the transformation vector (Fig. 1). As *C. reinhardtii* transformants carrying the His-tagged D1 reaction center protein that also confer phototrophic growth have never been reported before and because they could serve as a very good tool for studying many other aspects of the PSII complex, we decided to further assess these transformants in terms of photosynthetic characteristics and physiology. Hereafter, the three transformant lines are sometimes referred to as HisD1-1, HisD1-2, and HisD1-3, respectively.

For subsequent studies, the *cw-15* (serving as WT reference strain) and the three transformants were grown in the TBP medium whereas the FUD7 host was grown in the normal TAP medium. The reason is because, like the HSM, the TBP medium only allows photoautotrophic

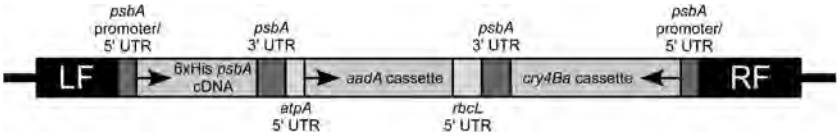

Fig. 1 Schematic of the vector carrying a histidine-tagged *psbA* construct used to generate all three transformants in this work. Left- and right-recombination fragments (*LF* and *RF*, respectively) were cloned from parts of the endogenous chloroplast genome, serving as the sites for homologous recombination. The histidine-tagged *psbA* cDNA is driven by its own *psbA* promoter, 5′ and 3′ UTR. A selectable marker for this vector is an *aadA* construct conferring spectinomycin resistance. This vector is coated to the gold particles before bombardment into *C. reinhardtii* FUD7 cells as described in the "Materials and methods" section

growth of the algae. However, $NaHCO_3$ present in the TBP medium promotes faster growth rate than the HSM minimal medium. Fig. 2 shows growth curves of the HisD1-1, HisD1-2, and HisD1-3 in comparison with that of the WT control and the FUD7 host strain when cultured under LL condition. With HCO_3^- as the only carbon source in the TBP medium, all the cultures including the WT reference strain grew slowly and could not reach stationary phase even after 18 days. From the result, the three transformant lines grew at ~50 % slower rate than that of the WT (Fig. 2). It is important to note that in this autotrophic medium, the *psbA*-less host could not grow due to its lack of photosynthetic capability.

The next analysis we performed was to verify that these putative transformants indeed expressed the His-tagged version of the PsbA protein. Total proteins were extracted from all three transformant lines as well as from the WT and the CC-744 *psbA*-deletion host, resolved by SDS-PAGE followed by Western blot analyses with polyclonal antibodies raised against the PSII D1 protein and monoclonal antibody specific to the 6× histidine tag. Fig. 3a shows that all strains except the FUD7 host contained the 32-kDa PsbA subunit of the PSII as probed by D1-specific polyclonal antibodies. When probing with the 6× His-tag monoclonal antibody, only the proteins from the transformants HisD1-1, HisD1-2, and HisD1-3 were cross-reacted (Fig. 3b), confirming that they indeed expressed the 6×His-*psbA* construct. We also probed the blot with polyclonal antibodies against the LHC-II proteins to determine the structural organization of the PSII antenna complex. As the primary antibodies we employed could cross-react with multiple forms of the LHC-II proteins, five protein bands from the WT sample were clearly detected (Fig. 3c, WT lane). In the CC-744 *psbA*-less host, only two major bands and one very faint band could be observed using the same antibodies (Fig. 3c, CC-744 lane). This result implies that the in the absence of the PsbA reaction center protein, the PSII complex in FUD7 mutant host may not be assembled and that could lead to degradation of certain LHC-II antenna proteins. Upon complementation with our vector construct containing 6× His *psbA* cDNA, all transformants had the same pattern of the LHC-II bands as that of the WT (Fig. 3c), suggesting that the His-tagged D1 protein could properly be integrated into the PSII holocomplex and the antenna protein profile was restored. This result also denotes that the 6× histidine tag present at the N terminus of the PsbA protein does not hinder proper assembly of the PSII complex as suggested earlier (Sugiura et al. 1998).

Another set of physiological and photosynthetic parameters we determined in these transformants were their Chl content and the PSII quantum efficiency (F_v/F_m ratio). Chl

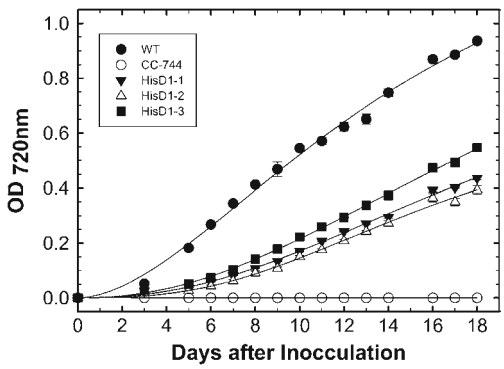

Fig. 2 Growth curves of *C. reinhardtii* WT, the *psbA*-less mutant (*CC-744*) and three transformant lines carrying His-tagged D1 reaction center protein. The cultures were grown in TBP medium under LL of ~50 μmol photons m^{-2} s^{-1}. Cell densities were measured by light scattering effect at OD_{720nm}. Data presented are averages of 3 independent experiments ± SE. Note that all transformants grew slower than the WT and that the CC-744 could not grow in the TBP medium

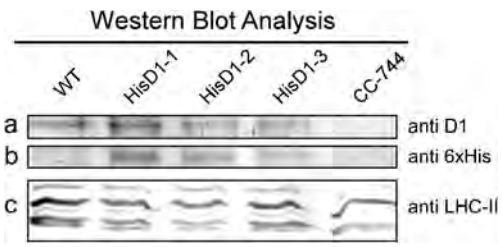

Fig. 3 Western blot analysis of SDS-PAGE-resolved proteins from *C. reinhardtii* WT, HisD1-1, HisD1-2, HisD1-3, and CC-744. Total proteins equivalent to 0.8 nmol of chl were loaded on each lane and were separated by standard SDS-PAGE followed by electrotransfer onto nitrocellulose membranes. The blots were subsequently probed with (**a**) polyclonal antibodies specific to the D1 reaction center protein, (**b**) monoclonal antibody raised against 6× histidine tag, and (**c**) polyclonal antibodies against the LHC-II polypeptides. As the secondary antibodies were conjugated with alkaline phosphatase enzyme, the positive cross-reactions were visualized by colorimetric assay

per cell of the WT was ~4.4×10^{-15} mol cell^{-1} while the values for HisD1-1, HisD1-2, and HisD1-3 were ~9.7, 9.5 and 9×10^{-15} mol cell^{-1}, respectively (Table 1). The higher Chl/cell values of the transformants over the WT cultures could probably be due to their larger cell size (result not shown). In terms of the Chl *a*/*b* ratio, value for the WT was about 3.6 when grown in the TBP medium (Table 1). For the three transformants, the ratios of Chl *a* to Chl *b* were about 2.2 for HisD1-1, 2.9 for HisD1-2 and 2.7 for HisD1-3. Since Chl *b* is only associated with the light-harvesting polypeptides whereas Chl *a* can be found in both the antenna and the photosystem core proteins, Chl *a*/*b* ratio can be used as a rough indicator for the Chl antenna size (Melis 1998; Yokthongwattana et al. 2009); the higher the value (usually more than 5), the smaller the antenna size. The slightly lower Chl *a*/*b* ratio in the transformants suggests that they have similar or even slightly larger Chl antenna size when compared to that of the WT, consistent with the Western blot profile in Fig. 3c. In terms of the PSII quantum efficiency determined as the F_v/F_m ratio, the *cw-15* strain had value of ~0.80 (Table 1). This value indicated that the WT cells were in healthy state under the LL phototrophic growth condition. Interestingly, when all transformants were grown photoautotrophically in the TBP medium, they manifested significantly lower F_v/F_m values of ~0.2–0.3 (Table 1), suggesting that their PSII activities were somehow compromised. The lower PSII quantum efficiency is consistent with the slower growth rates of the transformants (Fig. 2).

To further assess the photosynthetic characteristics of these transformants, we determined their light-saturation curves of photosynthesis (P vs. E curves) in comparison to that of the WT. In TBP medium, WT *C. reinhardtii* exhibited typical light-saturation curve of photosynthesis with saturation irradiance at ~200 μmol photons m^{-2} s^{-1} and P_{max} of ~10 mmol O_2 [mol Chl]$^{-1}$ s^{-1} (Fig. 4, solid circles). All three transformants, on the other hand, could evolve O_2 at much lower rates than that of the WT under low irradiances (Fig. 4), consistent with the growth rates in Fig. 2. However, when irradiance increased, photosynthesis of the three transformants exceeded that of the WT. Rates of O_2 evolution in HisD1-1, HisD1-2, and HisD1-3 were saturated at ~600 μmol photons m^{-2} s^{-1} with the P_{max} values of ~15, 14, and 16 mmol O_2 mol Chl^{-1} s^{-1}, respectively (Fig. 4 and Table 1).

Altogether, these results confirmed that the histidine tag present at the N terminus of the D1 subunit did not affect assembly and function of the PSII complex, albeit with its functional activities were somehow hampered at low irradiances. Having transformants of the model alga carrying His-tagged PsbA protein at hand, we attempted to exploit such tag for purification of the PSII D1 subunit and its associated proteins. By passing the NP-40-solubilized thylakoid membranes of the HisD1-1 transformant onto standard Ni^{2+}-NTA column, we could purify the proteins specifically bound to the Ni^{2+} resin. Figure 5a shows the silver-stained SDS-PAGE profile of proteins from different fractions during the purification steps. In Fig. 5a, lane 1 represents the crude NP-40 solubilized thylakoids before loading onto the column, lane 2 is the last wash fraction from the column before elution and lane 3 is the eluted proteins. The crude fraction contained a lot of proteins as envisioned by the dark smear after silver staining (Fig. 5a, "crude" lane). After several washes, it was clear that proteins unspecifically bound to the Ni^{2+} column were completely removed. This was confirmed by the fact that there was no detectable band, even with silver staining, in the "last wash" lane (Fig. 5a). When the washed column was eluted with elution buffer containing 200 mM imidazole, several proteins were released from the column (Fig. 5a, eluted lane). The presence of the PsbA protein in the "eluted" fraction was confirmed by Western blot with polyclonal antisera against the D1 protein (Fig. 5b, Western blot panel). It is important to note that we only used a small column for this simple purification to show the plausibility of purifying the His-tagged D1 subunits and its associated proteins. Therefore, the specific enrichment of D1 proteins in the "eluted" lane cannot be observed. As the PsbA was the only protein containing histidine tag in the transformants, the result in Fig. 5 also demonstrated that

Table 1 Chlorophyll content, chlorophyll *a*/*b* ratio, and photosynthetic characteristics of *C. reinhardtii* WT and the three transformants carrying histidine-tagged D1 protein

Parameter	WT	HisD1-1	HisD1-2	HisD1-3
Chl/cell (x10^{-15} mol cell^{-1})	4.35±0.12	9.67±0.68	9.45±0.82	8.97±0.38
Chl *a*/*b* ratio	3.58±0.04	2.17±0.02	2.89±0.02	2.66±0.04
F_v/F_m	0.796±0.015	0.215±0.047	0.319±0.043	0.271±0.019
Photosynthetic saturation irradiance (μmol photons m^{-2} s^{-1})	200	600	600	600
Maximum rate of O_2 evolution (mmol O_2 [mol Chl]$^{-1}$s^{-1})	10.27±0.37	15.02±0.08	14.17±0.22	15.81±0.45

Cells were grown photoautotrophically in TBP medium under 50 μmol photons m^{-2} s^{-1} illumination. Analyses were performed according to what described in the "Materials and methods" section. Data presented are averages from 3 independent experiments±SE. Note that the CC-744 host could not grow in this type of medium, and, therefore, their parameters could not be assessed

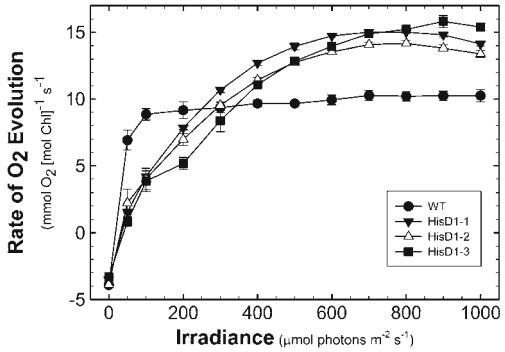

Fig. 4 Light saturation curves of photosynthesis of *C. reinhardtii* WT and all the His-tagged PsbA transformants. Rates of O_2 evolution of cells grown in TBP medium under LL of ~50 μmol photons m^{-2} s^{-1} were measured as a function of irradiance. Data points are averages of 3 independent experiments±SE

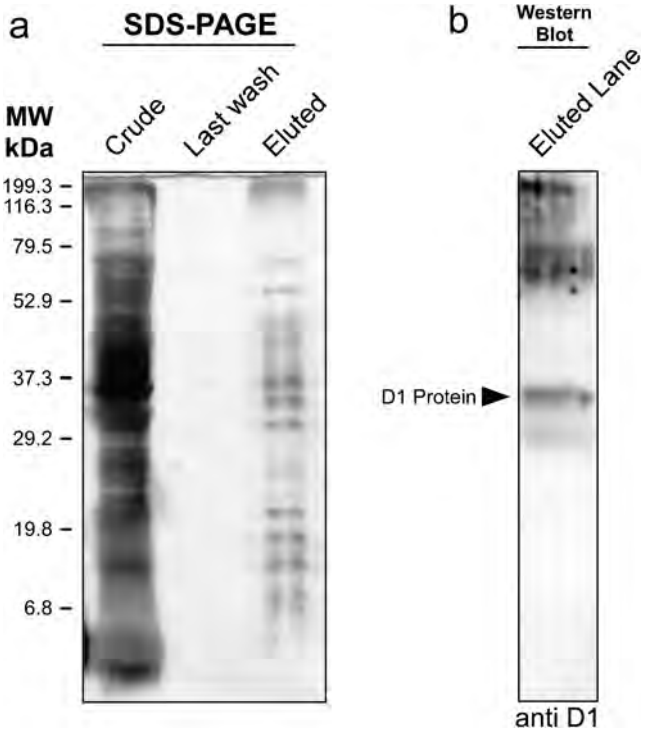

Fig. 5 SDS-PAGE and Western blot analysis of protein fractions during the purification of the His-tagged PsbA and its associated proteins using Ni^{2+} column. **a** SDS-PAGE profile visualized by silver staining. *Lane 1* is the "crude" NP-40-solubilized thylakoid membranes that contains large amount of input proteins before loading onto the column. *Lane 2* represents the "last wash" fraction showing that proteins unspecifically bound to the column were completely removed. *Lane 3* is the protein fraction "eluted" from the column using 200 mM imidazole that contains multiple polypeptide bands. **b** Western blot analysis of the eluted fraction. The polyclonal antibodies raised again the PSII D1 protein were employed as the primary antibody

other proteins in association with the His-tagged D1 subunit could also be co-purified by a standard Ni^{2+} column. As we do not have specific antibodies toward the other PSII subunits, identities of the other protein bands beside the D1 protein could not be determined. However, the band pattern of the eluted proteins in this study was similar to the previously reported SDS-PAGE profile of the purified PSII complex of the His-tagged PsbD transformant reported by Sugiura et al. (1998).

Discussion

Photosynthetic organisms with histidine tag attached to any of the PSII components have been proven as very useful tools for isolation and purification of reaction center complex. Among the PSII core subunits, histidine tag has been successfully placed at the C terminus of D2, CP43, CP47, PsbH and at the N terminus of Cyt b_{559} (Sugiura et al. 1998; Sugiura and Inoue 1999; Suzuki et al. 2003; Cullen et al. 2007; Fey et al. 2008). In most cases, the transformants carrying the His-tagged version of those PSII subunits could grow well photoautotrophically although their photosynthetic performances were not up to the par with that of the WT counterpart. The exception was the placement of the 6× histidine tag at the N terminus of the PsbA subunit. In the previous report by Sugiura et al. (1998), the H-D1 transformant could not grow in the absence of acetate. It was suggested that 6× histidine tag placed at the N terminus of the D1 protein somehow lead to instability of the PSII holocomplex. This suggestion has been widely accepted and cited in the literature until today. In contrast to the existing belief, we present in this study a successful generation of *C. reinhardtii* transformants harboring the PsbA subunit with 6× histidine residues fused at its N terminus that are capable of photoautotrophic growth. Our results in this paper proved that the 6× histidine tag present at the N terminus of the D1 protein did not affect the PSII assembly. The evidence supporting the stable assembly of the PSII complex in the His-D1-1, HisD1-2, and HisD1-3 transformants was their photoautotrophic growth (Fig. 2) as well as their ability to evolve O_2 (Fig. 4). The amount of the D1 protein in the transformants, as assessed by Western blot analysis in Fig. 3b, also supports this. If the histidine tag imposes any instability to the D1 protein and/or the PSII structure, one would expect the level of the steady-state D1 protein in the transformants to be significantly lower than that of the *cw-15* WT reference strain. Moreover, restoration of the LHC-II profile (Fig. 3c) to the same pattern as that of the WT control instead of having only 3 bands like their FUD7 transformation host also supports this claim. Since we basically subcloned the exact same construct of the 6×His *psbA* cDNA from the pBAH158 used in the study of Sugiura et al. (1998), phototrophic competency of our transformants could probably be due to the usage of different host strain for transformation. The host employed by

Sugiura et al. (1998) was the *psbA* deficient mutant (ac-u-ε) while the one used in this study was the FUD7 (ac-u-β). As both of these mutants were defective in the PsbA protein, the dissimilar photosynthetic characteristics upon complementation with the same set of 6×His *psbA* construct could originate from the unknown background differences between the two.

Although our transformants could confer photoautotrophic growth, their PSII activities, determined by the slower growth rates and lower F_v/F_m ratios, were not at the same level as that of the WT. As it was previously demonstrated that intron-less version of the *psbA* gene introduced into the *psbA*-less host did not affect the PSII activity of the transformant in term of Q_A photoreduction (Minagawa and Crofts 1994), the use of *psbA* cDNA in this work should not be accounted for this phenotype. It is possible that even though the presence of the histidine tag at the N terminus of the PsbA protein may not lead to total instability of the whole structure, its fitness in terms of enzymatic activity could somehow be affected. Alternatively, as our WT reference strain had different genetic background from the FUD7 host, the lower F_v/F_m and slower growth rates phenotype in the transformants could probably be inherited from the unknown defect in the transformation host itself.

It is interesting to note that HisD1-1, HisD1-2, and HisD1-3, albeit having lower F_v/F_m ratio, had higher P_{max} than the WT. Based on the evidence provided in this paper, it is difficult to provide an accurate interpretation regarding this observation. We can, however, speculate that in these transformants, association between the peripheral antenna complexes and the reaction center core could somehow be defective. With such defect, energy transfer between the LHC-II and the reaction center core might be hampered. Under low irradiances, less effective photon energy could reach the reaction center, giving rise to lower photosynthetic rates than the WT. At high light intensities that saturate photosynthesis of the WT control cells, the actual photon reaching the reaction center of the transformants could be significantly lower, leading to higher saturation irradiance and higher P_{max}. However, we do not claim that this speculated phenotype originates from the histidine tag present at the N terminus of the D1 subunit of the PSII. Such defect could already be part of the background genetics of the FUD7 host. This hypothesis as well as other unexplainable questions regarding the physiology of these transformants needs further investigation.

In addition to the physiological analyses, we also performed a simple purification of the tagged D1 protein along with its associated proteins using standard Ni^{2+} column. It is clear from our results that in the presence of 6× histidine tag, the PsbA protein could be effectively purified even with our simple procedure. Moreover, a number of proteins tightly associated with the D1 subunit could also be co-purified. With further optimization of the purification protocol, these transformants could serve as a good tool for purification of the PSII holocomplex for further studies.

In summary, this paper presents evidence showing that the histidine tag fused at the N terminus of the PsbA subunit of the PSII did not lead to total instability of the complex. Our transformants could grow photoautotrophically, albeit with lower efficiency than the *cw-15* control cells. These transformants could become very useful tools for other researchers working on the PSII complex and particularly D1 protein.

Acknowledgments This work was supported by funding, in part, from Mahidol University, The Office of the Higher Education Commission, and Thailand Research Fund. TJ was a graduate student supported by the Royal Golden Jubilee Ph.D. Program. The authors thank Prof Anastasios Melis for providing the polyclonal antibodies against the D1 and LHC-II proteins and Dr Sarawut Jitrapakdee for monoclonal antibody specific to 6× histidine tag. We also thank Dr Jun Minagawa for providing the plasmid pBAH158.

References

Arnon D (1949) Copper enzymes in isolated chloroplasts. Polyphenol oxidase in *Beta vulgaris*. Plant Physiol 24:1–5

Bumba L, Tichy M, Dobakova M, Komenda J, Vacha F (2005) Localization of the PsbH subunit in photosystem II from the *Synechocystis* 6803 using the His-tagged Ni-NTA nanogold labeling. J Struct Biol 152:28–35

Cullen M, Ray N, Husain S, Nugent J, Nield J, Purton S (2007) A highly active histidine-tagged *Chlamydomonas reinhardtii* photosystem II preparation for structural and biophysical analysis. Photochem Photobiol Sci 6:1177–1183

Fey H, Piano D, Horn R, Fischer D, Schmidt M, Ruf S, Schröder WP, Bock R, Büchel C (2008) Isolation of highly active photosystem II core complexes with a His-tagged Cyt b_{559} subunit from transplastomic tobacco plants. Biochim Biophys Acta 1777:1501–1509

Goldschmidt-Clermont M (1991) Transgenic expression of aminoglycoside adenine transferase in the chloroplast: a selectable marker of site-directed transformation of *Chlamydomonas*. Nucleic Acid Res 19:4083–4089

Guenther JE, Melis A (1990) The physiological significance of photosystem II heterogeneity in chloroplasts. Photosynth Res 23:105–110

Haußuhl K, Andersson B, Adamska I (2001) A chloroplast DegP2 protease performs the primary cleavage of the photodamaged D1 protein in plant photosystem II. EMBO J 20:713–722

Juntadech T, Yokthongwattana K, Tangphatsornruang S, Yap Y-K, Angsuthanasombat C (2012) Efficient transcription of the larvicidal *cry4Ba* gene from *Bacillus thuringiensis* in transgenic chloroplasts of the green algal *Chlamydomonas reinhardtii*. Adv Biosci Biotechnol, in press

Kato Y, Sakamoto W (2009) Protein quality control in chloroplasts: a current model of D1 protein degradation in the photosystem II repair cycle. J Biochem 146:443–469

Kim JH, Nemson JA, Melis A (1993) Photosystem II reaction center damage and repair in *Dunaliella salina* (green alga). Analysis under physiological and irradiance-stress conditions. Plant Physiol 103:181–189

Lindahl M, Spetea C, Hundal T, Oppenheim AB, Andersson B (2000) The thylakoid FtsH protease plays a role in the light-induced turnover of the photosystem II D1 protein. Plant Cell 12:419–431

Melis A (1998) Photostasis in plants: mechanisms and regulation. In: Williams TP, Thistle A (eds) Photostasis and related phenomena. Plenum, New York, pp 207–221

Melis A (1999) Photosystem-II damage and repair cycle in chloroplasts: what modulates the rate of photodamage? Trends Plant Sci 4:130–135

Melis A, Spangfort M, Andersson B (1987) Light-absorption and electron-transport balance between photosystem II and photosystem I in spinach chloroplasts. Photochem Photobiol 45:129–136

Minagawa J, Crofts AR (1994) *Chlamydomonas reinhardtii*: a PCR-spliced *psbA* gene in a plasmid conferring spectinomycin resistance was introduced into a *psbA* deletion. Photosynth Res 42:121–131

Mulo P, Sirpiö S, Suorsa M, Aro E-M (2008) Auxiliary proteins involved in the assembly and sustenance of photosystem II. Photosynth Res 98:489–501

Nixon PJ, Michoux F, Yu J, Boehm M, Komenda J (2010) Recent advances in understanding the assembly and repair of photosystem II. Ann Bot 106:1–16

Polle JEW, Benemann JR, Tanaka A, Melis A (2000) Photosynthetic apparatus organization and function in the wild type and a chlorophyll *b*-less mutant of *Chlamydomonas reinhardtii.* Dependence on carbon source. Planta 211:335–344

Sueoka N (1960) Mitotic replication of deoxyribonucleic acid in *Chlamydomonas reinhardtii*. Proc Natl Acad Sci USA 46:83–91

Sugiura M, Inoue Y (1999) Highly purified thermo-stable oxygen-evolving photosystem II core complex from the thermophilic cyanobacterium *Synechococcus elongatus* having His-tagged CP43. Plant Cell Physiol 40:1219–1231

Sugiura M, Inoue Y, Minagawa J (1998) Rapid and discrete isolation of oxygen-evolving His-tagged photosystem II core complex from *Chlamydomonas reinhardtii* by Ni^{2+} affnity column chromatography. FEBS Lett 426:140–144

Suzuki T, Minagawa J, Tomo T, Sonoike K, Ohta H, Enami I (2003) Binding and functional properties of the extrinsic proteins in oxygen-evolving photosystem II particle from a green alga, *Chlamydomonas reinhardtii* having His-tagged CP47. Plant Cell Physiol 44:76–84

Takahashi S, Badger MR (2011) Photoprotection in plants: a new light on photosystem II damage. Trends Plant Sci 16:53–60

Yokthongwattana K, Melis A (2006) Photoinhibition and recovery in oxygenic photosynthesis: mechanism of a photosystem-II damage and repair cycle. In: Demmig-Adams B, Adams WW III, Mattoo AK (eds) Photoprotection, photoinhibition, gene regulation and environment, Advances in photosynthesis series. Springer, Dordrecht, pp 175–191

Yokthongwattana K, Chrost B, Behrman S, Casper-Lindley C, Melis A (2001) Photosystem II damage and repair cycle in the green alga *Dunaliella salina*: involvement of a chloroplast-localized HSP70. Plant Cell Physiol 42:1389–1397

Yokthongwattana K, Jin E, Melis A (2009) Chloroplast acclimation, photodamage and repair reactions of photosystem-II in the model green alga *Dunaliella salina*. In: Ben-Amotz A, Polle JEW, Rao DVS (eds) The alga *Dunaliella*: biodiversity, physiology, genomics and biotechnology. Science, New Hampshire, pp 273–299